

**AN ASSESSMENT OF THE USE OF REMOTE SENSING TO  
ESTIMATE CATCHMENT RAINFALL FOR USE IN HYDROLOGICAL  
MODELLING AND DESIGN FLOOD ESTIMATION**

**Khodani Khakhu**

Submitted in partial fulfilment of the  
requirements for the degree of MSc Hydrology

Environmental Hydrology

School of Agricultural, Earth and Environmental Sciences

University of KwaZulu-Natal

Pietermaritzburg

August 2022

## PREFACE

I ..... declare that

- (a) The research reported in this thesis, except where otherwise indicated, is my original work.
- (b) This thesis has not been submitted for any degree or examination at any other university.
- (c) This thesis does not contain text, data, figures, pictures, graphs, or tables from another document unless it is specifically acknowledged as being sourced from the original document. Where other sources have been quoted, then:
  - i) their words have been paraphrased/re-written, and the general information attributed to them has been referenced, and
  - ii) where their exact words have been used, their writing has been placed inside quotation marks and referenced.
- (d) Where I have reproduced a publication, of which I am an author, co-author, or editor, I have indicated in detail which part of the publication was actually written by myself alone and have fully referenced such publications.
- (e) This document does not contain text, graphics or tables copied and pasted from the Internet, unless they are specifically acknowledged, and the source is detailed, both in the document and in the References section.

Signed:..........

Date: .....

## **SUPERVISOR'S APPROVAL**

As the candidate's supervisor, I have approved this review and proposal for submission:

Signed:.....

Date: .....

## ABSTRACT

The accurate estimation of catchment rainfall is crucial, especially in hydrological modelling and flood hydrology which is used for the planning and design of hydrological infrastructures such as dams and bridges. Traditionally, catchment rainfall is estimated by making use of ground-based point rainfall measurements from rain gauges. The literature review conducted in this study supports that there is evidence of a decrease in the number of operational ground-based rainfall stations in South Africa which presents a challenge when estimating catchment rainfall for use in hydrological modelling and design flood estimation. Thus, innovative ways are required to estimate catchment rainfall and to improve the estimation of catchment design rainfall.

This study investigated the use of remote sensing as an alternative way to estimate catchment design rainfall. To do this, a pilot study was first used to develop and test the methodology using a quaternary catchment that was selected based on the raingauge density. This was followed by the application of a refined methodology in another quaternary catchment which was used to verify the results that were obtained in the pilot study.

After a comprehensive review of the literature, the remote sensing product selected for this study was the CHIRPS rainfall product. The methodology adopted first validated the remotely sensed rainfall data using the observed rainfall data and the estimated remotely sensed rainfall values were bias corrected using the observed rainfall data. The statistics that were used for validating are MAE, MBE, RMSE and D. The method that was used for bias correction was empirical quantile mapping. Issues encountered, and as documented in the literature, include the unavailability of long periods of observed quality rainfall data and the limited and uneven spatial distribution of rainfall stations.

Catchment rainfalls were estimated using observed rainfall, and this was assumed as the best estimate and was compared to the catchment rainfalls that were estimated using the bias-corrected remotely sensed rainfalls. The performance of CHIRPS rainfall was varied among the approaches and the selected catchments.

Nevertheless, the results from this study still show the potential of the use of remotely sensed rainfall to estimate catchment design rainfalls. At the daily timescale, satellite-derived and observed rainfall were poorly correlated and variable among locations. However, monthly and annual rainfall totals were in closer agreement with historical observations than the daily values.

Despite the varied performance , the result of the study shows that CHIRPS rainfall product can be used to estimate catchment rainfall for hydrological modelling and flood frequency analysis.

By acknowledging that the performance of remote sensing products is robust, it is of importance to note that the performance of the results presented is strictly for the catchments and stations selected for this project as well as the methods selected to validate and correct the bias in remotely sensed rainfall. The recommendations from the study are that a similar study is conducted in another region where there is even distribution of stations and a long record of quality observed rainfall beyond the year 2000 and consideration of the methods to identify outliers before making any meaningful estimations such as catchment rainfall from rainfall data.

Keywords: Catchment rainfall, Design rainfall, Hydrological modelling, Remote sensing

## **ACKNOWLEDGMENTS**

I would like to acknowledge and express my sincere thanks and appreciation to the following people for their help and support that was provided throughout this study:

- God.
- Sponsors (NFSP, RAENG and NRF).
- Professor J.C. Smithers (Supervisor)
- Lecturer's
- Family
- Peers

My help comes from the Lord, the maker of heaven and earth. – Psalms 121:2 NIV

# TABLE OF CONTENTS

	Page
ABSTRACT .....	iv
ACKNOWLEDGMENTS .....	vi
LIST OF FIGURES .....	xi
LIST OF TABLES .....	xiii
LIST OF ABBREVIATIONS .....	xv
1. INTRODUCTION.....	17
2. LITERATURE REVIEW.....	19
2.1 Rainfall Observation and Monitoring Network.....	19
2.1.1 Daily raingauge observations .....	19
2.1.2 Raingauge network status in South Africa .....	19
2.2 Estimation of Catchment Design Rainfalls.....	21
2.2.1 Using observed point rainfall data.....	22
2.2.1.1 Interpolation from point measurements .....	22
2.2.1.2 Use of adjustment factors.....	23
2.2.1.3 Areal reduction factors.....	24
2.2.2 Using remote sensing .....	25
2.2.3 Design rainfall estimation.....	32
2.3 Verification and Bias Correction of Remotely Sensed Data .....	32
2.4 Chapter Summary .....	34

3.	STUDY METHODOLOGY .....	37
3.1	Catchments Selection.....	38
3.2	Rainfall Station Selection .....	41
3.3	Remote Sensing Product Selection .....	43
3.4	Extraction and Processing of Remote Sensing Rainfall Data.....	46
3.4.1	Using ArcMap .....	46
3.4.2	Using Python .....	47
3.4.3	Using Google Earth Engine to extract point pixel values .....	47
3.4.4	Using Google Earth Engine to extract mean catchment rainfall .....	48
3.5	Performance of RS Data .....	48
3.6	Bias Correction .....	50
3.7	Estimation of Daily Catchment Rainfall.....	51
3.7.1	Using observed rainfall: Weighted stations.....	51
3.7.2	Using remotely sensed rainfall .....	52
3.7.2.1	Weighted pixels.....	52
3.7.2.2	Driver pixel (pptcor) .....	53
3.7.2.3	Corrected GEE .....	53
3.8	Estimation of Catchment 1-Day Design Rainfall .....	55
4.	APPLICATION TO CATCHMENT S60A: PILOT STUDY.....	56
4.1	Assessment of the performance and bias correction.....	56
4.2	Sensitivity to Period Length .....	63



4.3	Estimation of Catchment Rainfall .....	64
4.3.1	Validation of method of catchment rainfall correction .....	64
4.3.2	Assessment on a daily scale .....	65
4.3.3	Assessment on a monthly scale .....	69
4.4	Estimation of Catchment 1-Day Design Rainfall .....	72
5.	APPLICATION TO CATCHMENT U20F .....	74
5.1	Assessment of the performance and bias correction.....	74
5.2	Catchment Rainfall Estimates.....	80
5.2.1	Assessment on a daily scale .....	80
5.2.2	Assessment on a monthly scale .....	83
5.2.3	Sensitivity to the spatial density and influence of Thiessen weights .....	86
5.2.3.1	Assessment using daily accumulation.....	87
5.2.3.2	Assessment using regression statistics.....	88
5.3	Estimation of Catchment 1-Day Design Rainfall .....	90
6.	DISCUSSIONS, CONCLUSIONS, AND RECOMMENDATIONS.....	92
7.	REFERENCES.....	97
8.	APPENDIX A: PYTHON CODE TO EXTRACT CHIRPS RAINFALL DATA FROM MULTIPLE STATIONS .....	107
9.	APPENDIX B: PYTHON SCRIPT TO EXTRACT CHIRPS RAINFALL DATA FROM A SINGLE STATION .....	108
10.	APPENDIX C: CODE TO EXTRACT RESAMPLED CHIRPS DAILY RAINFALL IN GOOGLE EARTH ENGINE .....	109

11. APPENDIX D: A CODE TO ETRACT CHIRPS CATCHMENT RAINFALL FROM THE GOOGLE EARTH ENGINE ..... 112

12. APPENDIX E: EXAMPLES OF EXCEL SPREADSHEETS ..... 114

13. APPENDIX F: CODE TO ESTIMATE CATCHMENT DESIGN RAINFALLS IN THE R-STUDIO ..... 117

14. APPENDIX G: RESULTS OF BIAS CORRECTION STATISTICS IN CATCHMENT S60A..... 120

15. APPENDIX H: RESULTS OF BIAS CORRECTION STATISTICS IN CATCHMENT U20F..... 122

## LIST OF FIGURES

	Page
Figure 2.1: Active rainfall stations for water resource assessment (Pegram <i>et al.</i> , 2016) ...	20
Figure 2.2: Data availability of rainfall from active raingauges by a year (Pegram <i>et al.</i> , 2016) .....	21
Figure 3.1: Summary of the study methodology .....	37
Figure 3.2: Catchment S60A .....	39
Figure 3.3: Catchment U20F .....	40
Figure 3.4: Example of Thiessen polygons constructed ArcMap .....	51
Figure 4.1: Validation statistics for bias correction at a daily scale .....	58
Figure 4.2: Validation statistics for bias correction at a monthly scale.....	59
Figure 4.3: Validation statistics for bias correction at an annual scale .....	60
Figure 4.4: Assessment of performance of bias correction on a pixel-station basis for the best performed station (0079730 0) and poorly performed station (0101719A8) .....	62
Figure 4.5: Comparison of bias correction at different time scales for station 0079396 .....	64
Figure 4.6: Correlation between catchment rainfall derived from the weighted pixel values and the Google Earth Engine-derived catchment rainfall <b>before</b> they were bias corrected.....	65
Figure 4.7: Correlation between catchment rainfall derived from the weighted pixel values and the Google Earth Engine-derived catchment rainfall <b>after</b> they were bias corrected.....	65
Figure 4.8: Accumulated daily catchment rainfalls for different approaches .....	67
Figure 4.9: Frequency distribution for daily catchment rainfalls .....	68

Figure 4.10: Monthly catchment rainfalls comparison between different approaches.....	69
Figure 4.11: Frequency distribution curve for the monthly catchment values.....	71
Figure 4.12: Estimation of 1-day catchment design rainfall using different approaches .....	73
Figure 5.1: Validation statistics for bias correction at a daily scale .....	75
Figure 5.2: Validation statistics for bias correction at a monthly scale.....	76
Figure 5.3: Validation statistics for bias correction at an annual scale .....	77
Figure 5.4: Assessment of performance of bias correction on a pixel-station basis for the best performing (0270086 A) and poorly performing (0269744 S) station .....	79
Figure 5.5: Accumulated daily catchment rainfalls for different approaches .....	80
Figure 5.6: Frequency distribution for daily catchment rainfalls .....	82
Figure 5.7: Catchment rainfalls comparison between different approaches .....	83
Figure 5.8: Frequency distribution curve for the monthly catchment values.....	85
Figure 5.9: Catchment U20F showing the station's distribution and the Thiessen polygons.....	86
Figure 5.10: Accumulated daily catchment rainfalls estimated using weighted pixels .....	87
Figure 5.11: The estimation of catchment rainfalls using an areal weighting of stations/pixels for the 10 and 3 stations/pixels distribution .....	89
Figure 5.12: Estimation of 1-day catchment design rainfall values for different return periods.....	91

## LIST OF TABLES

	Page
Table 2.1: Summary of RS products reviewed .....	28
Table 3.1: Catchment S60A, selected raingauges, and selected driver station in bold text.....	42
Table 3.2: Catchment U20F, selected raingauges, and selected driver station in bold text.....	42
Table 3.3: Criteria used to select the RS product.....	44
Table 3.4: Criterion used to select the RS product against the RS products reviewed. ....	45
Table 4.1: MBE difference between RAW and CORRECTED rainfalls for each station.....	61
Table 4.2: Daily catchment rainfalls MAE summary statistics for all approaches compared to the Weighted station approach.....	67
Table 4.3: Total monthly catchment rainfalls MAE summary statistics for all approaches compared to the weighted station approach.....	70
Table 4.4: Catchment design rainfalls MAE statistics for all approaches compared to the Weighted station approach.....	72
Table 5.1: MBE difference between RAW and CORRECTED rainfalls for each station.....	78
Table 5.2: Daily catchment rainfalls MAE summary statistics for all approaches compared to the Weighted station approach.....	81
Table 5.3: Total monthly catchment rainfalls MAE statistics for all approaches compared to the weighted station approach.....	84

Table 5.4:	Catchment design rainfalls MAE statistics for all approaches compared to the weighted station approach.....	90
Table E.1:	An example spreadsheet of calculation of bias correction factors.....	114
Table E.2:	An example of the calculation of catchment rainfall using areal weights .....	115
Table E.3:	Results of the catchment median rainfalls, station median rainfalls, and the adjustment factors for the selected driver station in Catchment S60A.....	116
Table E.4:	Results of the catchment median rainfalls, station median rainfalls, and the adjustment factors for the selected driver pixel in catchment U20F.....	116
Table G.1:	Bias correction statistics at a daily scale.....	120
Table G.2:	Bias correction statistics at a monthly scale .....	120
Table G 3:	Bias correction statistics at an annual scale .....	121
Table H.1:	Bias correction statistics at a daily scale.....	122
Table H.2:	Bias correction statistics for the monthly scale.....	122
Table H 3:	Bias correction statistics for the annual scale .....	123

## LIST OF ABBREVIATIONS

Acronym	Description
APHRODITE	Asian Precipitation Highly Resolved Observational Data Integration Towards Evaluation of Water Resources
ARC	Africa Rainfall Climatology
CHIRPS	Climate Hazards Group IR Precipitation Station
CMORPH	Climate Prediction Center Morphing Technique
CPC	Climate Prediction Center
CRU TS	The Climatic Research Unit Timeseries
ECMWF	European Centre for Medium-Range Weather Forecast
ERA-Interim	ECMWF Re-Analysis Interim
FEWS	Famine Early Warning Systems
GPCC	The Global Precipitation Climatology Centre
GPCP	Global Precipitation Climatology Project
GPM	Global Precipitation Measurements
MAP	Mean Annual Precipitation
MSWEP	Multi-Source Weighted Ensemble Precipitation
NASA	National Aeronautics and Space Administration
NERC	Natural Environment Research Council
NCAS	National Centre for Atmospheric Science
NOAA	National Oceanic Atmospheric Administration
PERSIANN	Precipitation Estimation from Remote Sensing Information Using Artificial Neural Network
RFE2	Rainfall Estimation version2

<b>Acronym</b>	<b>Description</b>
RS	Remote Sensing
TAMSAT	Tropical Application of Meteorology Using Satellite
TRMM 3B42	Tropical Rainfall Measuring Mission product 3B42
TMPA	TRMM Multi-satellite Precipitation Analysis
UC Irvine	University of California, Irvine
USGS	United States Geological Survey



# 1. INTRODUCTION

Rainfall data are needed for many purposes, e.g. for hydrological modelling and design rainfall estimation. Ciach (2003) describes rainfall as the main driving force and key input in many hydrological processes. Generally, long term and good quality rainfall records are recommended for use (Gericke, 2018). This is because the statistical analysis and the conclusions that are drawn from the analysis of rainfall data can only be as accurate as the data on which they are based (DWS, 2014). Frezghi and Smithers (2008) expressed that, for hydrological modelling, such as design flood modelling, long sequences of rainfall at a fine spatial and temporal resolution are necessary.

According to Schulze *et al.* (2007), the most convenient method to monitor accurate and long record rainfall is through the use of raingauges. Pegram *et al.* (2016) noted that Remote Sensing (RS) means of estimating rainfall are limited both internationally and in South Africa. Generally, RS records are not as trusted as observed records from the rain gauges. Dembélé *et al.* (2016) recommended that remotely sensed rainfall data should be validated with gauged observations before making meaningful conclusions based on the RS data. However, Awange *et al.* (2016) argue that, even though raingauges provide trusted observed rainfall estimates at a point, satellite and radar provide cost-effective means of complementing rainfall field data. This blended approach to estimating rainfall, especially with the gradual decrease of operating gauge stations in South Africa, should be pursued. For example, Makapela *et al.* (2015) recommended that both remote sensing and gauged observed rainfall should be combined to produce effective up-to-date estimations.

Many hydrological assessments are done at a catchment level. To estimate catchment rainfall, point rainfall has historically been used. This is owing to the unavailability until relatively recently, uncertainty and errors that have been associated with using remotely sensed rainfall estimates. This statement is supported by the use of satellite-driven simulations specifically in flood events. According to Sawunyama and Hughes (2008), spatially interpolated point rainfall data are currently widely used as input to hydrological modelling even though the accuracy in terms of both time and space remains a major concern. Therefore, spatial rainfall estimated using remote sensing is becoming a viable substitute and mainline product.

There are different methods of estimating catchment rainfall from point rainfall observations. For example, the Department of Water and Sanitation uses the areal averaged method to convert

point design rainfalls to catchment design rainfalls (DWS, 2014), while the ACRU hydrological model makes provision for the use of adjustment factors to adjust daily point rainfalls to best represent catchment daily rainfall (Smithers and Schulze, 2004a). In both examples, areal rainfall is estimated using point rainfall data from raingauges. Therefore, it is important to investigate other approaches to estimate areal rainfalls that result in better estimates of spatial rainfall and take into consideration ungauged catchments and the currently declining raingauge network, both internationally and in South Africa.

The primary aim of this study is to use remotely sensed rainfall to improve the estimation of catchment rainfall for use in hydrological modelling and assess different methods of estimating both catchment rainfall and catchment design rainfall. This is to (a) address the challenge of few stations with long records of rainfall data and (b) address the gap that exists when deriving catchment design rainfalls for flood studies in less gauged catchments. The study aims were achieved by the following objectives:

- (a) Assessing the availability of remotely sensed rainfall data and selecting the best option for use in South Africa.
- (b) Evaluating the performance of the selected remotely sensed rainfall estimation product by comparing it against gauged data and, if necessary, bias correcting the remotely sensed rainfall data using approaches that are used internationally.
- (c) Estimating catchment rainfall using observed rainfall and adjusting remotely sensed rainfall to some approaches that traditionally use observed rainfall to estimate catchment rainfall for comparison.
- (d) Assessing the performance of catchment rainfalls and the impact of adjusted approaches in (c) on the performance of the design rainfall estimation.

This study is structured as follows: Chapter 2 provides a detailed literature review. Chapter 3 introduces the detailed methodology that was followed to carry out this study and this includes the selection of catchments, selection of stations, and selection of remote sensing product to use in the study. Chapter 4 contains the results of the pilot study. In Chapter 5, a refined methodology is applied in another catchment so that the results obtained in the pilot study can be confirmed. Chapter 6 contains a discussion of the results from the study, draws conclusions, and give recommendations for future research.

## **2. LITERATURE REVIEW**

This chapter contains a detailed literature review of the study which includes to the observed rainfalls, remotely sensed rainfalls and the estimation of design catchment rainfalls.

### **2.1 Rainfall Observation and Monitoring Network**

This chapter provides a review of gauged rainfall observations and raingauge network status in South Africa. This is followed by a review of the use of remotely sensed rainfall data.

#### **2.1.1 Daily raingauge observations**

Raingauges are the primary source of observed rainfall data which provides accurate estimates at the point of measurement (Kruger and Nxumalo, 2017). Although many scientists have high confidence in rainfall measurement using raingauges, considerable deficiencies in rainfall measurement using raingauges remain a problem (Ciach, 2003). Many of these problems are outlined by Smithers and Schulze (2004a) to be a result of the physical characteristics and the location of the raingauge.

Numerous studies have been conducted to investigate the accuracy of using raingauges to measure point rainfall (e.g. Allerup and Madsen, 1980; Wood *et al.*, 2000; Ciach, 2003). According to Smithers and Schulze (2004a), since a raingauge is an obstacle to wind, it is unrealistic to assume that a raingauge reading represents the actual rainfall at the site because of turbulence around the gauge. For example, Tyson *et al.* (1976) found that at Cathedral Peak in the Kwazulu-Natal Drakensberg, a Nipher-type windshield increased catch deficiency by an average of 9.2%. Hence, assuming that the observed point rainfall from raingauges is representative of the true rainfall, the catch deficiencies caused by the aerodynamic interaction with a raingauge and the surrounding topography are ignored. In addition, errors associated with rainfall measurement using a raingauge are not limited to systemic errors, but also human errors from incorrectly reading the rainfall amounts. Therefore, it is accepted that raingauges provide fair rainfall measurements, however, there are considerable inaccuracies associated with it (Smithers and Schulze, 2004a).

#### **2.1.2 Raingauge network status in South Africa**

The availability of observed rainfall data and long records remains a challenge in South Africa (Kruger and Nxumalo, 2017; Suleman, 2020). One of the factors contributing to this challenge

is the decline in the number of active rainfall stations (Schulze *et al.*, 2007; Pitman, 2011; Pegram *et al.*, 2016). This is evident in Figure 2.1, where the trend of active rain stations in South Africa indicates a significant decline that started in the 1990s. As a result of this continuous decline in active rainfall stations, obtaining long records of quality rainfall data has become more challenging (Nomqophu, 2020). This is an issue in hydrological modelling as most hydrological models were calibrated using point rainfall measurements from raingauges. As seen in Figure 2.2, the blue vertical lines only appear when a year has data and the white space means there were no data recorded at that time for available active stations (Pegram *et al.*, 2016). This has resulted in the implementation of more innovative approaches to estimate rainfall information such as through Remote Sensing (RS), however, the accuracy related to remotely sensed rainfall remains a concern (Makapela *et al.*, 2015). Therefore, a dense network of raingauges is required in order to obtain reliable estimates of the spatial distribution of rainfall as mentioned by Pegram *et al.* (2016).

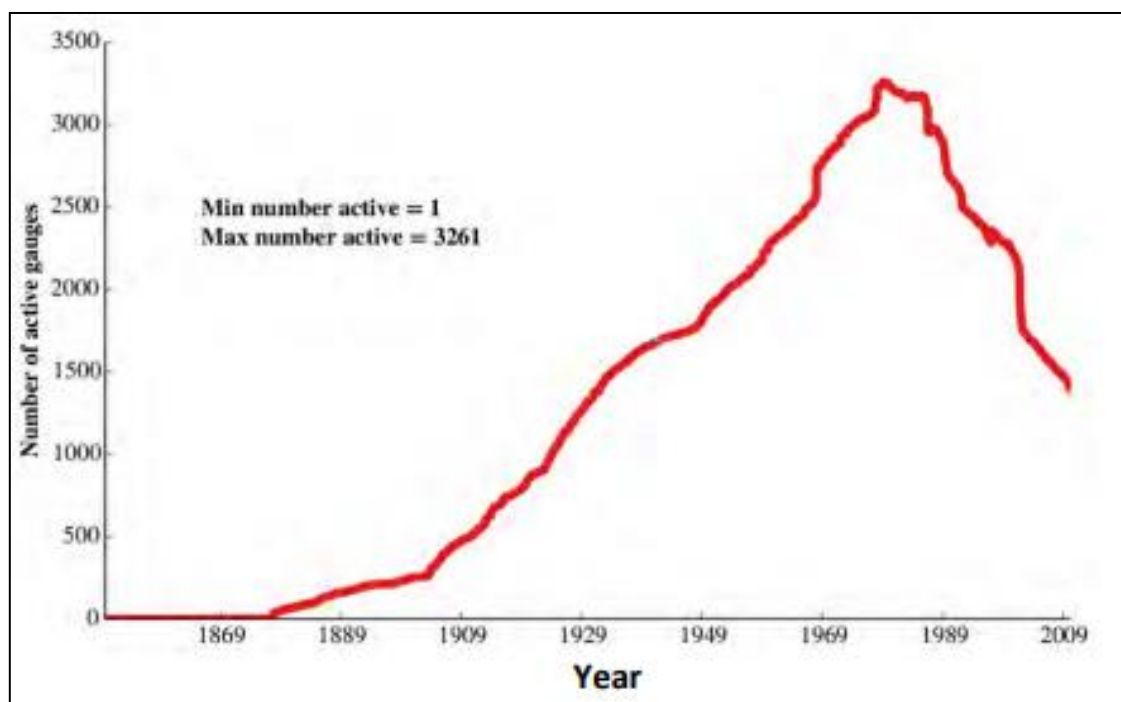


Figure 2.1: Active rainfall stations for water resource assessment (Pegram *et al.*, 2016)

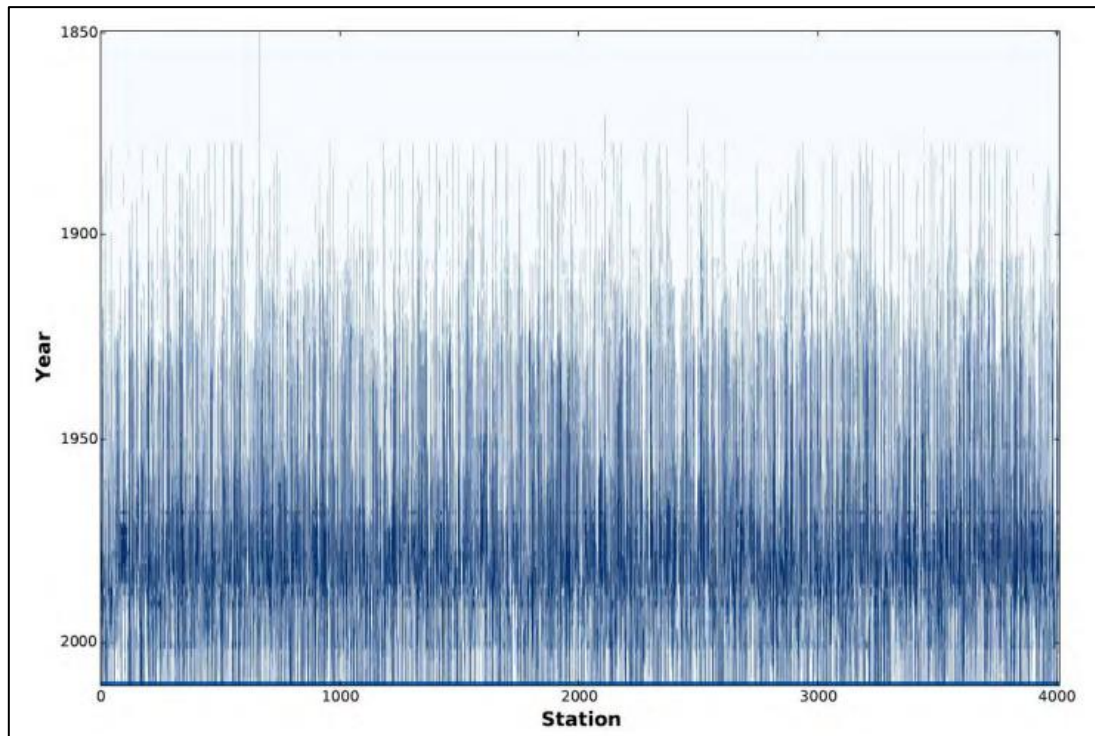


Figure 2.2: Data availability of rainfall from active raingauges by a year (Pegram *et al.*, 2016)

According to Hutchinson (1974), Mishra (2013), and Xu *et al.* (2013) a network of raingauges should be designed to allow the adequate representation of the spatial variability of rainfall within a catchment. This is important, especially when estimating catchment rainfall because a dense raingauge network is essential to obtain an accurate estimate of the areal rainfall (Nomqophu, 2020). Rodda (1972), cited by Abtew *et al.* (1995) summarised the problems of network design in the early 1970s as: (a) the number of raingauges required, (b) the location of these gauges, and (c) the length of operation. These problems still prevail 48 years later which emphasises the need to implement new ways to estimate rainfall information to complement raingauge measurements.

## 2.2 Estimation of Catchment Design Rainfalls

According to Pietersen *et al.* (2015), design rainfall is the rainfall information taken from observed rainfall data which constitutes a rainfall depth and duration associated with a given return period or annual exceedance probability. While many studies have focused on estimating design rainfall at a point (Smithers *et al.*, 2002; Smithers and Schulze, 2003; Smithers and Schulze, 2004b; Xu and Tung, 2008; Yang *et al.*, 2010; Haddad *et al.*, 2011), it is also important to estimate design rainfall from spatial estimates such as by converting remotely sensed

measured rainfall to a catchment design value for use in the risk assessment and design of hydrological structures. This section contains a review of approaches that are considered when estimating catchment design rainfall. This includes the use of observed point rainfall estimates and details of the approaches followed. Thereafter, the use of RS data to estimate catchment design rainfall is detailed.

### **2.2.1 Using observed point rainfall data**

Point rainfall estimates are the most fundamental hydrological element required for most rainfall-runoff modeling and the estimation of design rainfall (Arnaud *et al.*, 2011). According to DWS (2014), the accuracy of point measurement of rainfall in hydrological modelling is important because the statistical analysis and the conclusions that are drawn from them can only be as accurate as of the data on which they are based. There are different approaches to using point rainfall measurements to estimate catchment design rainfalls, it can be either by first adjusting the observed point rainfall and converting it to a catchment rainfall and then the catchment rainfall to estimate catchment design rainfalls or by converting the estimated catchment rainfall, derived from the observed point rainfall values, to point design rainfall values and then adjusting these to catchment design rainfalls by using an appropriate factor.

#### **2.2.1.1 Interpolation from point measurements**

To estimate spatial rainfall from point rainfall data, interpolation methods are used such as Inverse Distance Weighting (IDW), Kriging, and Thiessen Polygons (TP) amongst others (Faisal and Gaffar, 2012; Mendez and Calvo-Valverde, 2016). TP is the most widely used interpolation method as it accurately estimates average point rainfalls over a catchment (Taesombat and Sriwongsitanon, 2009). As explained by Stellman *et al.* (2001), Faisal and Gaffar (2012), and Keblouti *et al.* (2012). TP uses Thiessen weights estimated by the ratio of the area of a polygon containing a station to the total area of the catchment. To estimate the area of each polygon around each raingauge, connecting lines joining each pair of rainfall gauge stations are drawn. Then, lines acting as perpendicular bisectors to the connecting lines are drawn to produce polygons around each gauge. The area of each polygon is then determined and is called the control area. The ratio is then used as a weighting factor to be applied when estimating the average point rainfall. Equation 2.1 is used to estimate Thiessen weights. With the advancement in technology, TP, as well as IDW, can now be performed by making use of the Geographical Information System (GIS) which takes a lot of time when done manually for a number of gauge stations (Hu *et al.*, 2019).

$$W = \frac{A_{\text{station}}}{A_{\text{catchment}}} \quad (2.1)$$

where

$W$  = Thiessen weights,

$A_{\text{station}}$  = area of polygon surrounding the station (km<sup>2</sup>), and

$A_{\text{catchment}}$  = total area of catchment (km<sup>2</sup>).

### 2.2.1.2 Use of adjustment factors

In the *ACRU* model (Schulze, 1995), point rainfall data are adjusted to estimate catchment rainfall by applying month-by-month adjustment factors to convert the point rainfall data to areal rainfall (Smithers, 1995; Clark, 2019). This is done using the driver station which is the station selected to drive the hydrological processes in the catchment. The application of month-by-month adjustments is because there is variation in the weather generation mechanism for each season at a given location. There are two utilities designed to select the driver station. The first utility is the daily rainfall data extraction utility developed by Kunz (2004). This utility selects stations based on station names or geographical areas. Details of the selected stations are then used to select the driver station. The *CalcPPTCor* rainfall adjustment utility (Pike, 2004) was developed to assist the user in selecting the most representative rainfall station for a particular catchment and automatically calculates rainfall adjustment factors required for each sub-catchment simulated using the *ACRU* model (Clark, 2019). This software uses information from the geographic and climatological characteristics of the selected stations in the study area to calculate month-by-month rainfall adjustment factors. This is done mainly to account for the regional, seasonal, and daily diversity of rainfall (Dent *et al.*, 1989; Lynch *et al.*, 2004; Pegram *et al.*, 2016). The usual procedure for use in southern Africa would be for the catchment to be overlaid on a map of Mean Annual Precipitation (MAP) derived from Lynch *et al.* (2004) from which a weighted catchment MAP is determined.

The criteria in the input file to the *CalcPPTCor* software allow the user to have options in choosing the best station for the site. *CalcPPTCor* also requires the user to supply average altitude, MAP, and median monthly rainfall information for each catchment. The ArcView Grid Extractor utility can be used for this purpose. The geographic coordinates of each station are used by *CalcPPTCor* to identify the position of the specified rainfall station in the gridded

rainfall and altitude surfaces for South Africa (Lynch *et al.*, 2004). The program then automatically extracts the relevant altitude, MAP, and the 12 median monthly rainfall totals for each station from the gridded information. The gridded median monthly rainfall surfaces were developed by Lynch (2004). The ratios between the catchment median monthly rainfall and each station's median monthly rainfall are then calculated using Equation 2.2 for each sub-catchment to adjust the daily or monthly total of rainfall to best represent the catchment rainfall (Smithers and Schulze, 2004a). The driver station can also be selected manually by using the same criteria as the criteria provided by the mentioned tools.

$$\text{pptcor} = \frac{\text{CatchmentMMR}}{\text{StationMMR}} \quad (2.2)$$

where

pptcor = precipitation correction factor, and  
MMR = Median Monthly Rainfall.

### 2.2.1.3 Areal reduction factors

Areal Reduction Factors (ARFs) have historically been used to estimate the areal average design rainfall over a catchment. Observed rainfall monitored at a point does not represent the catchment's rainfall given the temporal and spatial non-uniformity of rainfall (Alexander, 1990; Van der Spuy and Rademeyer, 2016). Hence it is necessary to convert point design rainfall into catchment design rainfall which generally requires a reduction in the point rainfall intensity which is related to the catchment area ( $\text{km}^2$ ) and storm duration (h) (Pietersen *et al.*, 2015; Van der Spuy and Rademeyer, 2016). ARFs are dependent on catchment location, characteristics, and the method of estimating the ARFs. Some studies have used storm-centered and other geographic-centered approaches. Relevant ARF studies conducted in South Africa are: (i) Van Wyk (1965), (ii) Wiederhold (1969), (iii) Alexander (1980) and (iv) Alexander (1990; 2001). The mathematical expressions used in each method and a detailed review is provided by Pietersen *et al.* (2015) and their use and figures from which the mathematical expressions are derived are detailed in the SANRAL Drainage Manual (SANRAL, 2013). However, most studies use Equation 2.3 because it is an update from the previous equations and uses one variable (Gericke and Du Plessis, 2011; Pietersen *et al.*, 2015).

$$\text{ARF} = [-6944.3 \ln(A) + 115\,731.9]^{0.4} \quad (2.3)$$

where

ARF = areal reduction factor, and



A = catchment area (km<sup>2</sup>).

### 2.2.2 Using remote sensing

The use of RS to estimate the spatial distribution of rainfall has for some time been proposed as a solution to overcome the challenge of declining rainfall stations in South Africa (Awange *et al.*, 2016; Kruger and Nxumalo, 2017). Although the accuracy of RS rainfall has been questioned, for example, by Awange *et al.* (2016), it has become the most valuable tool to estimate rainfall at different spatial and temporal scales (Keblouti *et al.*, 2012). Often RS products are used to gather information about rainfall, evaporation, soil moisture, and runoff. When used to estimate rainfall information, it provides a cost-effective means of complementing field observed data as it can cover a large area and provide rainfall information in ungauged catchments (Chen *et al.*, 2019).

Various RS products have been developed and investigated to assess the accuracy of remotely sensed rainfall, for example, Rainfall Estimation version2 (RFE2) and Tropical Rainfall Measuring Mission product (TRMM) by Mashingia *et al.* (2014), Global Precipitation Climatology Project (GPCP), Precipitation Estimation from Remote Sensing Information Using Artificial Neural Network (PERSIANN) and Climate Prediction Center Morphing Technique (CMORPH) by Pombo *et al.* (2015), and Famine Early Warning Systems (FEWS) by Artan *et al.* (2007). Thorne *et al.* (2001) compared Tropical Application of Meteorology Using Satellite (TAMSAT) and Climate Prediction Center (CPC), Hessels (2015) compared and validated TRMM 3B42, and Du Plessis and Kibii (2021) compared daily and monthly rainfall data derived from Climate Hazards Group IR Precipitation Station (CHIRPS) with observed rainfall data from 46 stations evenly distributed across South Africa. The results showed that satellite products can represent the temporal and spatial variability of rainfall within a region. However, there is high variation in the accuracy of the remotely sensed products, with variation from product to product and between locations (Maswanganye, 2018). Another finding is that products that are combined with rain gauge data or bias corrected with observed rainfall are more accurate, however, the accuracy depends on the topography and density of the rain gauge network. In many cases, the accuracy was mainly affected by factors related to elevation, relative relief, longitude, and latitude. Therefore, bias correction is recommended before the application of remotely sensed rainfall data (Habib *et al.*, 2014a; Maswanganye, 2018).

Liu *et al.* (2015) reported the erratic performance of RS products. Three widely used satellite products i.e. TRMM, CMORPH, and PERSIANN, were evaluated over a subtropical catchment at different time scales. On a daily scale, CMORPH had the best performance. On a monthly and annual scale, TRMM had the best performance with PERSIANN having the worst performance at all time scales considered. The study concluded that TRMM was a more reliable product and has good potential for hydrological applications. Global Precipitation Measurements (GMP), which is the updated version of TRMM, is the recommended product for future usage.

Recent development reveals that remotely sensed rainfall can also be used in hydrological models. This is evident in a study that was conducted by Suleman (2017) and Suleman *et al.* (2020) to investigate the use of satellite-derived rainfall in the *ACRU* hydrological model to simulate streamflow. The satellite rainfall products chosen for investigation included TRMM 3B42, FEWS ARC2, FEWS RFE2, TAMSAT-3, and GPM. Generally, the results of the analyses indicated that the TRMM 3B42 overestimated rainfall volumes whereas the other products underestimated rainfall volumes.

Lakew *et al.* (2020) investigated the hydrological performance of several global RS products in a data-scarce region for daily simulation. TRMM Multi-Satellite Precipitation Analysis (TMPA), ERA-Interim (ERA-Interim), Global Precipitation Climatology Centre (GPCP), and Multi-Source Weighted Ensemble Precipitation (MSWEP) were used for this purpose. The results indicate that the MSWEP performed better than the rest of the products. Based on the results, the study recommended the use of MSWEP with bias correction to use in the Blue Nile catchment. A similar study was done by Shayeghi *et al.* (2020) using the Asian Precipitation Highly Resolved Observational Data Integration Towards Evaluation of Water Resources (APHRODITE), ERA-Interim, TMPA, and PERSIANN data to compare against gauged datasets for use in the Variable Infiltration Capacity (VIC) model. APHRODITE and ERA-Interim gave better rainfall estimates at a daily time scale than other products. Further, the hydrological assessment indicated that PERSIANN is the best rainfall dataset for capturing the streamflow and peak flows for the studied area.

One of the limitations in many of the studies is that results from one region do not necessarily give the confidence for use in another region which has differences in catchment meteorological and physical characteristics. Kruger and Nxumalo (2017) express the thought that remotely sensed rainfall records are not as trusted as observed records from raingauges, therefore, it is

advisable to incorporate both or use *in-situ* measurement to validate RS measurements to produce effective up-to-date predictive and analytical output. Table 3.1 contains a summary review of some of the most used and most reviewed RS products to estimate rainfall information.

Table 2.1: Summary of RS products reviewed

<b>RS Product</b>	<b>Data Availability</b> [Years of Record]	<b>Data accessibility</b> [Bias Correction]	<b>Spatial Resolution</b> [Spatial Coverage]	<b>Temporal Resolution</b> [Product Updates]	<b>Gauged/Satellite/Radar/Model Based</b>	<b>Product Producer</b>	<b>Accuracy and Performance (Key Findings)</b>	<b>Source of Information</b>
TRMM	1997-2015 [18]	Free [Not required]	0,2°×0,25°, 0,5°×0,5 ° [50°N and 50°S]	Hours to monthly [Stopped]	Gauged/Satellite	NASA	Accurate at the tropics. Fair measurements at mid-latitudes.	(Huffman <i>et al.</i> , 2010; Liu <i>et al.</i> , 2012; Hessels, 2015; Makapela <i>et al.</i> , 2015; Pombo <i>et al.</i> , 2015; NCAR/UCAR, 2019)
GMP	2000-Present [20]	Free [Not required]	0,1°×0,1° [60°N and 60°S]	Sub-daily, Daily, Monthly [30 Minutes]	Gauged /Satellite	NASA/JAXA	Poor performance in sparse raingauges but acceptable measurements	(Adler <i>et al.</i> , 2003; Liu <i>et al.</i> , 2012; Blumenfeld, 2015; NCAR/UCAR, 2019)
GPCP	1996-2020 [36]	Free [Corrected]	1°×1°, 2,5°×2,5° [Global]	Daily, Monthly [Regularly]	Gauged/Satellite	NASA/GSFC	Underestimate rainfall at low precipitation rates.	(Grody, 1991; Wilheit <i>et al.</i> , 1991; Kummerow and Giglio, 1995; Adler <i>et al.</i> , 2003; Hessels, 2015; Makapela <i>et al.</i> , 2015; NCAR/UCAR, 2019)

<b>RS Product</b>	<b>Data Availability</b> [Years of Record]	<b>Data accessibility</b> [Bias Correction]	<b>Spatial Resolution</b> [Spatial Coverage]	<b>Temporal Resolution</b> [Product Updates]	<b>Gauged/Satellite/Radar/Model Based</b>	<b>Product Producer</b>	<b>Accuracy and Performance (Key Findings)</b>	<b>Source of Information</b>
TAMSAT	1983-Present [37]	Free [Required]	0,0375°×0,0375° [Africa]	10Days-Decadal [February 2019]	Gauged/Satellite	NOAA	Underestimate/overestimate rainfall in coastal and mountainous regions.	(Grimes <i>et al.</i> , 1999; Thorne <i>et al.</i> , 2001; Maidment <i>et al.</i> , 2014; Awange <i>et al.</i> , 2016; Dembélé <i>et al.</i> , 2016; Maidment <i>et al.</i> , 2017; Dinku <i>et al.</i> , 2018)
CMORPH	1998-Present [22]	Free [Required]	0,25°×0,25°, 0,1°×0,1° [60°N and 60°S/ 8km×8km]	Sub-daily, Daily [February 2019]	Satellite	NOAA/CPC	Inconsistent results for different areas. Inaccurate in coastal and orographic areas.	(Joyce <i>et al.</i> , 2004; Joyce <i>et al.</i> , 2010; Hessels, 2015; Makapela <i>et al.</i> , 2015; Pombo <i>et al.</i> , 2015; Awange <i>et al.</i> , 2016; Xie <i>et al.</i> , 2017; NCAR/UCAR, 2019)
FEWS NET	2001-Present [19]	Free [Not required]	0,1°×0,1° [20°W and 55°E, 40°N and 40°S]	Hourly [Daily]	Gauged/Satellite	FEWS/USGS/ NOAA	Inaccurate results in dry summer areas over East and West Africa.	(Novella and Thiaw, 2013; Makapela <i>et al.</i> , 2015; Awange <i>et al.</i> , 2016; Maswanganye, 2018) <a href="#">ENREF 49</a>

<b>RS Product</b>	<b>Data Availability</b> [Years of Record]	<b>Data accessibility</b> [Bias Correction]	<b>Spatial Resolution</b> [Spatial Coverage]	<b>Temporal Resolution</b> [Product Updates]	<b>Gauged/Satellite/Radar/Model Based</b>	<b>Product Producer</b>	<b>Accuracy and Performance (Key Findings)</b>	<b>Source of Information</b>
CRU TS	1901-2019 [118]	Request [Required]	0,5°×0,5° [90°N and 90°S]	Monthly [Timely interval]	Gauged/Model	NERC/NCAS	Inconsistent performance and accuracy.	(Mitchell and Jones, 2005; Harris <i>et al.</i> , 2014; NCAR/UCAR, 2019)
ERA-Interim	1979-2019 [40]	Free [Not required]	0,75°×0,75° [90°N and 90°S]	6 Hourly, Daily, Monthly [Stopped]	Gauged/Satellite/Model	ECMWF	Performs more reasonably at the escarpments than on the coast. Provide accurate results.	(Thépaut <i>et al.</i> , 1996; Dee <i>et al.</i> , 2011; Hersbach and Dee, 2016; Hoffmann <i>et al.</i> , 2019; NCAR/UCAR, 2019)
ERA5	1950-Present [70]	Free [Required]	0.3°×0.3° [Globally]	Hourly, Monthly [Daily]	Model	ECMWF	Accurate measurements but uncertain at the coast of the continent.	(Hersbach and Dee, 2016; Chen <i>et al.</i> , 2019; Hoffmann <i>et al.</i> , 2019; NCAR/UCAR, 2019)
CHIRPS	1981-Present [41]	Free [Not required]	0,05°×0,05° [50°N and 50°S]	Daily, Monthly Averages [May 2020]	Gauged/Satellite	UCSB	Fair performance with high accuracy for a large amount of precipitation than in arid and semi-arid areas. Performs better on a monthly scale.	(Funk <i>et al.</i> , 2012; Funk <i>et al.</i> , 2014; Hessels, 2015; Funk <i>et al.</i> , 2017; Dinku <i>et al.</i> , 2018; Du Plessis and Kibii, 2021; Funk <i>et al.</i> , 2007)

<b>RS Product</b>	<b>Data Availability</b> [Years of Record]	<b>Data accessibility</b> [Bias Correction]	<b>Spatial Resolution</b> [Spatial Coverage]	<b>Temporal Resolution</b> [Product Updates]	<b>Gauged/Satellite/Radar/Model Based</b>	<b>Product Producer</b>	<b>Accuracy and Performance (Key Findings)</b>	<b>Source of Information</b>
GPCC	1901-Present [119]	Request [Corrected]	0,5°×0,5°, 2,5°×2,5° [Global]	Sub-daily, Daily, Monthly [Monthly]	Gauged	NOAA	Accurate measurements depend on the density of the station network.	(Shepard, 1968; Rudolf and Schneider, 2005; Darand and Zand, 2016; Pegram <i>et al.</i> , 2016; NCAR/UCAR, 2019)
PERSIAN	1983-2020 [20]	Free [Required]	0,25°×0,25° [60°N and 60°S]	Sub-daily, Daily [Quarterly]	Satellite/Radar	UC-Irvine	Reasonable results in plateau basins with high climate variability. More accurate on a monthly scale.	(Hong <i>et al.</i> , 2004; Hessels, 2015; Pombo <i>et al.</i> , 2015; Awange <i>et al.</i> , 2016; Maggioni <i>et al.</i> , 2016; NCAR/UCAR, 2019)

### 2.2.3 Design rainfall estimation

Probability distributions are fitted to extreme rainfall events and used to estimate the design values for specific return periods (Smithers and Schulze, 2003). They use mathematical equations which are also referred to as probability functions to derive design values (Van der Spuy et al., 2016). The probability distribution models that are usually used in the South Africa to estimate design rainfall are but are not limited to, the Log-normal (LN), Pearson Type III (P3), Log-Pearson Type III (LP3), Generalized Extreme Value (GEV), Generalized Pareto, Generalized Logistic and Gumbel distributions (EV1) (Gericke, 2018)

The GEV Probability distribution is widely used internationally. For example, the GEV is recommended as the best probability distribution internationally in the United Kingdom (Flood Studies Report, 1975) Cited by Hosking *et al.* (1985) and in South Africa (Smithers, 1996), (Smithers, 2000), and (Smithers and Schulze, 2003). The advantage for using GEV probability distribution was that it combines three sub-types of distributions into one based on the value of the skewness coefficient and it is a flexible distribution. Additionally, the distribution model that is the best fit for a respective rainfall duration is to be applied to any rainfall duration.

### 2.3 Verification and Bias Correction of Remotely Sensed Data

Even though remotely sensed rainfall data are useful for spatial estimates of rainfall, it is also evident that satellite rainfall estimations are contaminated with significant systemic and random errors (Yeh *et al.*, 2020). Research by Bhatti *et al.* (2016) indicates that satellite-based rainfall estimates are not always reliable. In such instances, RS products may require validation and bias correction before they can be useful for further hydrological applications and to gain confidence in the computed remotely sensed rainfall-based estimations.

Many studies conducted to assess bias correction conclude that bias correction improves simulations. For example, a study of the effect of bias correction on satellite rainfall estimation by Habib *et al.* (2014a) indicated that applying space and time-fixed bias correction schemes may result in reduced rainfall bias in CMORPH by up to 50%. Mei *et al.* (2016) pointed out that some mismatches between the satellite-based rainfall estimations and observed rainfall data from raingauges are due to the absence or not enough raingauges in a catchment for a fair comparison. In support of this, Bhatti *et al.* (2016) added that time series of raingauge data are not reliable and may influence hydrological assessments and modelling studies. These studies have provided more insight into the assessment of the accuracy of spatial rainfall estimates.



Considering data scarcity in poorly gauged regions, it is important to assess whether remotely sensed estimates are suitable to act as a substitute or to supplement data sources to estimate rainfall. Moulin *et al.* (2009) conducted a study to investigate where the uncertainties in mean areal precipitation stem from. One hypothesis was that it may be due to model performance and another hypothesis was that it may be due to the use of unrepresentative gauges stations. For the methodology, model performance, as well as mean areal precipitation estimated from raingauges, were assessed. The results indicate that some errors stem from the spatial estimates from raingauges. Based on the above-referenced studies it can be concluded that not all uncertainties in spatial estimates of rainfall are from the use of the remote sensing data and therefore gauge distribution within and around a catchment needs to be assessed as well.

Before bias correction can be performed, traditionally, remotely sensed estimates need to be verified against ground-based estimates. Validation and verification are done to assess the accuracy of remotely sensed rainfall estimates. If the verification suggests any doubt in the accuracy of the remotely sensed estimates, then the remotely sensed estimates should be adjusted to reduce the bias.

There are several statistics to verify remotely sensed rainfall and bias correction methods that are applicable to reduce the error of remotely sensed rainfall data in comparison with the gauged based rainfall estimates (Shrestha *et al.*, 2011; Fang *et al.*, 2014; Habib *et al.*, 2014b; Bhatti *et al.*, 2016; Mei *et al.*, 2016). Some of the bias correction techniques estimate the ratio between gauge and satellite estimates and multiply the ratio by the satellite estimates to arrive at the biased corrected rainfall estimate. Habib *et al.* (2014a) used a multiplicative bias factor, also termed the multiplicative shift technique, to correct the daily CMORPH estimates. Moulin *et al.* (2009) estimated and corrected uncertainties of mean areal precipitation by using a model that estimates error in simulated rainfall, and Yeh *et al.* (2020) calculated correlation coefficients between the gauged rainfall observation at the Taiwan Central Weather Bureau (CWB) and the Global Satellite Mapping of Precipitation (GSMaP) accumulated rainfall data using elevation models. After the elevation levels were determined, the rainfall data that was estimated by the GSMaP was compared with the actual rainfall data that was collected using the CWB stations. Accordingly, the systemic errors in the four types of elevation categorization were identified, and a regression equation was determined by fitting the curve in the GSMaP–CWB scatter plot to correct the GSMaP systemic errors. Essentially, the recommendations of the techniques that are used to verify and correct remotely sensed rainfall data from different

studies vary with RS products and study objectives. For example, Soriano *et al.* (2018) recommend using the quantile mapping polynomial bias correction method for precipitation. These sentiments were shared by many other studies (Ghimire *et al.*, 2019; Ayugi *et al.*, 2020; Katiraie-Boroujerdy *et al.*, 2020; Enayati *et al.*, 2021). However, Chen *et al.* (2013) argue that results from bias correction performance are location dependent and that careful validation should always be performed, especially on studies in new regions.

## **2.4 Chapter Summary**

Challenges associated with the decline of the gauged network of rainfall stations in South Africa and their implications on spatial rainfall estimations have been well documented in the literature. Many hydrological calculations require an estimation of catchment rainfall and traditionally point rainfall from raingauges is used. This highlights the need to invest in research into solutions to overcome the challenges associated with obtaining long records of quality rainfall data. The use of poor quality and inadequate rainfall data in hydrology may result in both social and economic consequences in resource planning and for the building of hydrological infrastructures such as dams and bridges.

Based on the literature reviewed, it is widely acknowledged that the accuracy of predictions from a hydrological model depends heavily on the quality and accuracy of the input rainfall data. Currently, the traditional way to estimate catchment rainfall for use in hydrological modelling utilises observed rainfall data from raingauges. Point rainfall estimated from raingauges is converted to spatially represent catchment rainfall. Point rainfall data are also used as input into many hydrological models to verify and calibrate satellite-based estimation of rainfall. However, the inaccuracy associated with deriving estimates of catchment rainfall from point rainfall at appropriate space and time scales has long been noted by several researchers as a major problem (Frezghi and Smithers, 2008; Haydon and Deletic, 2009; Arnaud *et al.*, 2011). Generally, the higher the number and density of raingauges within a catchment result in increased accuracy of the estimation of spatial catchment rainfall. Therefore, catchment rainfall estimated from a very sparse raingauge network is prone to bias.

South Africa and many other countries are experiencing a rapid decline in operational raingauge stations (Pegram *et al.*, 2016). This is an increasing challenge that raises questions related to the accuracy of catchment rainfall and catchment design rainfall. Accurate estimation of catchment rainfall requires that the estimations are derived from a dense gauge station network.

In addition, the decline of operating rain gauges in the past decades has become an issue even in hydrological modelling as most hydrological models require the input of point rainfall measurements from raingauges. This has resulted in a paradigm shift from using interpolation techniques to spatially represent point rainfall measurements for use in hydrological modelling to the use of remotely sensed rainfall data in hydrological modelling.

Even though RS has not been widely applied in South Africa, some studies (Sawunyama and Hughes, 2008; Maswanganye, 2018; Clark, 2019) have been conducted to gain confidence in the use of remotely sensed rainfall estimates to improve the spatial representation of rainfall estimates for use in hydrological modelling. Remotely sensed rainfall data are becoming more readily available and will eventually replace ground-based measurements and be used to recalibrate hydrological models that were calibrated using point gauged rainfall data unless the declining network of rain gauge stations is reversed. However, in the interim, RS measurements offer a way to complement ground-based measurements. Even so, RS data still require validation and, if there is bias in the estimations, bias correction is recommended before making meaningful estimations using RS data.

Concerning the issue of scale, rainfall data from raingauges are a better representation of the temporal scale while remotely sensed rainfall data provides a better representation of spatial variation of rainfall (Frezghi and Smithers, 2008). Therefore, it is necessary to assess the use of both in an attempt to represent both the temporal and spatial scales of rainfall data. For example, in the ACRU hydrological model, point rainfall from raingauges provides a good representation of temporal scale at daily time step and the values are adjusted to estimate catchment rainfall. In addition, the use of remotely sensed rainfall data could therefore potentially improve, replace, or be used alternatively to improve the spatial representation of rainfall that could be used to estimate catchment design rainfall. The result will be improved estimation of catchment design rainfall and enable estimation in ungauged catchments in South Africa.

When estimating catchment design rainfalls, different approaches are available to use such as estimating design rainfall at a point and using ARFs to convert the point design rainfall to catchment design rainfall. Other approaches adjust the point rainfall to represent the catchment rainfall and use the estimated catchment rainfall to estimate catchment design rainfalls such as by using the adjustment factors as done in the ACRU hydrological model. However, interpolation of multiple points observed rainfalls has traditionally been used to estimate catchment rainfalls which are later converted to catchment design rainfalls. The discussions

around the estimation of catchment design rainfalls require that regardless of the source of rainfall, rainfall data should be reviewed and checked for accuracy before using it and that considerable care should be taken to make sure that the rainfall data are sensible.

### 3. STUDY METHODOLOGY

This chapter provides details of the methodology followed to carry out this study. The general methodology followed is summarised in Figure 3.1 and the acronyms used to refer to the methods are included in bold text in brackets. Initially, a study pilot was conducted, and these results are documented in Chapter 4. A refined methodology was implemented in another catchment with some adjustments to the criteria used to select the catchment and rainfall stations based on the results that were obtained from the pilot study. The results for the additional catchment are presented and discussed in Chapter 5.

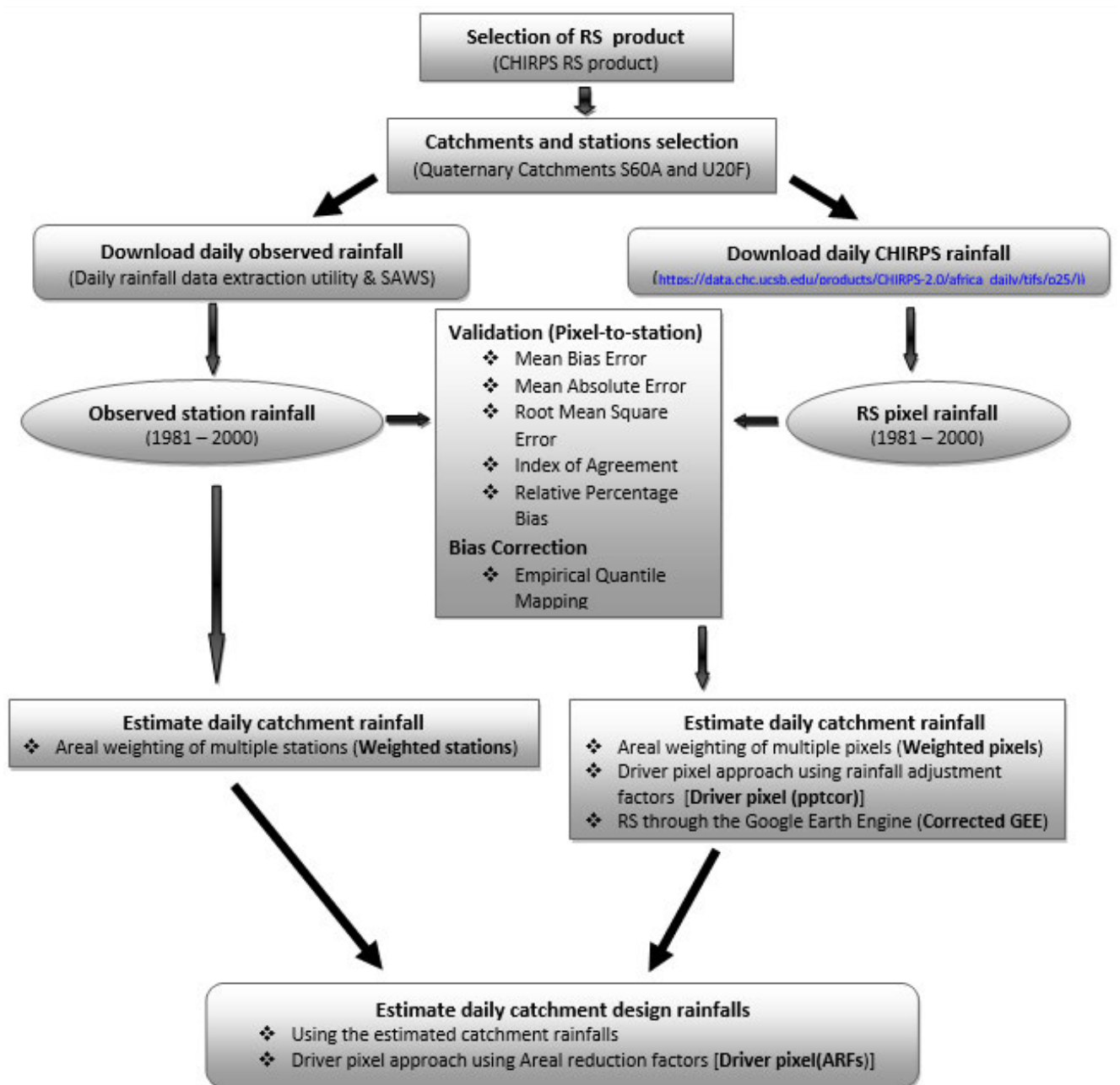


Figure 3.1: Summary of the study methodology

### 3.1 Catchments Selection

The catchments were selected from the South African quaternary catchments which can be accessed from the Department of Water and Sanitation (DWS) site (available from <https://www.dws.gov.za/iwqs/wms/data/000key2data.asp>). The selection for the pilot study was based on: (i) stations with the available selected full record length inside and around the catchment (1981-2010), and (ii) the density and spatial distribution of stations that have the selected record length. The selected record length was based on the availability of station data. With the above criteria, Quaternary Catchment S60A (Area = 328.34 km<sup>2</sup>) which is located in the Eastern Cape Province was selected for the pilot study, and the location is presented in Figure 3.2

After studying the results obtained from the pilot study catchment, the selection criteria were adjusted to select another catchment for further analysis. For the second catchment, the following additional criteria was added: (iii) catchments in different climatic regions. Catchment S60A is in a semi-arid area of Western Cape province. The second catchment selected is situated in Kwazulu-Natal province in the Mngeni Catchment in Quaternary Catchment U20F (Area = 458.99 km<sup>2</sup>). This area is in humid region of Kwazulu-Natal province. The location of Catchment U20F is shown in Figure 3.3.

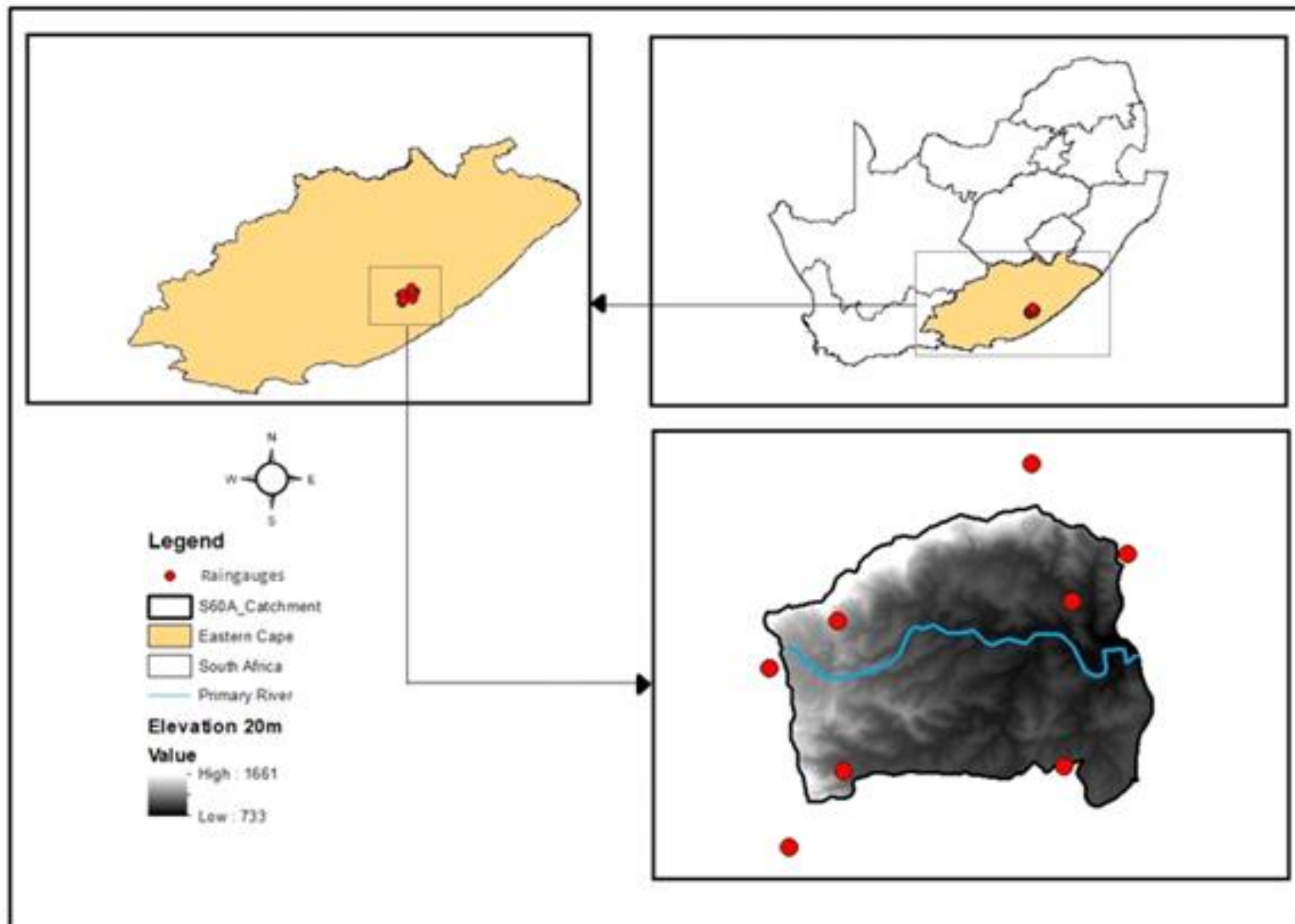


Figure 3.2: Catchment S60A

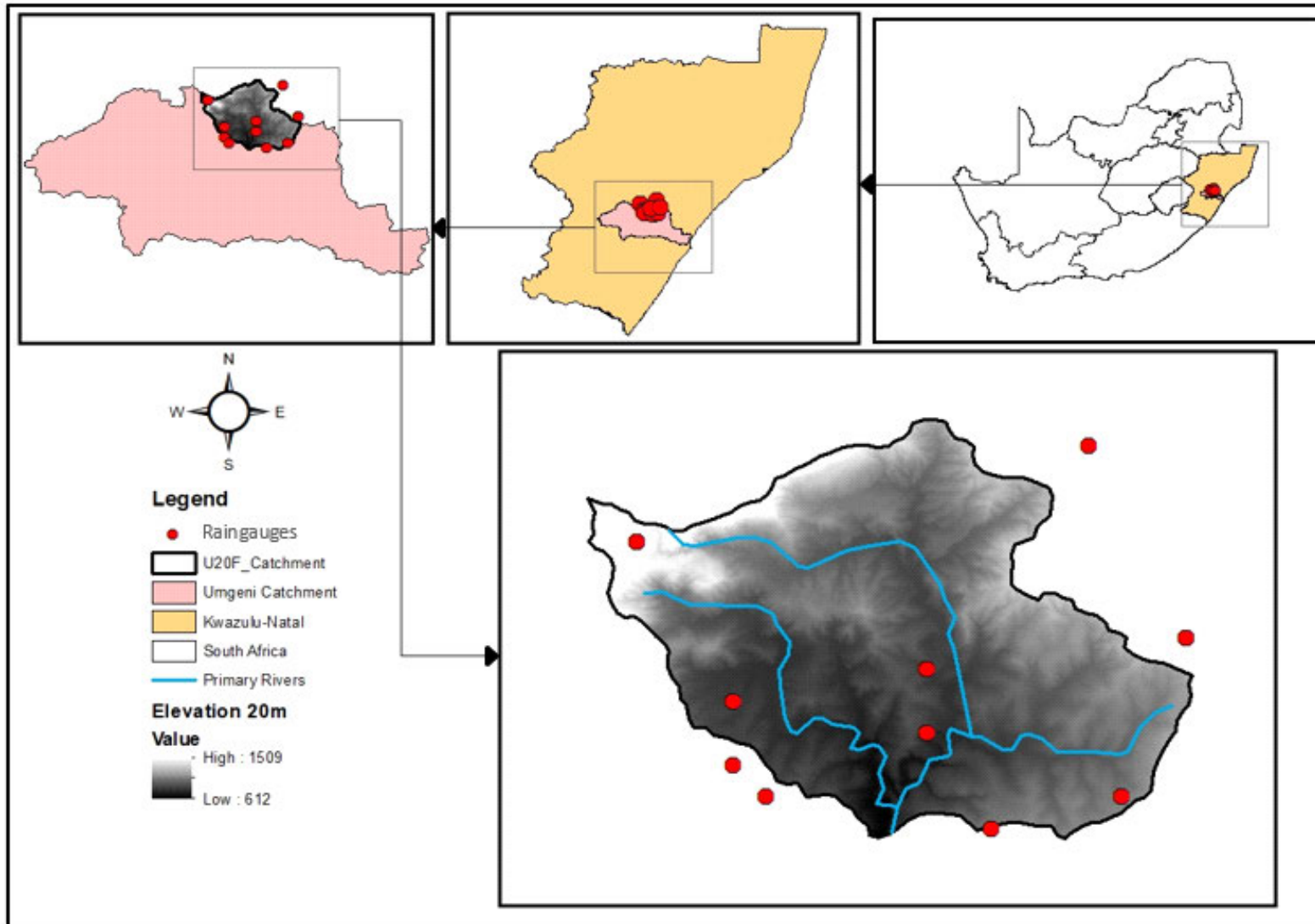


Figure 3.3: Catchment U20F



### 3.2 Rainfall Station Selection

Initially, both catchments had a more stations distribution. The daily observed data was available from the Lynch *et al.* (2004) database (1981 to 1999/2000) and additional data was requested from the South Africa Weather Services (SAWS) for the period from 2000 to 2010. The period of data was selected to be 1981-2010 for the station selection at Catchment S60A because both observed, and RS rainfall data were available for this period. However, after a careful review of the additional data available from SAWS, it was noticed that there were challenges with the station-based data beyond the year 2000 due to missing data, the unavailability of nearby stations to infill the missing data, and that many of the stations available from the Lynch database were not monitored by SAWS after 2000. Considering the project aims and objectives, the observed data ideally should not be missing and infilled to enable accurate comparisons. Therefore, the record period was adjusted to 1981-2000 so that long periods of infilled missing rainfall data could be avoided. After reviewing the actual rainfall dataset, it was noted that some stations had rainfall data up to the year 1999 while other stations had rainfall data up to the year 2000 in the Lynch database, therefore, even with the adjusted period length, SAWS data was used to supplement the Lynch data up to the year 2000. Rainfall stations were selected from both inside and surrounding catchment areas based on:

- (i) rainfall stations with record length covering 1981 to 2000,
- (ii) little or no missing data in the selected period length,
- (iii) high station data reliability,
- (iv) inclusion of stations outside the catchment boundary (within 3.5 km) for the construction of TP so that the TP completely overlays the catchment boundaries, and
- (v) stations that contribute to the total Thiessen weight of the catchment which was determined by using the TP (some stations were useful to completely overlay the TP over the catchment, but they had no contribution to the total catchment weights).

The selection of catchment and stations was done simultaneously by considering both the criteria for selecting a catchment and those for selecting stations. The same procedure was followed when selecting stations in the U20F Catchment. Details of the stations selected are summarised in Table 3.1 for Catchment S60A and Table 3.2 for Catchment U20F. It is important to note that the summarised statistics contained in the tables (except for the Thiessen weights) were obtained from the Lynch database and they apply for the available record length

of each station on the Lynch rainfall database and not the selected record length used in this study. The bold station in each table is the selected driver station of the catchment.

Table 3.1: Catchment S60A, selected raingauges, and selected driver station in bold text

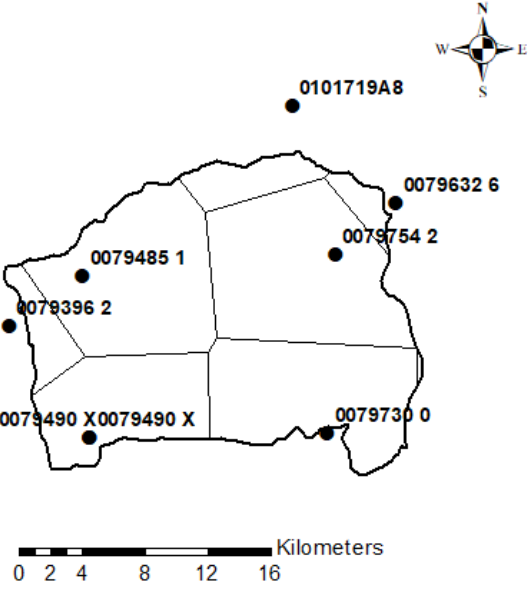
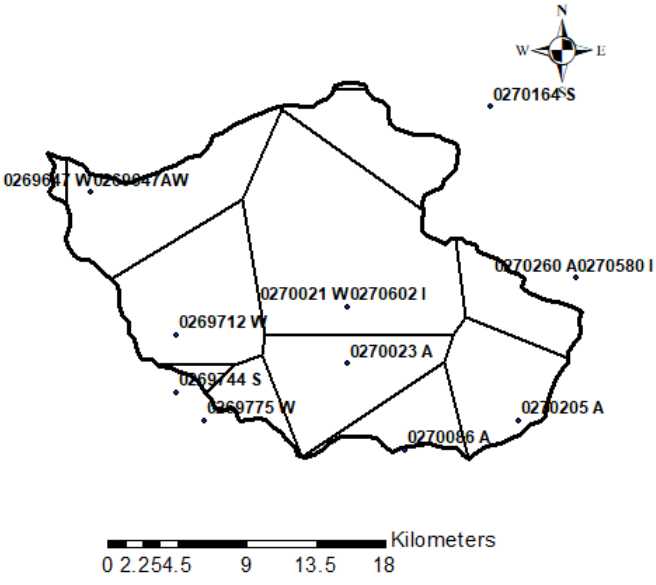
Catchment S60A (Area = 328.34 km <sup>2</sup> )							
	Station Number	Missing days	Infilled (%)	Reliable (%)	Thiessen weights (%)	MAP (mm)	Altitude (m)
	0101719A8	0.0	85.4	14.6	0.05	726	1102
	0079632 6	0.1	8.3	91.7	0.02	935	1102
	0079754 2	0.0	6.5	39.5	0.27	681	799
	0079730 0	0.1	29.5	70.4	0.22	903	829
	0079490 X	0.0	11.7	88.3	0.16	990	947
	0079396 2	0.0	19.9	80.1	0.04	809	905
	<b>0079485 1</b>	<b>0.1</b>	<b>26.2</b>	<b>73.7</b>	<b>0.24</b>	<b>920</b>	<b>952</b>

Table 3.2: Catchment U20F, selected raingauges, and selected driver station in bold text

Catchment S60A (Area = 458.99 km <sup>2</sup> )							
	Station Number	Missed (%)	Infilled (%)	Reliable (%)	Thiessen weight (%)	MAP (mm)	Altitude (m)
	0270260A	1.1	77.2	21.7	0.06	736	981
	0270205A	1.9	78.9	19.2	0.09	772	912
	0270086A	43.3	50.7	6	0.05	934	903
	0270023A	1.4	77.2	21.4	0.11	954	723
	<b>0270021W</b>	<b>16.3</b>	<b>43.7</b>	<b>40</b>	<b>0.29</b>	<b>808</b>	<b>767</b>
	0270164S	1.8	71	27.2	0.08	851	1084
	0269647W	70.4	0	29.6	0.14	1259	1288
	0269712W	23.2	57.3	19.4	0.14	1101	767
	0269744S	22.6	31	46.6	0.01	907	789
	0269775W	23.2	57	19.8	0.03	749	697

### 3.3 Remote Sensing Product Selection

The application of the methodology was continued by selecting a suitable rainfall RS product. A number of criteria were developed to select suitable RS products to use in the study. These are presented in Table 3.3. In Table 3.4, each RS product reviewed in Section 2.2.2 is compared against the criteria. The preferred requirement for each criterion is indicated in brackets and “Yes” indicates that the product meets the required criteria while blank indicates that it does not. Based on a careful review of the RS products, consideration of the criteria, and the comparison of the criteria against the RS products reviewed, the CHIRPS product was selected as the best product. The CHIRPS RS rainfall product is available in daily temporal resolution and has a record length of 41 years starting from 1981 to present, it is a widely used RS product with free and unlimited access to the dataset. It is a bias-corrected product with good reviews reported in the literature (references for CHIRPS rainfall data are available in Table 2.1) in terms of performance and reliability.

There is, however, uncertainty with the daily time period used in the development of the CHIRPS dataset, i.e. 08:00 – 08:00 or 00:00 - 00:00. The uncertainty was because the stations that were used to develop the CHIRPS rainfall dataset were from different regions that use different local time 24-h periods in their daily rainfall data. This is supported by the response from one of the developers Pete (2021), who responded that “a number of different sources were used and none of which record their start and end times for a day, and because of this reason, the exact estimate of the day's precipitation is the best guess”. CHIRPS daily rainfall was available in Tag Image File Format (TIFF) and was obtained from the CHIRPS website ([https://data.chc.ucsb.edu/products/CHIRPS-2.0/africa\\_daily/tifs/p25/](https://data.chc.ucsb.edu/products/CHIRPS-2.0/africa_daily/tifs/p25/)) and extracted using the Google Earth Engine (GEE).

Table 3.3: Criteria used to select the RS product.

<b>Criterion</b>	<b>Explanation</b>
Temporal resolution	A product suitable to estimate daily values was targeted for the estimation of catchment rainfall on a daily scale. Design rainfalls were estimated at a 1-day duration for up to 20 year return periods.
Record length	Gericke (2018b) stated that longer records of rainfall increase the reliability of design rainfall, and generally, record lengths that are less than 10 years are not acceptable for design rainfall estimation. Therefore, to increase the reliability of design rainfall estimation, a product with rainfall record lengths of up to 20 years was selected.
Spatial resolution	The study areas selected are quaternary catchments that have catchment areas >500km <sup>2</sup> , therefore a product with a fine spatial resolution was targeted for more accurate results.
Spatial coverage	Since the study is based in South Africa, RS product that has good spatial coverage of South Africa was considered to increase the reliability of results.
Data availability and reliability	Readily available data with free access and free use was the ideal selection for this study. Further, data from the frequently updated product were prioritised.
Bias correction	Bias correction of remotely sensed data is recommended before they can be used for hydrological applications. This study targeted a product that has been bias corrected. However, the performance of the selected RS product will be evaluated and, if necessary, bias corrected for the selected local catchments.
Performance and accuracy	An RS product that has reported high performance and accuracy in areas with characteristics similar to the selected study areas was prioritised. This was done with the acknowledgment that RS products can perform differently even on catchments with similar characteristics.

Table 3.4: Criterion used to select the RS product against the RS products reviewed.

Criteria	TRMM	GMP	GPCP	TAMSAT	CMORPH	FEWS NET	CRU TS	ERA-Interim	ERA5	CHIRPS	GPCC	PERSIANN
<b>Temporal Resolution (daily)</b>	Yes	Yes	Yes	Yes	Yes	Yes		Yes	Yes	Yes	Yes	Yes
<b>Record length up to the year 2000 (&gt;10 Years)</b>				Yes			Yes	Yes	Yes	Yes	Yes	Yes
<b>Spatial resolution (Fine) :</b> Fine $\leq 0.25^\circ$ Medium $0.26^\circ - 0.5^\circ$ Coarse $> 0.5^\circ$	Yes	Yes			Yes	Yes				Yes		Yes
<b>Spatial Coverage (South Africa)</b>	Yes	Yes	Yes	Yes	Yes	Yes	Yes	Yes	Yes	Yes	Yes	Yes
<b>Data Availability (Free access)</b>	Yes	Yes	Yes	Yes	Yes	Yes		Yes	Yes	Yes		Yes
<b>Data reliability (Frequently updated)</b>		Yes	Yes	Yes	Yes	Yes	Yes		Yes	Yes	Yes	Yes
<b>Bias Correction (Not required)</b>	Yes	Yes	Yes			Yes		Yes		Yes	Yes	
<b>Daily Time Step (08:00 – 08:00)</b>												

### 3.4 Extraction and Processing of Remote Sensing Rainfall Data

The extraction and processing of the CHIRPS raster pixels were firstly done using ArcMap software, then using a coded script in python software, and finally using the GEE software and a coded script. The details of the process followed using the software are detailed below.

#### 3.4.1 Using ArcMap

The CHIRPS rainfall dataset was initially processed using ArcMap in ArcGIS. Considering that each raster image (band) represented one day of rainfall, and the amount of data that needed to be processed (1981 to 2000), it was not feasible to continue to use ArcMap to process the CHIRPS rainfall data for the selected period length. ArcMap based processing is valuable and recommended for processing short record lengths such as a day, week, a month, and up to one year. It can also be used when processing RS data for monthly and annual scales because it requires a considerable amount of time, faster network connectivity, and a very large computer Random Access Memory (RAM) space. Thus, ArcMap was used in this study to develop the concepts to be included when processing the rainfall dataset using the coded scripts. The steps followed for the processing are presented below:

- (a) In ArcMap, catchment shapefiles and CHIRPS TIFF files were added using the *Add* feature (in this study, TIFF files were added one month per run).
- (b) The catchment area was clipped from TIFF files and all selected stations using the *Clip Analysis Tool* that is found in the *ArcToolbox* to work with a smaller volume of data and for faster processing.
- (c) Each band from  $0.025^\circ$  (CHIRPS resolution) was resampled to  $0.00025^\circ$  to generate a finer resolution so that each raster pixel is more representative of a point rainfall. This was done using the *Resample Data Management tool* which is found in the *ArcToolbox*.
- (d) Each of the resampled bands was converted to raster points using the *Raster to Points Conversation Tool* which is found in *ArcToolbox*.
- (e) Using the *Identify tab*, the value of the raster points closest to all the selected rainfall stations were extracted using the *Grind Values* (also called pixel values) for each raster TIFF file.

### **3.4.2 Using Python**

Python Spyder Version 3.8 (Raybaut, 2009) was used to process the CHIRPS rainfall dataset. Two scripts were developed. The first script was used to simultaneously extract data from multiple stations by using the Geopandas as the main library and adjustments were made for different stations' shapefiles. The Python libraries and packages that were used included the following:

- (i) Geopandas - combines the capabilities of the data analysis library Pandas with other packages for managing spatial data
- (ii) Pandas - an open source Python package that is most widely used for data science or data analysis and machine learning tasks,
- (iii) OS - used to read contents, change, and identify the current directory,
- (iv) Rasterio (a module for raster processing that you can use for reading and writing several different raster formats in Python),
- (v) Scipy. sparse -provides tools for creating sparse matrices using multiple data structures, as well as tools for converting a dense matrix to a sparse matrix, and
- (vi) Numpy - works together with pandas to provide support for multi-dimensional arrays

The detailed use of the libraries used is described in Wasser et al. (2019). The full script that was used in this study is found in Appendix A. Another separate script was created to extract data from a single station where there are missing values because the first script could not read some of the raster images, and adjustments were made for each station. The second script is in Appendix B.

### **3.4.3 Using Google Earth Engine to extract point pixel values**

The importance of resampling remotely sensed raster data is detailed by Baboo and Devi (2010). The CHIRPS raster dataset has a spatial resolution of 0.25° which is coarse compared to the catchment areas and the distribution of stations and it was noted that frequently more than one rainfall station is contained within a single raster pixel. To avoid such instances, resampling and interpolation were adopted using another script in GEE. Similarly, to the use of Python, a coded script was developed for use in GEE to resample and interpolate the raster pixels so that each value extracted from a raster pixel has a smaller footprint over the raingauge site. The observed rainfall stations selected for the study were added as shapefiles to GEE and used as a guide to extract the pixel rainfall values corresponding to each of the selected stations.

The resampling performed was from 0.25° spatial resolution (27750 m) to 0.0045° spatial resolution (approximately 500 m). The resampling to a resolution of 500 m was to ensure that the resampled raster pixels are finer and still represent good coverage within the catchment to maintain the good spatial estimates from the RS product. The sensitivity of the resolution of the resampling was assessed and it was observed that there was no significant difference in the values extracted using both 0.0025° and 0.0045° resolutions. The interpolation technique that was applied is bilinear. Bilinear interpolation is an extension used for interpolating functions of two variables on a rectilinear two-dimensional (2D) grid by using linear interpolation, first in one direction, and then again in a 90° direction. The outcome was resampled and interpolated raster pixels values which had a resolution of 0.0045°. The GEE code used in the study is documented in Appendix C.

#### **3.4.4 Using Google Earth Engine to extract mean catchment rainfall**

After the extraction of point raster values, RS was used to estimate the mean rainfall directly from the selected catchment. This was carried out using code in GEE. For this purpose, catchment shapefiles were added to GEE. The code was used to specify the RS rainfall product, catchment shapefiles, product band, variable to be downloaded, units of the variable, the time step of the variable, and to extract the mean areal rainfall for Catchments S60A and U20F. The code extracts and averages rainfall within the catchment boundaries. This method of estimating mean catchment rainfall is better than using the scripts because there are fewer individual calculations to be done. The details of the code are specified in Appendix D.

#### **3.5 Performance of RS Data**

Validation between the observed station and RS data was done on a pixel to station basis. Each pixel value was validated using the corresponding station rainfall. The statistics that were used for validating remotely sensed pixel values are the Mean Bias Error (MBE), Root Mean Square Error (RMSE), Mean Absolute Error (MAE), Index of Agreement (D), and Relative Bias Percentage Bias (%BIAS). The statistics were estimated using the Agricultural and Meteorological software which was developed by Jinghao *et al.* (2009). The agricultural and meteorological software is software that is used to automatically calculate statistics for two sets of a dataset. The equations that were used to estimate the values of the selected statistics are presented below:



- (i) Mean Bias Error (MBE) is primarily used to estimate the average bias in the model and captures the average bias in the prediction. A positive bias or error in a variable (such as speed) means that the data from the datasets are overestimated and vice versa.

$$\text{MBE} = \frac{1}{n} \sum_{i=1}^n (P_i - O_i) \quad (3.1)$$

where

$P_i$  = RS rainfall for day =  $i$  (mm),

$O_i$  = observed rainfall for day =  $i$  (mm), and

$n$  = number of observations.

- (ii) Root Mean Square Error (RMSE) is used to measure of the sum of difference between values predicted by a model and the observed values. These individual differences are also called residuals, and the RMSE serves to aggregate them into a single measure of predictive power.

$$\text{RMSE} = \sqrt{\frac{\sum_{i=1}^n (O_i - P_i)^2}{n}} \quad (3.2)$$

- (iii) Mean Absolute Error (MAE) is simply, as the name suggests, the mean of the absolute errors. For continuous variables, MAE represents the expected average error. The MAE and the RMSE can range from 0 to  $\infty$  and are indifferent to the direction of errors.

$$\text{MAE} = \frac{1}{n} \sum_{i=1}^n (|O_i - P_i|) \quad (3.3)$$

- (iv) Index of Agreement (D) is a standardized measure of the degree of model prediction error which varies between 0 and 1.  $D = 1$  indicates a perfect match, and  $D = 0$  indicates no agreement at all.

$$D = 1 - \frac{\sum_{i=1}^n (O_i - P_i)^2}{\sum_{i=1}^n (|O_i - \bar{O}| + |O_i - \bar{P}|)^2} \quad 0 \leq D \leq 1 \quad (3.4)$$

where

O = average observation values.

- (v) Relative Bias in Percentage (%BIAS) - The relative bias provides a measure of the magnitude of the bias in percentage. Sometime the bias is expressed in relative terms (relative bias) making it possible to evaluate the size of the bias with respect to the true unknown parameter to estimate. This value is multiplied by 100 if one need relative bias in percentage.

$$\%BIAS = \frac{\sum_{i=1}^n (P_i - O_i)}{\sum_{i=1}^n O_i} \times 100 \quad (3.5)$$

### 3.6 Bias Correction

After verification of RS pixel rainfall using station rainfall, bias correction was performed. The technique that was used for bias correction was the Empirical Quantile Mapping (EQM) method. Details of the EQM method to correct bias in rainfall are included in Ghimire *et al.* (2019). EQM works by adjusting daily precipitation in a form of multiplicative factor using an observed and simulated rainfall as shown in Equation 3.7. The estimated correction factor is multiplied by the corresponding RS rainfall for each day. An example of calculations is shown in Table E.1 in Appendix E. In the Table E.1, dayObs and daySim (RS) are the day number in the original time series. To estimate the percentiles, Equation 3.6 was used.

$$\text{Percentile} = \frac{\text{Rank}}{n+1} 100 \quad (3.6)$$

where

Rank = rank of a numeric value when compared to a list of other numeric values  
and

n = total number in series

$$\text{Correction factor} = \frac{\text{Observed rainfall (mm)}}{\text{RS rainfall (mm)}} \quad (3.7)$$

where

Observed rainfall = rainfall from the stations (mm) and

RS rainfall = rainfall from CHIRPS product (mm)

### 3.7 Estimation of Daily Catchment Rainfall

This section documents the methodology followed to estimate the catchment rainfalls. To achieve this, catchment rainfall was estimated using both the observed station rainfall and remotely sensed CHIRPS rainfall data.

#### 3.7.1 Using observed rainfall: Weighted stations

In the Weighted Stations approach, the observed rainfall data from the selected rainfall stations were used. Using the spatial distribution of the selected stations, Thiessen polygons were constructed, and the areal weights of each station were estimated. Example of Thiessen polygons that were constructed for Catchment S60A in ArcMap is presented in Figure 3.4.

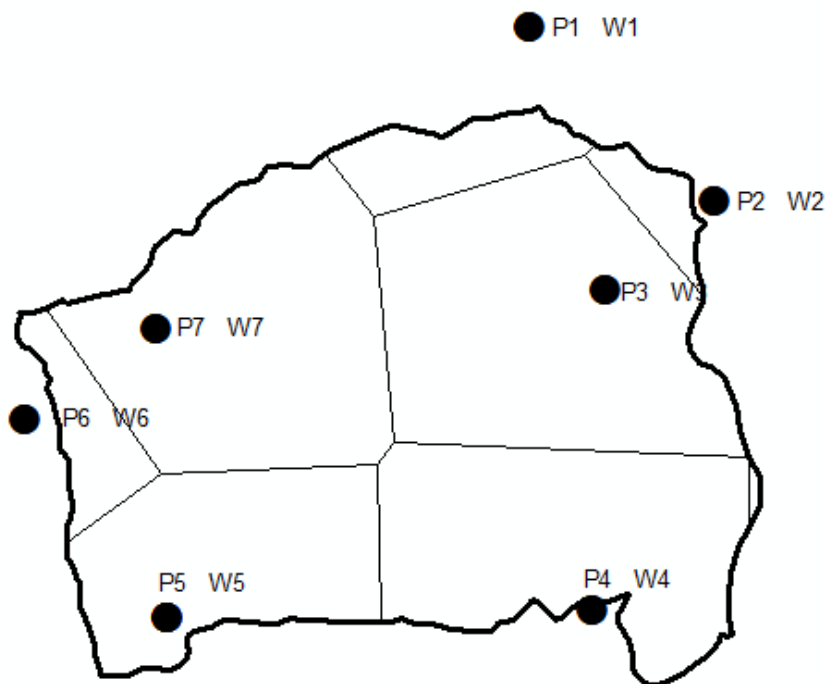


Figure 3.4: Example of Thiessen polygons constructed ArcMap

To estimate the areal weights, Equation 2.2 as detailed in Section 2.2.1.1 was used. The calculated areal weights for each station are used to calculate the contribution from each station to catchment rainfall for each time step. Using Equation 3.8, the weighted point observed

rainfalls were summed together to estimate the average catchment rainfall. An example of the portion of calculations is shown in the spreadsheet found in Appendix E Table E.2.

$$P_{ave} = \sum_{i=1}^n P_i \times W_i \quad (3.8)$$

where

$P_{ave}$  = weighted observed catchment rainfall (mm),

$n$  = number of observations,

$P_i$  = point observed rainfall for day =  $i$  (mm), and

$W_i$  = Thiessen weight for day =  $i$ .

### 3.7.2 Using remotely sensed rainfall

The RS pixel rainfall values that were extracted using code as described in Section 3.4.3 and bias corrected as described in Section 3.6 were used to estimate catchment rainfalls.

#### 3.7.2.1 Weighted pixels

Similar to area weighting the observed station rainfall data to estimate catchment rainfall, the bias corrected RS pixel values corresponding to the station location were used to estimate the average catchment rainfall using the same areal weights that were estimated using Equation 2.2. The reason for using selected pixels within the catchment and not all the pixels was because of the need to use observed rainfall data to bias correct the remotely sensed rainfall data before they could be used to derive meaningful estimations. The pixels were selected based on the location of the corresponding raingauges. The equation for estimating the averaged catchment rainfall from the pixel values was adjusted from Equation 3.8 and is presented in Equation 3.9. This method was used with observed data in the DWS (2014) report.

$$P_{ave\_x} = \sum_{x=1}^n P_x \times W_x \quad (3.9)$$

where

$P_{ave\_x}$  = averaged RS rainfall (mm),

- $n$  = number of observations,
- $P_x$  = point pixel rainfall for day =  $x$  (mm), and
- $W_x$  = Thiessen weight for day =  $x$ .

### 3.7.2.2 Driver pixel (pptcor)

Based on the criteria in

Table 3.1 and Table 3.2, driver stations were selected for each catchment. In the Driver Pixel (pptcor) approach, the data from the RS pixel located at the driver station is adjusted to represent the catchment rainfall. Traditionally, this approach is used with the observed data in the ACRU model. Hence in this study, the Driver pixel (pptcor) approach adopted the steps that are used when estimating catchment rainfall in the ACRU hydrological model using the driver station. To do this, the monthly median bias corrected pixel rainfall values were calculated using a pivot table in Excel. The monthly median catchment rainfall was estimated using the zonal statistics calculated in ArcMap from the gridded median monthly rainfall surfaces that were developed by Lynch *et al.* (2004). The rainfall adjustment factors were then calculated using Equation 3.10 which was adjusted from Equation 2.1 for the estimation of pixel rainfall adjustment factors. The calculated adjustment factors were multiplied by the daily pixel values for the corresponding month to derive the average catchment rainfall values. The results of the estimation of median rainfalls are presented in Appendix E Table E.3 for Catchment S60A and Table E.4 for Catchment U20F.

$$\text{pptcor} = \frac{\text{CatchmentMMR}}{\text{PixelMMR}} \quad (3.10)$$

where

- $\text{pptcor}$  = Precipitation Correction factors/ Rainfall adjustment factors,
- $\text{CatchmentMMR}$  = Catchment Median Monthly Rainfall, and
- $\text{PixelMMR}$  = Median Monthly Rainfall.

### 3.7.2.3 Corrected GEE

The RS data was used to spatially estimate catchment rainfall directly for the catchment by running code in GEE as described in Section 3.4.4. The catchment rainfall estimated using GEE was bias corrected to remove any bias in the RS pixel data. This section details a method to correct the RS catchment rainfall that was obtained from using the GEE software of any bias.

The assumption made was that the average bias in the estimated RS catchment rainfall is equal to the area weighted bias at the pixels at the raingauges which contribute to the catchment rainfall. However, bias could only be computed at pixels corresponding to stations, and therefore the catchment bias correction was based on those selected pixels. The bias correction factors obtained from using the quantile mapping method for each pixel corresponding to the selected station were used to correct the mean catchment rainfall estimated using the GEE software. The method adopted was through the use of Thiessen weights that were estimated for each station. The Thiessen weights of the selected stations are the same as those of the corresponding pixels. For this purpose, Pixel Weights (PW) that were previously estimated using the Thiessen polygons were used to multiply the calculated pixel-to-station bias correction factor (PC) for the bias correction factor that was estimated in each pixel. Equation 3.11 was used for this purpose and the sum of the multiplied values is the weighted catchment bias. The weighted catchment bias results were multiplied by the GEE catchment rainfall values to obtain the bias corrected GEE-based catchment rainfall as shown in Equation 3.12.

$$C_w = \sum_{i=1}^n PW_i \times PC_i \quad (3.11)$$

where

$C_w$  = daily weighted catchment bias correction factors,

$PW_i$  = assigned pixel Thiessen weight determined using corresponding station for day =  $i$ ,

$PC_i$  = pixel correction factor for day =  $i$ , and

$n$  = number of values.

$$\text{Corrected GEE} = C_w \times \text{GEE} \quad (3.12)$$

where

Corrected GEE = bias corrected catchment rainfall estimated using GEE,

$C_w$  = Daily weighted catchment bias correction factors, and

GEE = Catchment rainfall estimated using Google Earth Engine.

### 3.8 Estimation of Catchment 1-Day Design Rainfall

Catchment design rainfalls were estimated using the catchment rainfalls that were estimated using the methodologies that are detailed in Sections 3.6 and 3.7. The approaches that were used to estimate catchment rainfalls are: (i) areal weighting of multiple rainfall stations (Weighted stations), (ii) Areal weighting of multiple pixel rainfalls (Weighted pixels), (iii) the driver pixel using an adjustment factor (pptcor), and (iv) using RS through Google Earth Engine (Corrected GEE).

Another method that was used to estimate catchment design rainfalls was through the use of ARFs [Driver pixel(ARFs)]. In this approach, the bias corrected driver pixel values were used to estimate design rainfall at a point. To convert the point design rainfall to catchment design rainfall, ARFs were used. In practice, ARFs is used with the driver station to estimate catchment design rainfalls by either multiplying point catchment rainfall with ARFs and use the estimated catchment rainfall to estimate catchment design rainfall or by multiplying ARFs with the estimated point design rainfall. In this study, the same approach was adopted using the driver pixel to estimate catchment design rainfall by multiplying point catchment rainfall from a single pixel by ARFs.

The driver pixel used is the same as used in Section 3.7.2.2. The equation that was used for the estimation of ARFs is Equation 2.6. This equation uses one variable to estimate ARFs which is the catchment area. To convert the ARFs to a percentage value, Equation 3.13 is used.

$$\%ARF = \frac{ARF}{100} \quad 3.13$$

where

$\%ARF$  = areal reduction factors in percentage and

$ARF$  = areal reduction factors.

To estimate catchment design rainfalls using the estimated catchment rainfall estimated by the various methods, code in R-Software was used to fit the Generalised Extreme Value distribution (GEV) to the Annual Maximum Series (AMS) of the catchment rainfall data using L-moments (Smithers *et al.*, 2018). This code is presented in Appendix F. Given the limited length of record 20 years used in the analysis, the catchment design rainfall values were only estimated up to a return period of 20 years.

## 4. APPLICATION TO CATCHMENT S60A: PILOT STUDY

This chapter contains the results and discussion of the study methodology in a pilot study and includes the validation and bias correction, sensitivity analysis, and the estimation of design rainfalls. The summary of comparisons of catchment rainfall done are:

- (i) Areal weighted pixel rainfall (Weighted pixels) against the areal weighted observed daily rainfall method (Weighted stations).
- (ii) Driver pixel using rainfall adjustment factors [Driver pixel(pptcor)] against the areal weighted observed daily rainfall method (Weighted stations),
- (iii) Estimated catchment rainfall using RS through Google Earth Engine (Corrected GEE) against areal weighted observed daily rainfall (Weighted stations), and
- (iv) Driver pixel using ARFs [Driver pixel(ARFs)] against the areal weighted of observed daily rainfall method (Weighted stations) for the estimation of catchment design rainfall.

In the assessments, the Weighted stations approach is assumed to be the best estimate of daily catchment rainfalls and catchment 1-day design rainfalls.

### 4.1 Assessment of the performance and bias correction

Different statistics were used to investigate the performance of the point-to-pixel bias correction technique applied. These statistics were derived from verifying remotely sensed data using observed rainfall from raingauges and the statistics results are summarised in Table G.1, Table G.2, and Table G 3 in Appendix G. The performance of the bias correction was assessed on different temporal scales namely daily, monthly, and annually and are presented in Figure 4.1, Figure 4.2, and Figure 4.3 respectively. In Table 4.1 Both the tables and figures, MBE, RMSE, MAE, D, and %BIAS were used as verification statistics, and RAW is the original RS CHIRPS data and CORRECTED is the RS CHIRPS data after it was bias corrected.

At a daily time scale, more than 50% of the bias in remotely sensed rainfall was reduced even though there was still bias in the dataset. The presence of bias after bias correction is supported by a low value of D that was ranging from 0.31 for station 0079754 2 to 0.43 for station 0079730 0. At a monthly time scale, up to 80% bias was removed in all stations, and D values improved



from a minimum of 0.87 to a maximum of 0.93. The estimated error in values and bias that was high on a daily time scale was also reduced. At the annual scale, the error was reduced, and the bias was improved, however, D between the observed and the remotely sensed rainfall values was compromised. Generally, the bias correction method performed better on a monthly time scale.

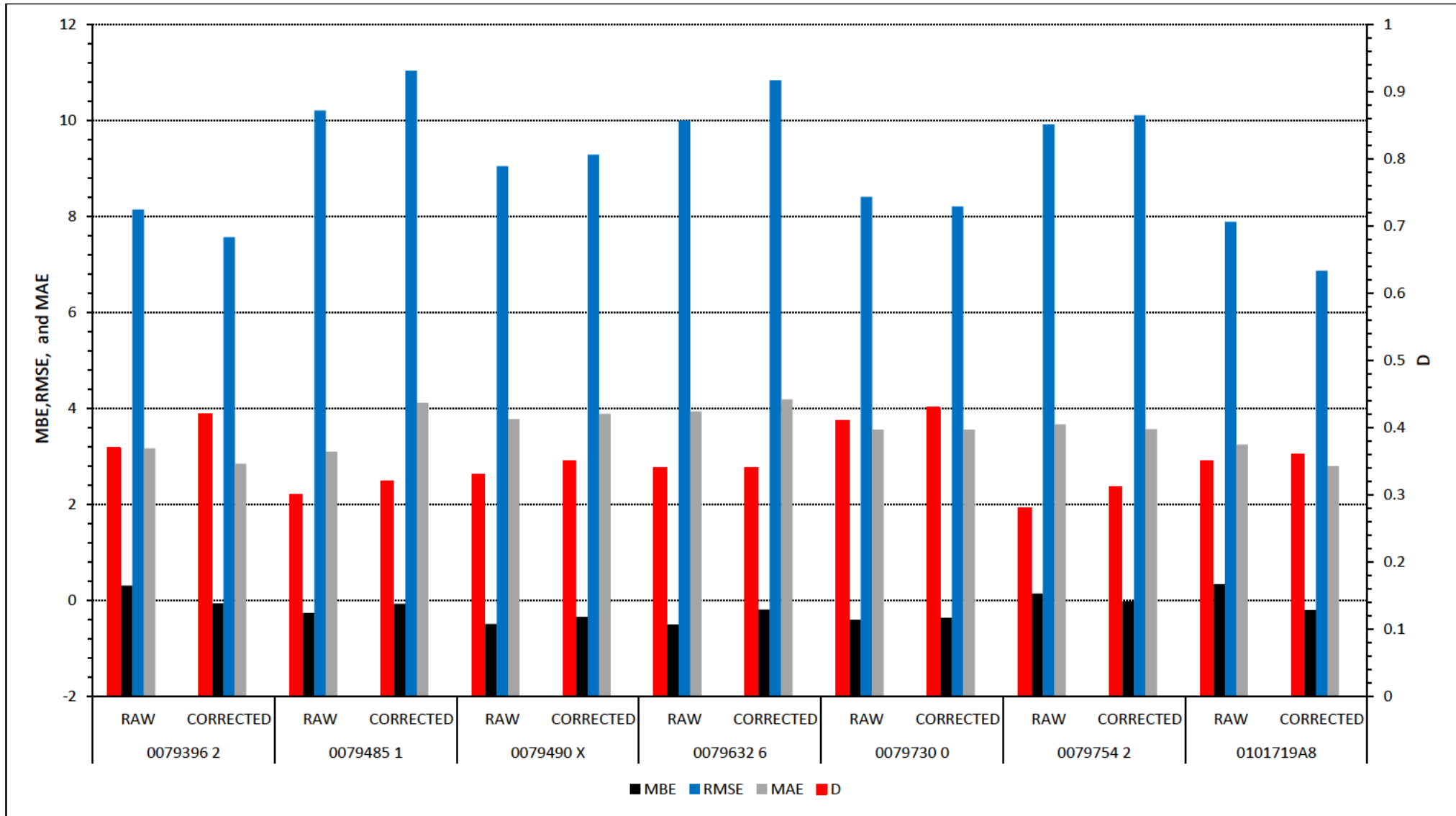


Figure 4.1: Validation statistics for bias correction at a daily scale

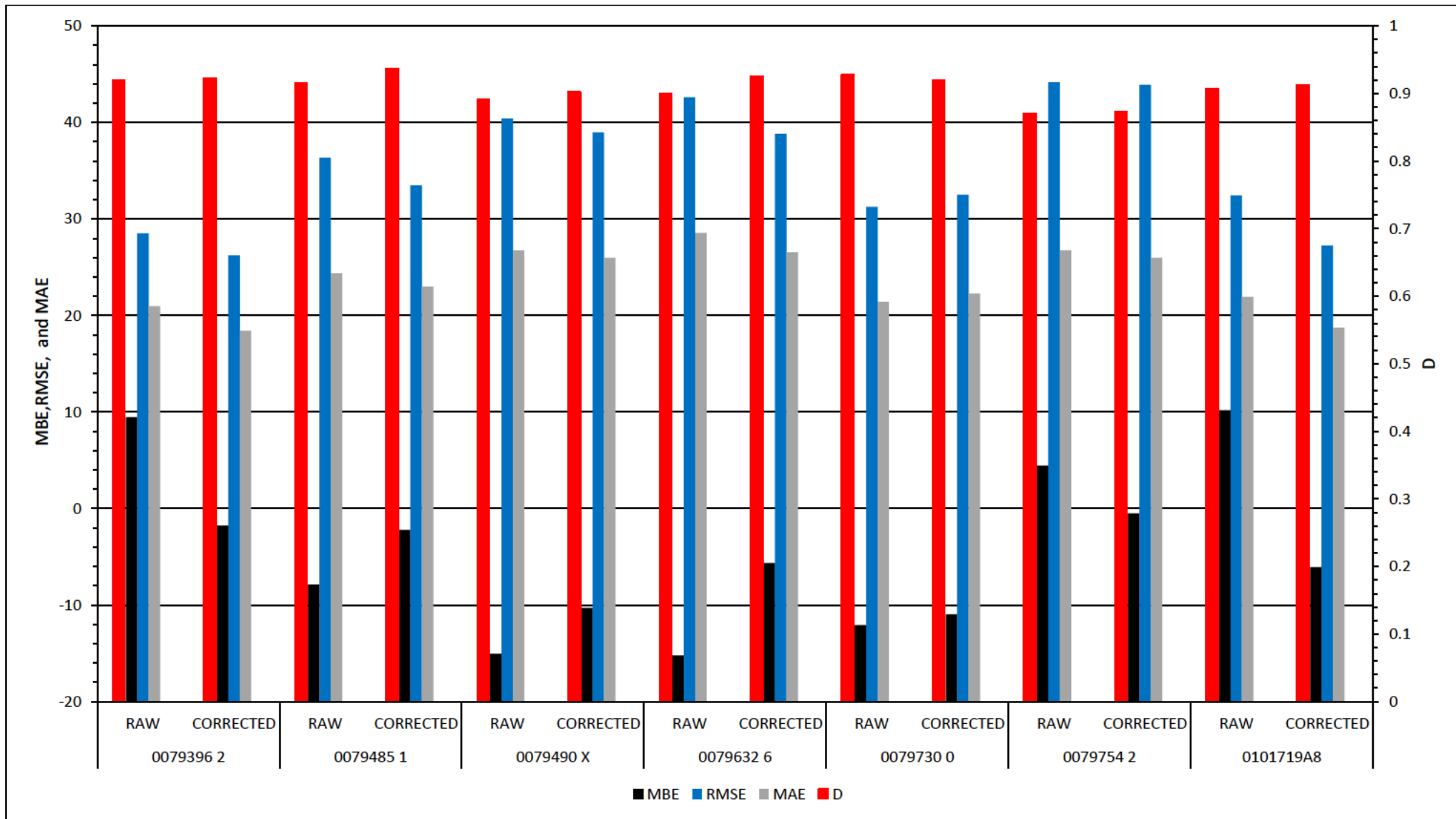


Figure 4.2: Validation statistics for bias correction at a monthly scale

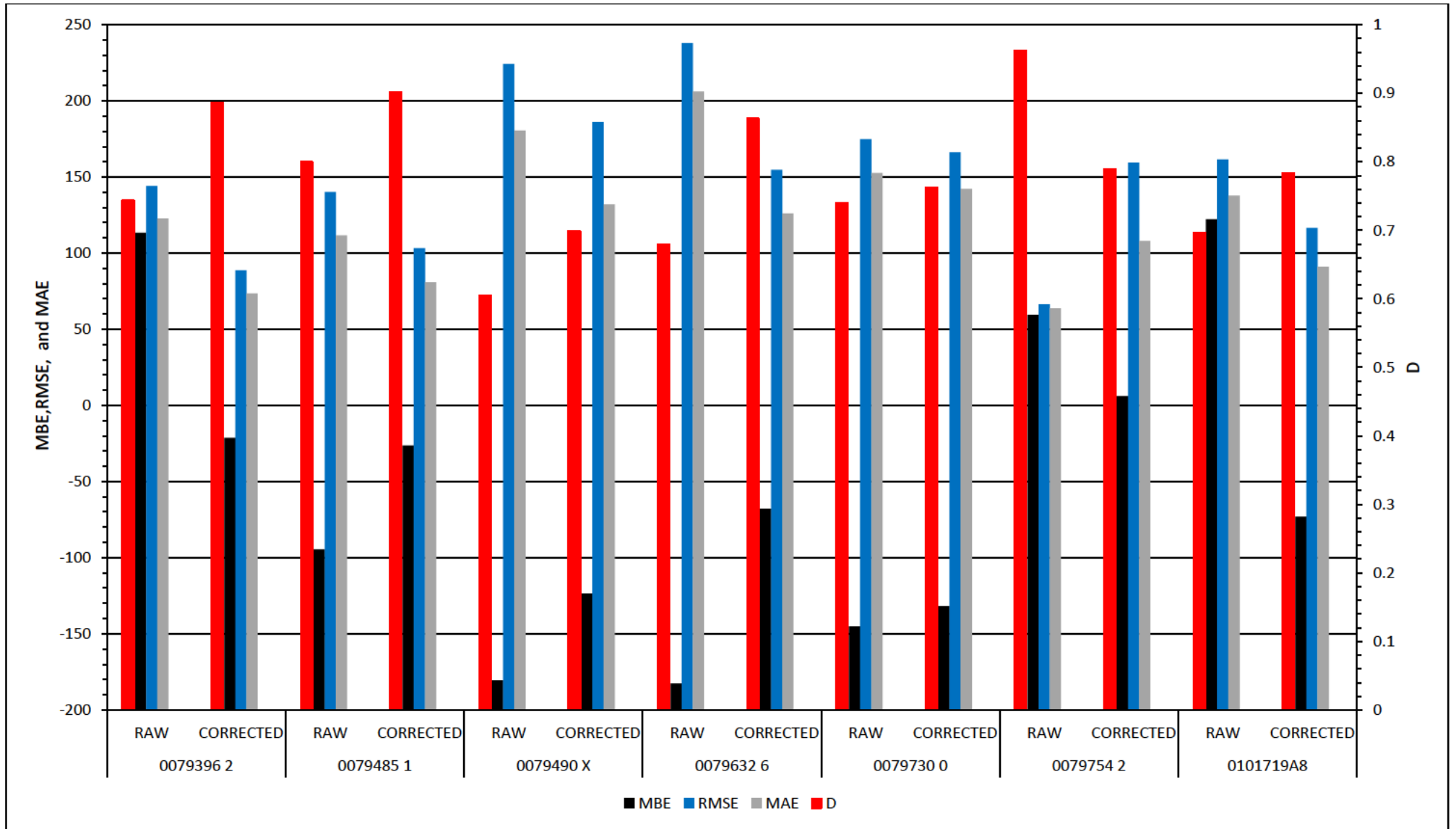


Figure 4.3: Validation statistics for bias correction at an annual scale

Based on the statistics presented in Figure 4.1- Figure 4.3, MBE difference values for each station were calculated and is presented in Table 4.1. Accordingly, the scatter plots in Figure 4.4 were developed which present the comparison of the raw rainfall data and the bias corrected rainfall against the observed rainfall at the station with the best and worst performance. The performance was assessed based on how much bias was reduced after the application of bias correction factors to the pixel values. In Figure 4.4, the legend at the bottom of the graphs represents all the graphs. For reference,  $R^2$  determines how well the RS data fits the observation data and the slope indicates the general performance. Each graph has the calculated statistics displayed.

Considering both the graphs and the statistics, Station 0079730 0 has been identified as the best performing station and Station 0101719A8 as the worst performing station based on the amount of bias that was reduced in at all time scales. The assessment between different scales also shows that quantile mapping for the bias correction of CHIRPS rainfall performs well at a monthly scale. This is because all stations had their bias reduced by a large amount at this time scale. Overall, as seen in Figure 4.4 , there is not much difference between the  $R^2$  and slope value between the best and poor performing stations before and after bias correction even though the  $R^2$  values are decreasing very slightly from RAW to CORRECTED for the best performing station and increasing for the poor performing station. Overall, the quantile mapping method for correcting bias in remotely sensed rainfall data performed well for all stations.

Table 4.1: MBE difference between RAW and CORRECTED rainfalls for each station

Stations	Differences in MBE		
	Daily	Monthly	Annually
0079396 2	0.37	11.24	134.86
0079485 1	-0.19	-5.69	-68.25
0079490 X	-0.15	-4.74	-56.89
0079632 6	-0.31	-9.56	-114.69
0079730 0	-0.04	-1.11	-13.27
0079754 2	0.16	4.95	53.30
0101719A8	0.54	16.27	195.25

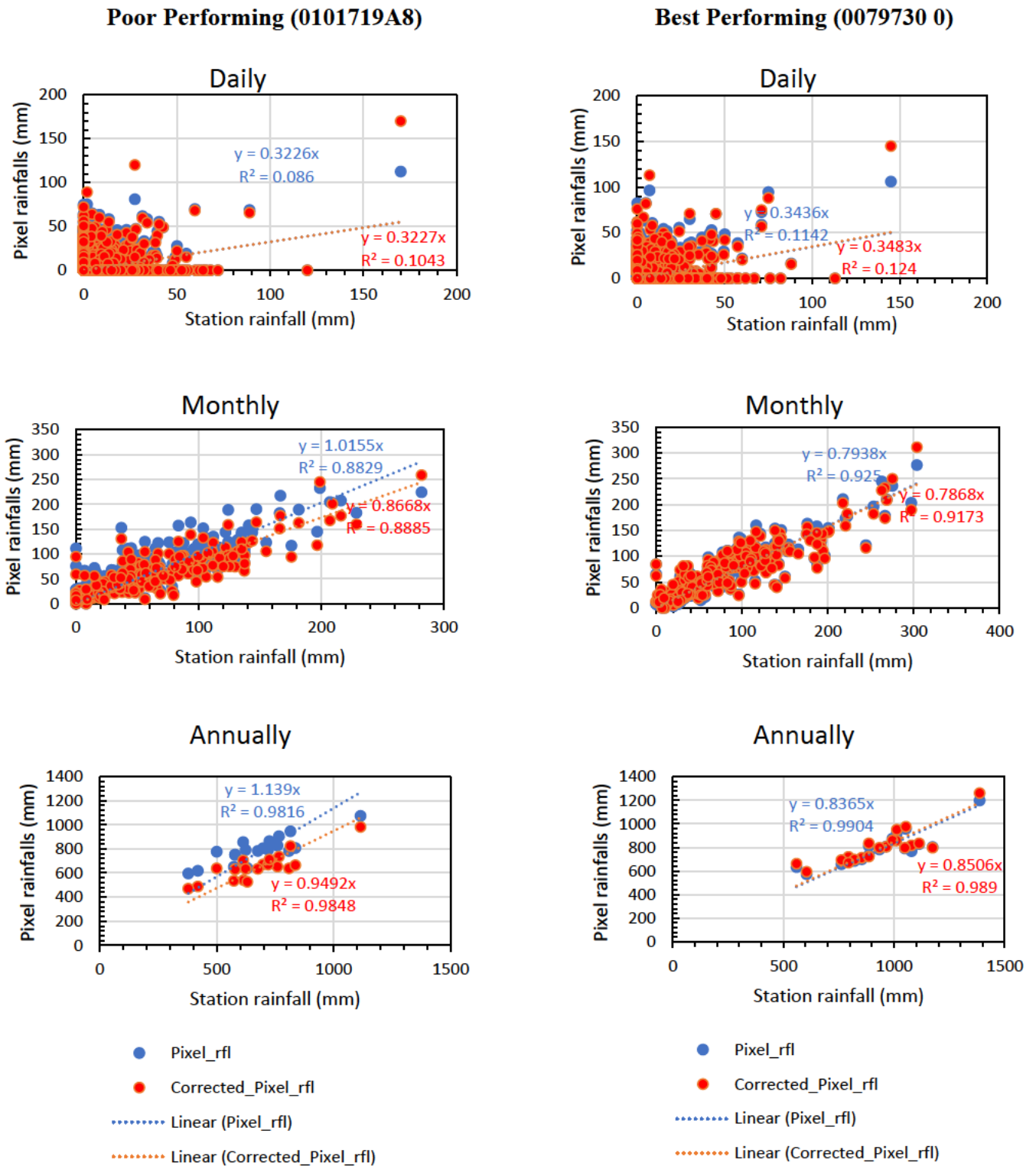


Figure 4.4: Assessment of performance of bias correction on a pixel-station basis for the best performed station (0079730 0) and poorly performed station (0101719A8)

## 4.2 Sensitivity to Period Length

This analysis aims to assess if bias correction based on empirical quantile mapping is affected if a different period of record was used and to assess if the period length used in this study had any impact on the results of bias correction. The original period length for Catchment S60A was from 1981 to 2000. Sensitivity to the period length was assessed using the remotely sensed rainfall values and corresponding observed rainfall values from Station 0079396. One station was used for this assessment because the results for all stations would be the same. For this analysis, the period length was incremented into increasing period lengths (1981-1985, 1981-1990, 1981-1995, and 1981-2000). The assessment was done by comparing the bias corrected pixel values from using different period lengths against the raw pixel rainfall values of the same period. For example, for the period length of 1981-1985, the observed rainfall data was used to correct the pixel values for the year 1981 to 1985, and the corrected pixel values of the same period (1981-1985) were then compared to the raw pixel values of the same period (1981-1985).

The results for all the comparisons are presented in Figure 4.5 for daily values. In the graph, the Corrected\_Pixel\_rfl is the corrected remotely sensed rainfall and the years in brackets indicate the period length that was used to estimate correction factors. To make the graph easy to read, the equations and the  $R^2$  values for the trendlines are placed at the top of the graph as 1981-1985, 1981-1990, 1981-1995, and 1981-2000 respectively. As observed in Figure 4.5, the correlation and the slope of each assessment show dynamic results. From the period length of 1981-1985 to the period length of 1981-1990, there was an increase in the  $R^2$  correlation from 0.94 to 0.95 and a decrease in the slope value from 1.04 to 0.98, and a decrease in both slope value and  $R^2$  value thereafter for all the other period lengths.

There is a good correlation at the low values and some variation in the higher values for the years 1981-1985. This could be due to some of the extreme rainfall values that could not be properly bias corrected which could be attributed to the effectiveness of the empirical quantile mapping method for the extreme rainfall values in short period length. Nonetheless, the differences in the correlation within all the regression plots is less than 1% and may be regarded as minimal. These results indicate that the bias correction method based on empirical quantile mapping is not significantly affected by a change in the period length of the dataset. However, these results could be influenced by the period length used as well as the RS product used in this project and therefore these results only apply to the study catchments, study period, stations rainfall values and the corresponding CHIRPS pixel rainfall values used.

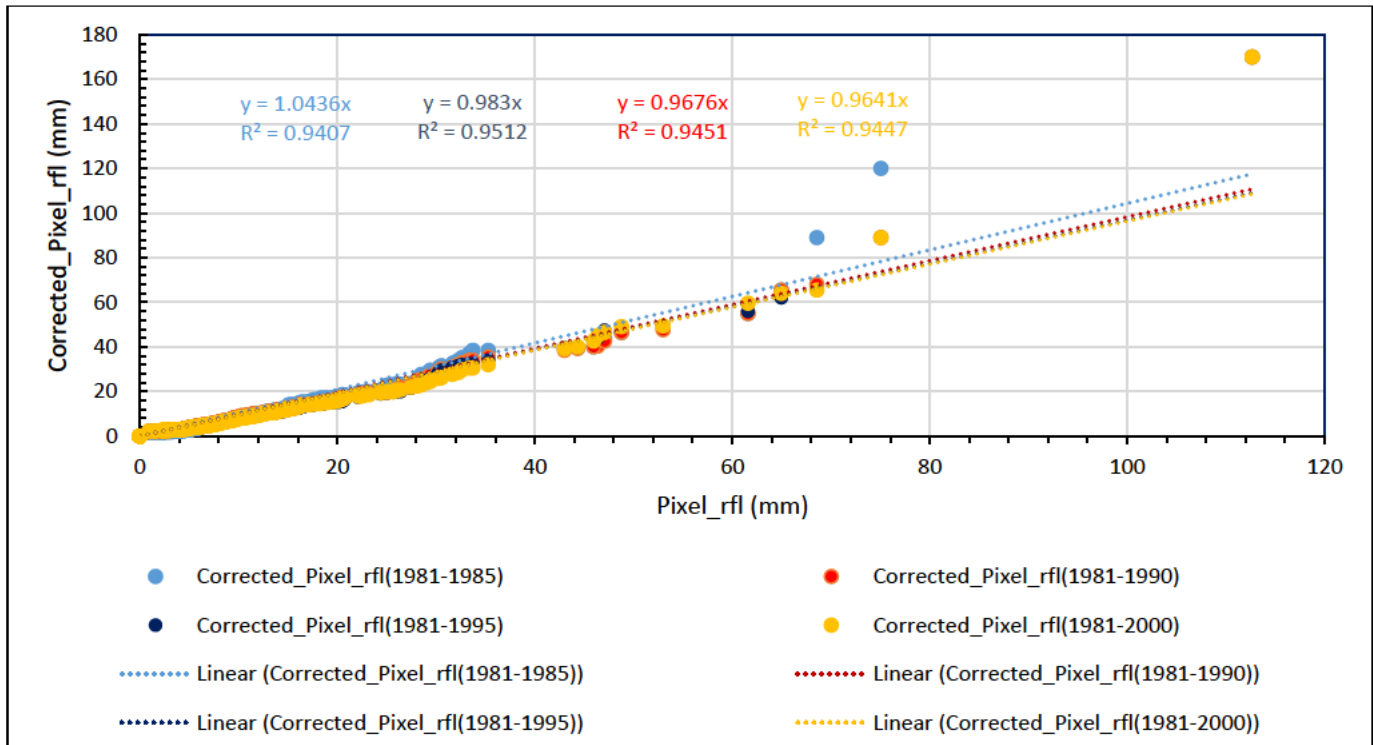


Figure 4.5: Comparison of bias correction at different time scales for station 0079396

### 4.3 Estimation of Catchment Rainfall

Given that the actual distribution of spatial rainfall is not known, the best estimate is the areal weighted observed daily rainfall data, therefore, all other estimates of catchment rainfall are assessed against catchment rainfall derived by interpolation of observed rainfall data.

#### 4.3.1 Validation of method of catchment rainfall correction

Catchment Rainfall that was estimated using the GEE was corrected of bias using an area weighting of the calculated bias correction values from the selected pixels at stations within the catchment. The method was adopted by assuming that each calculated pixel-to-station bias contributes to the total catchment bias according to the weight that each selected pixel contributes to total catchment rainfall. The contribution of pixel rainfall to total catchment rainfall was determined by using the Thiessen polygon to calculate the weight of each station. The calculated weight for each station contributing to the total catchment rainfall is the same as the weight for the corresponding pixel contributing to the catchment rainfall. The bias correction factors of each pixel where the stations are located were then areal weighted using the weights to estimate the average catchment correction factors. The GEE-derived catchment rainfall was then bias corrected by multiplying the GEE-derived catchment rainfall values by the averaged catchment bias correction factors.



The correlation results are summarised in Figure 4.6 and Figure 4.7, wherein the GEE-derived catchment rainfall and weighted pixel based catchment rainfall are compared before and after the application of bias correction. In Figure 4.6, the catchment rainfall that was derived from the pixel values before bias correction was performed and in Figure 4.7 the catchment rainfall that was derived from the pixel value after bias correction was performed, with the bias correction performed using the method presented in Section 3.7.2.3. Ideally, the slope of graphs and correlation from both comparisons should be the same. This would mean that, since the correlation and slope before bias correction was performed is the same as after bias correction was performed, it means that the method that was used to derive correction factors for the GEE catchment rainfall was valid and therefore the results can be fairly assessed against the Weighted station's catchment rainfall that is derived from observed rainfall.

From the results, it is evident that the method that was used to correct GEE derived catchment rainfall of possible bias by assuming that the bias at each pixel contributes to total catchment bias according to estimated station weight was valid.

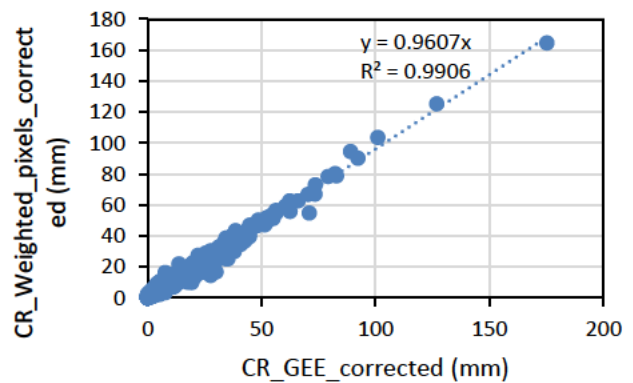
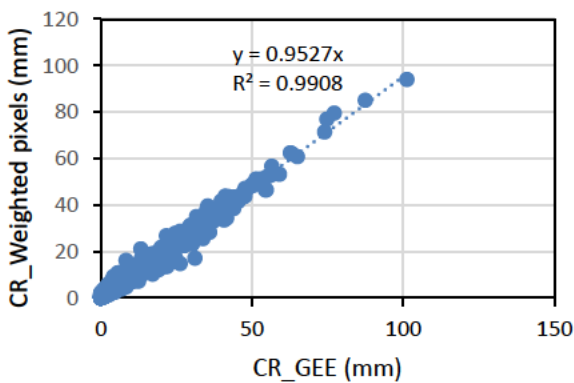


Figure 4.6: Correlation between catchment rainfall derived from the weighted pixel values and the Google Earth Engine-derived catchment rainfall **before** they were bias corrected

Figure 4.7: Correlation between catchment rainfall derived from the weighted pixel values and the Google Earth Engine-derived catchment rainfall **after** they were bias corrected

### 4.3.2 Assessment on a daily scale

Figure 4.8 presents the accumulated daily catchment rainfall derived by using the following approaches:

- (i) the areal weighting of multiple rainfall stations (Weighted stations),
- (ii) the areal weighting of multiple pixels (Weighted pixels),
- (iii) driver pixel using rainfall adjustment factors [Driver pixel (pptcor)], and
- (iv) RS through the Google Earth Engine (Corrected GEE),

All these methods estimate catchment rainfall differently as detailed in Section 3.7. The results from all the approaches were compared against the catchment rainfall derived from the areal weighting of multiple stations (Weighted stations) which is assumed to be the best estimate of actual catchment rainfall.

Figure 4.8 presents a comparison of accumulated daily catchment rainfalls and indicates that all the methods generally underestimate accumulated daily catchment rainfall with increasing time period. Considering the presented approaches that are being compared, it is clear that Weighted pixels have estimates that are much closer to the Weighted station accumulated daily rainfall followed by the Driver pixel(pptcor) approach. This could be the result of a similar approach to estimate catchment rainfall used in both the Weighted pixel approach and the Weighted station approach and the point rainfalls were obtained from the same geographical areas.

Further, the Driver pixel(pptcor) approach performs well because it is based on the selection of a pixel that best represents the catchment and therefore has a high contribution to the Weighted pixel derived catchment rainfall. The Corrected GEE approach is seen to underestimate the accumulated daily rainfalls more than other approaches. This may be due to the differences in the estimated rainfall depth because there was no clear indication of improvement of the rainfall depth and its accuracy needs to be improved.

The results in Figure 4.8 are supported by the frequency distribution shown in Figure 4.9 which present the non-exceedance frequency of daily catchment values in percentiles. All daily rainfall values up to the 75<sup>th</sup> non-exceedance percentile for is zero. Between the 75<sup>th</sup> and 87<sup>th</sup> non-exceedance percentiles, there is an underestimation of daily catchment values by all approaches, however, Weighted pixels approach has percentile values that are much closer to the Weighted station approach. Corrected GEE and Driver pixel(pptcor) had the worst performance especially in lower percentiles. This is seen in the summary of MAE statistics in Table 4.2, where the Weighted pixel had a low MAE value and Corrected GEE and Driver pixel(pptcor) had the values of MAE 8.57 and 8.56, respectively.

Table 4.2: Daily catchment rainfalls MAE summary statistics for all approaches compared to the Weighted station approach

Statistic	CR Corrected GEE	CR Weighted Pixel	CR Driver Pixel(pptcor)
MAE	8.57	3.92	8.56

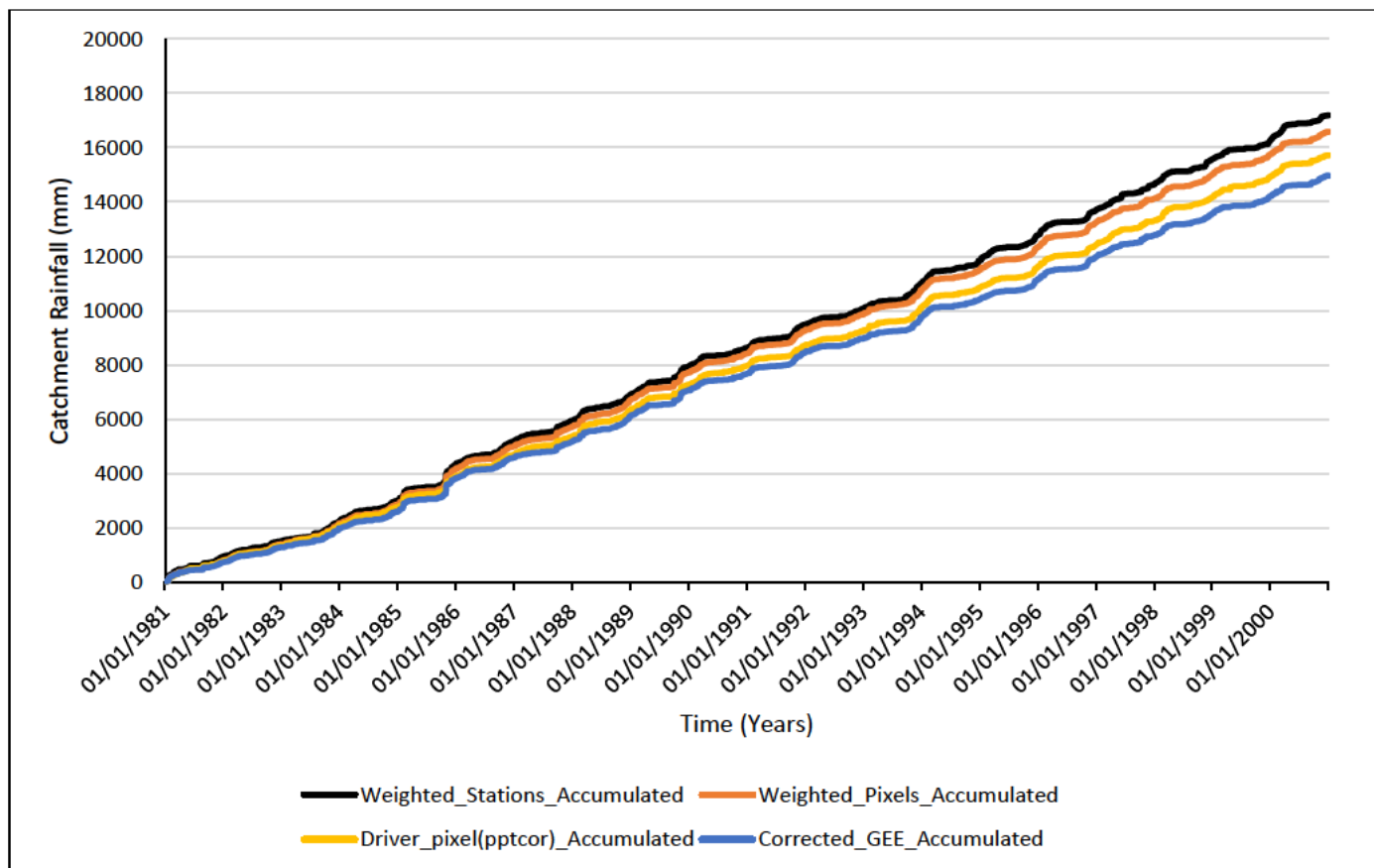


Figure 4.8: Accumulated daily catchment rainfalls for different approaches

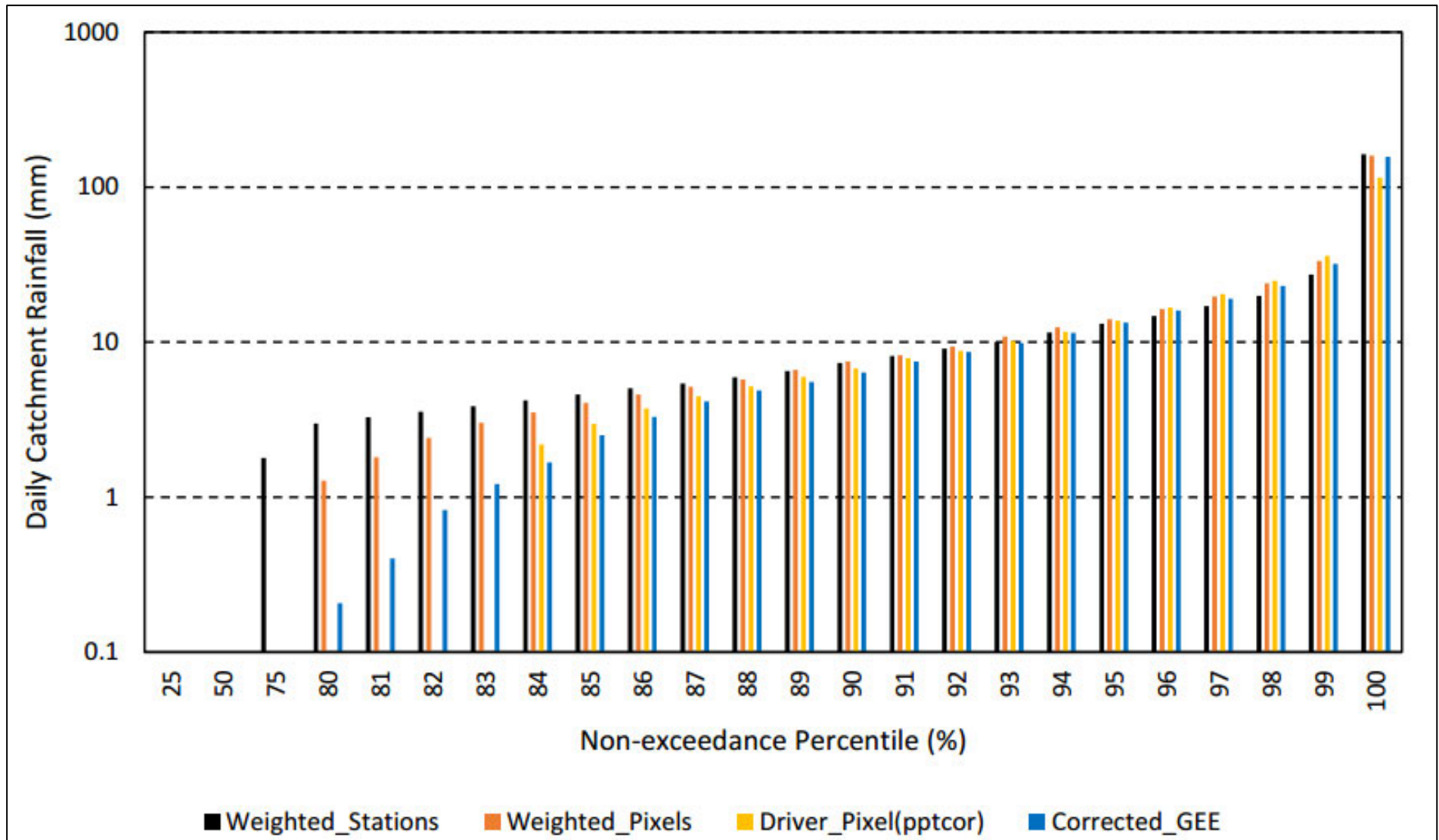


Figure 4.9: Frequency distribution for daily catchment rainfalls

### 4.3.3 Assessment on a monthly scale

Further assessment was done on a monthly scale. This is because the bias correction of the CHIRPS rainfall data showed better performance on a monthly scale. Figure 4.10 presents a scatter plot comparing catchment rainfalls derived using GEE (Corrected GEE), weighted pixels (CR\_Weighted pixel), and the Driver pixel approach [CR\_Driver\_pixel(pptcor)] against the weighted station approach (CR\_Weighted stations). CR represent catchment rainfalls. From Figure 4.10 it is evident that the driver pixel approach underestimates monthly catchment rainfalls by nearly 14% on average while the Corrected GEE approach overestimates by 10% on average. The weighted pixels approach slightly overestimate rainfalls by 2% on average and shows a better performance compared to other approaches.

These results are supported by the correlation coefficient ( $R^2$ ) and slope of each approach which is displayed on the graph. The difference in the correlation of all approaches is less than 0.04. These results are in the same order for the slope of the graphs. Overall, the results show a good potential of Weighted pixel approach to estimate monthly totals of catchment rainfall followed by Corrected GEE approach.

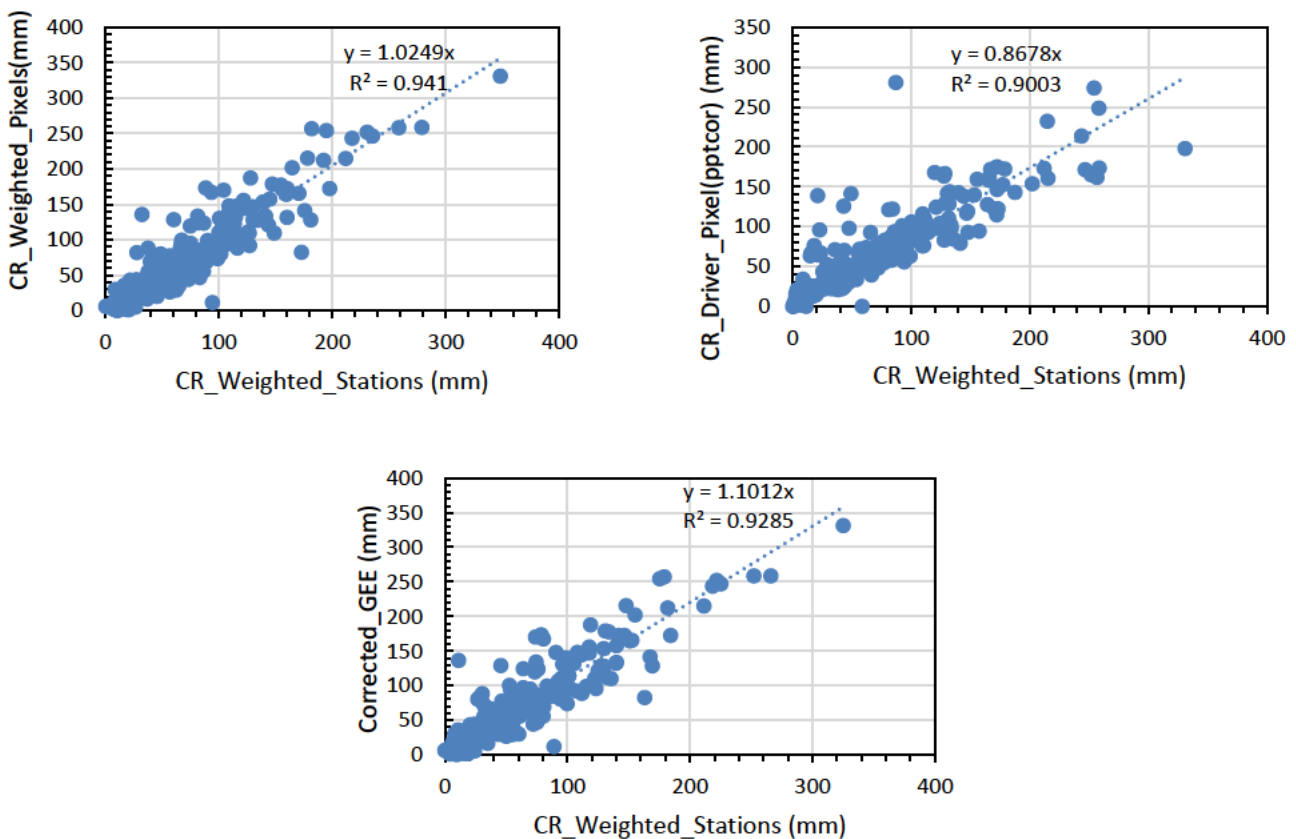


Figure 4.10: Monthly catchment rainfalls comparison between different approaches

Further assessment of catchment monthly rainfall was done using the frequency distribution shown in Figure 4.11. In the figure, less than 5% of estimated values did not exceed 10 mm catchment rainfall. All the approaches have a larger maximum (100<sup>th</sup> percentile) monthly catchment rainfall value compared to the Weighted station's approach except for the Driver pixel(pptcor). In terms of distribution performance, the Weighted pixel approach shows a similar distribution to the Weighted station approach while the distributions of the Corrected GEE and the Driver pixel(pptcor) approaches are less similar. This is supported by the values of MAE of the percentile values shown in Table 4.3, which present the estimated average error between the estimated catchment rainfalls in percentiles Overall, all approaches show a good potential to estimate monthly values of catchment rainfall.

Table 4.3: Total monthly catchment rainfalls MAE summary statistics for all approaches compared to the weighted station approach

<b>Statistic</b>	<b>CR Corrected GEE</b>	<b>CR Weighted Pixel</b>	<b>CR Driver Pixel(pptcor)</b>
MAE	17.7	15.4	18.2

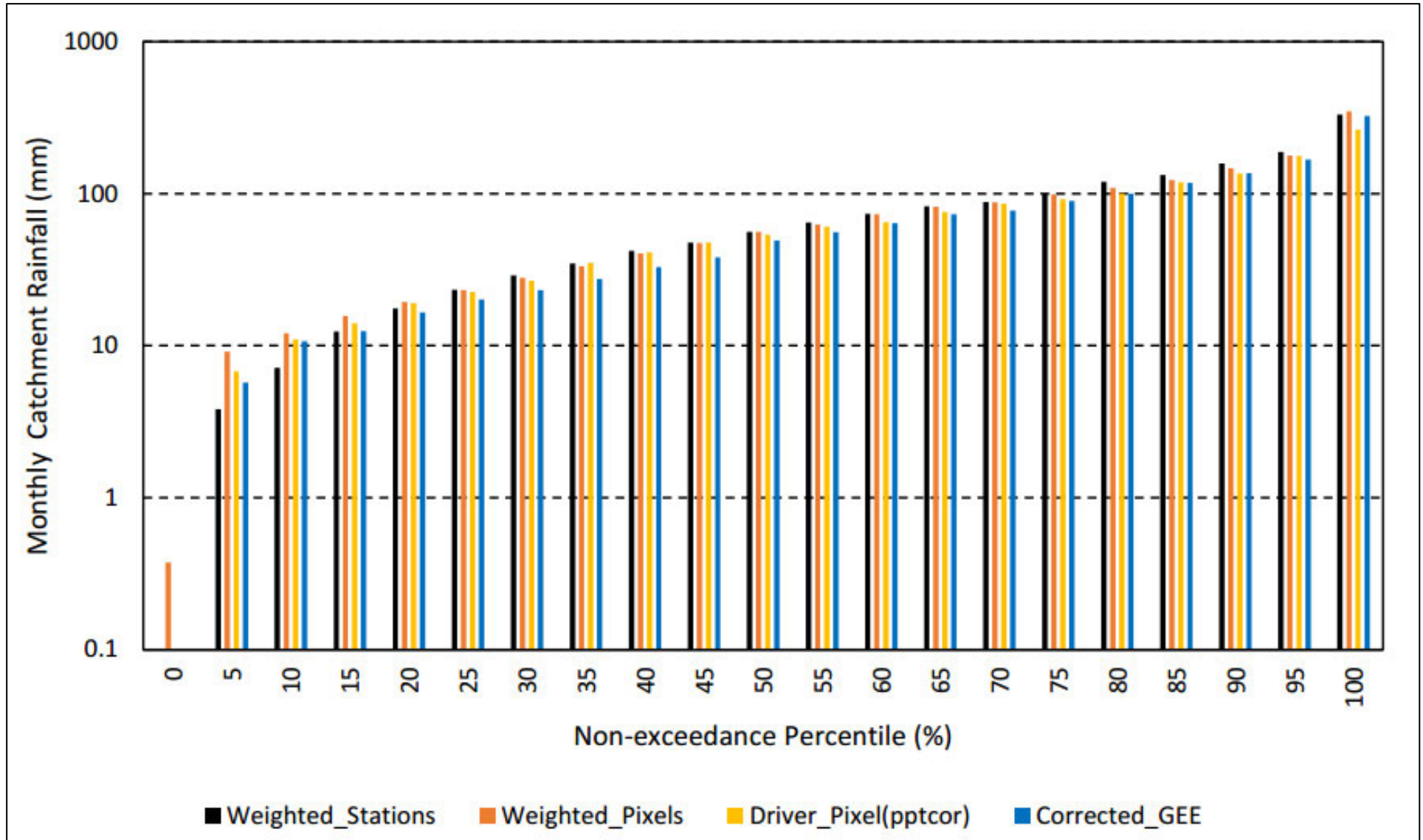


Figure 4.11: Frequency distribution curve for the monthly catchment values.

#### 4.4 Estimation of Catchment 1-Day Design Rainfall

The performance of 1-day design rainfalls estimated from the three approaches to estimate catchment rainfall, detailed in Section 3.7 and the Driver pixel approach using ARFs detailed in Section 3.8, was assessed. Given the limited length (20 years) of rainfall data used in this study, this analysis was limited to the 20 year return period event. The results are presented in Figure 4.12 which shows the design values for each return period. Based on the graph, the approaches performed better from the Weighted pixels followed by Corrected GEE with a similar performance. The Driver pixel(pptcor) approach overestimated design values for most return periods while the Corrected GEE is both underestimates and overestimates design rainfall values at different return periods. All approaches performed well for the 2-year return period except for the Driver pixel(pptcor) approach which overestimated the design values slightly higher than other approaches. Further analysis of the design values reveals a varying performance of all approaches against the Weighted station approach. RS (Driver pixel (ARFs) and Weighted pixels) show potential to perform better in high return periods. However, the MAE estimations in Table 4.4 show that the Weighted pixel approach has the lowest estimated error while the Driver pixel(pptcor) has the highest estimated error. Therefore, even though all approaches performed reasonably well, the Weighted pixel approach performed the best.

Table 4.4: Catchment design rainfalls MAE statistics for all approaches compared to the Weighted station approach

<b>Statistic</b>	<b>Corrected_GEE</b>	<b>Weighted_pixels</b>	<b>Driver_pixel (pptcor)</b>	<b>Driver pixel (ARF's)</b>
<b>MAE</b>	5.6	5.4	12.3	8.7



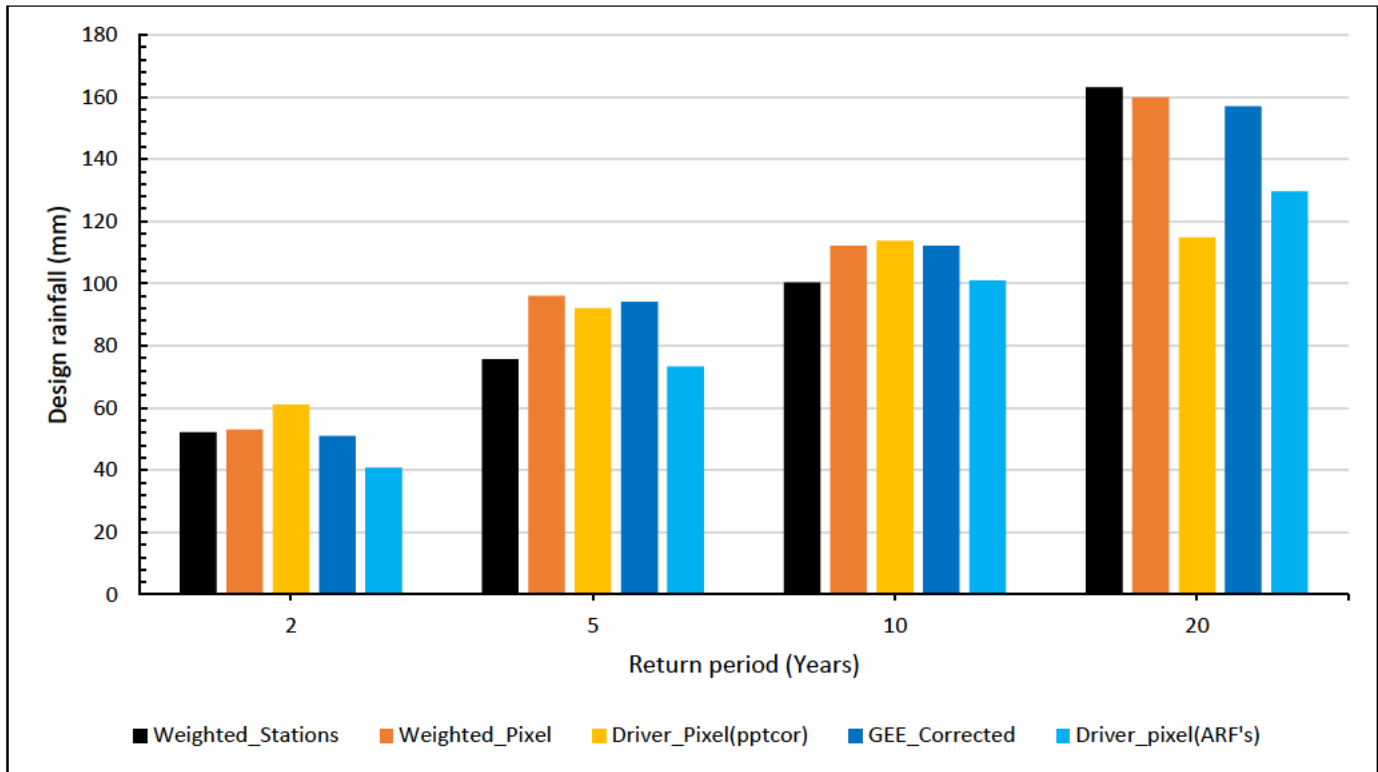


Figure 4.12: Estimation of 1-day catchment design rainfall using different approaches

## 5. APPLICATION TO CATCHMENT U20F

Using the results from the pilot study, further assessments were performed in Catchment U20F. The results from Catchment S60A showed the Weighted pixels approach as the best approach to estimate design rainfalls against the Weighted station approach, therefore, this chapter further investigates the performance at Catchment U20F. The difference between Catchment S60A and U20F is the climatic region, the catchment sizes, and how the distribution of stations in the catchment.

### 5.1 Assessment of the performance and bias correction

Validation was performed using the statistics MBE, RMSE, MAE, D, and %BIAS which is obtained by multiplying MBE by 100. Figure 5.1, Figure 5.2, and Figure 5.3 present the results of the statistics that were used to assess the performance of the bias correction for the daily, monthly, and annual scales, respectively. The values of the statistics are presented in Appendix H. As per the graphs, the bias correction performed significantly well.

On a daily scale, the bias is reduced in 8 out of 10 stations with bias reduced up to 0. The D between datasets ranged from 0.38 to 0.62 for the raw rainfall dataset and from 0.37 to 0.71 for the bias corrected rainfall values with Station 0269775 having the lowest values of the D values and Station 0270086 A having the highest D values. RMSE values are each increasing in corrected rainfall values while MAE values are decreasing in all stations.

At monthly and annual scales, the trends in performance are the same as at a daily scale. The bias was removed entirely at Stations 02270021 and 0269775. Based on results for all stations, the D value has increased up to 0.938 for raw data and 0.961 for the corrected values on a monthly scale. At an annual scale, D increased up to 0.91 for raw rainfall values and 0.94 for the corrected values. Station 0269775 has the lowest values of D but has the bias reduced to a value of 0 at all time scales while Station 0270086 has the highest values of D and an increased value of %BIAS present at all time scales.

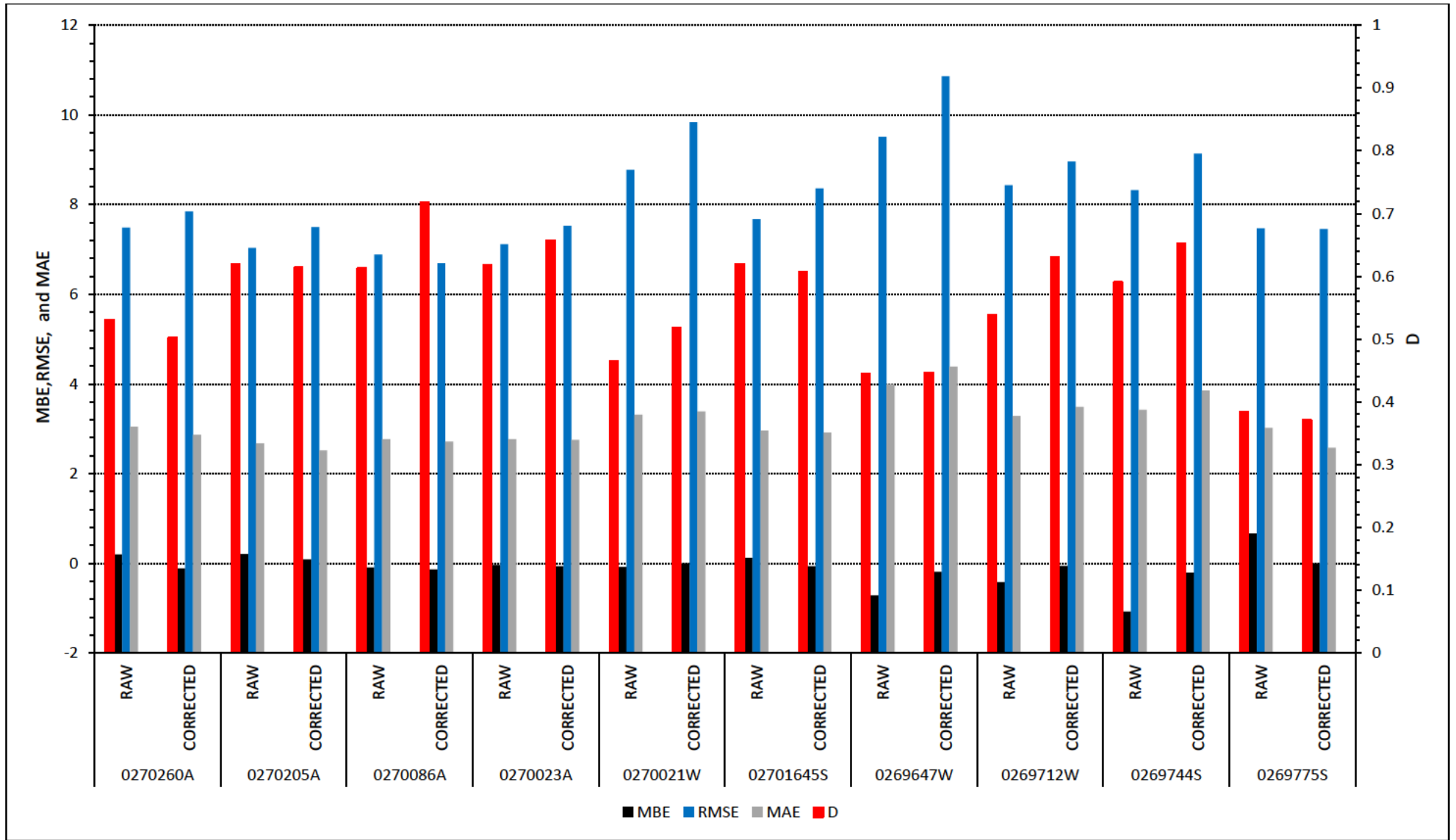


Figure 5.1: Validation statistics for bias correction at a daily scale

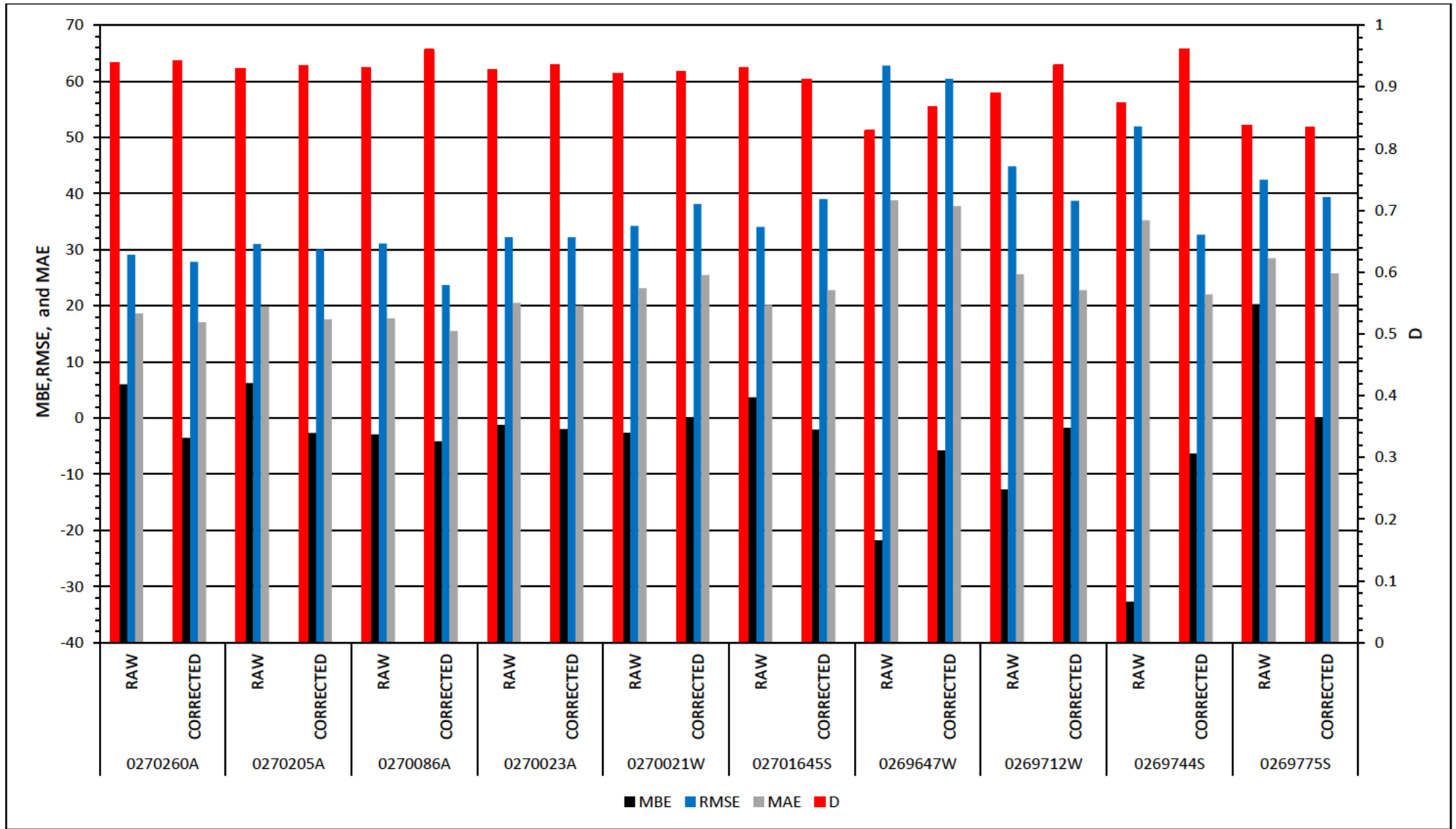


Figure 5.2: Validation statistics for bias correction at a monthly scale

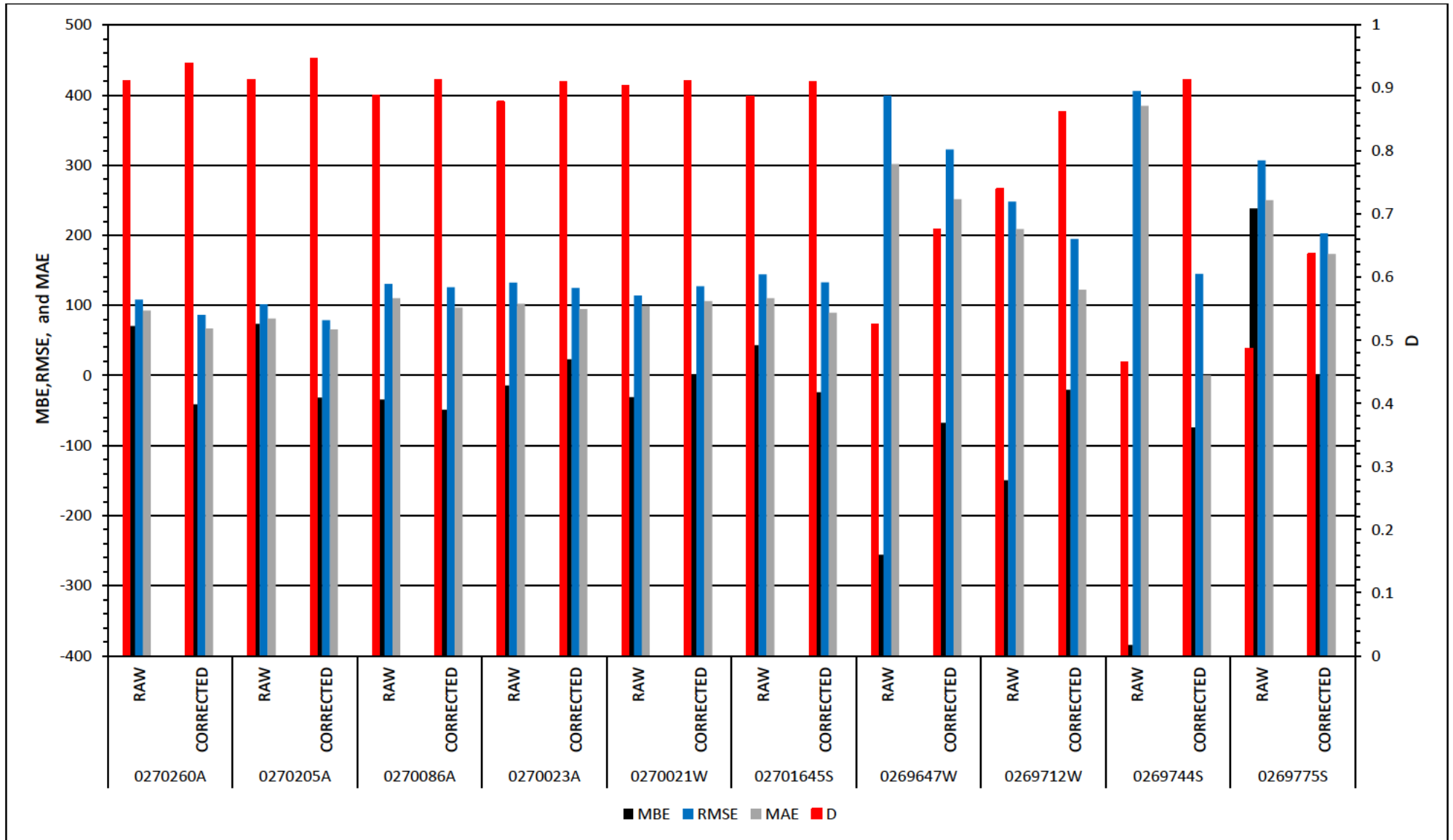


Figure 5.3: Validation statistics for bias correction at an annual scale

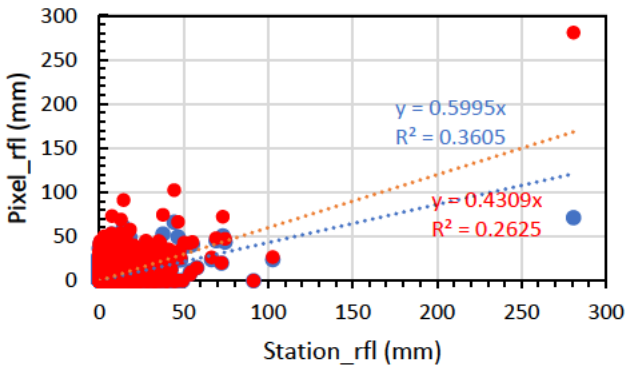
The Performance of pixel-to-station bias correction for Catchment U20F was further assessed using regression graphs. The graphs are presented in Figure 5.4. Even though some stations had %Bias reduced to 0, the criteria to select the best and poorly performing stations was the same as used in Catchment S60A which was to assess the amount of bias reduced after applying bias correction. The results of the differences in MBE between RAW and CORRECTED are presented in Table 5.1. Based on the statistics, Station 0270086 A was identified as the best performing and station 0269744 S as the worst performing. However, the regression statistics shows interesting results with decreasing slopes and R<sup>2</sup> values for both poor and best performing stations. Nonetheless, these results agree with results for Catchment S60A in the sense that bias correction between RAW and CORRECTED remotely sensed using empirical quantile mapping performs better in longer high temporal scales.

Table 5.1: MBE difference between RAW and CORRECTED rainfalls for each station

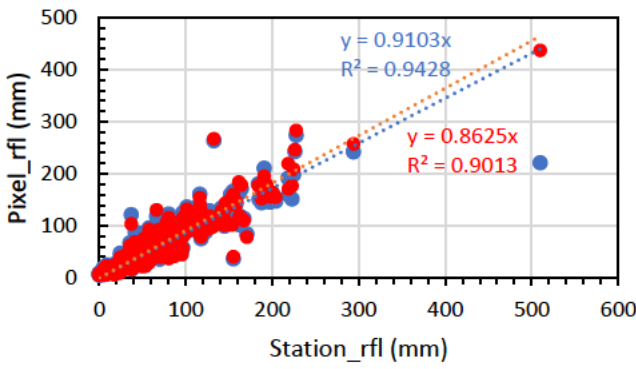
Stations	Difference in MBE		
	Daily	Monthly	Annually
0270260A	0.31	9.53	111.96
0270205A	0.12	8.92	104.84
0270086A	0.04	1.21	14.23
0270023A	0.02	0.75	-37.12
0270021W	-0.09	-2.64	-31.06
02701645S	0.19	5.72	67.20
0269647W	-0.53	-15.99	-187.86
0269712W	-0.361	-10.988	-129.109
0269744S	-0.869	-26.427	-310.519
0269775S	0.666	20.278	238.267

**Poor Performing (0269744 S)**

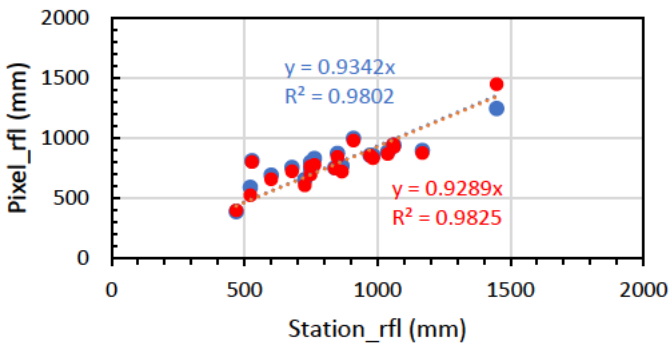
**Daily Scale**



**Monthly Scale**



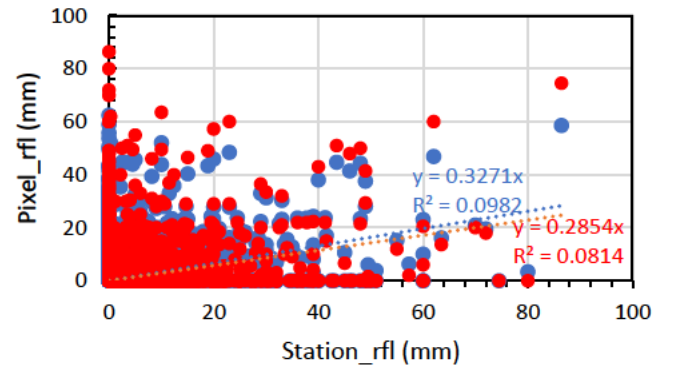
**Annual Scale**



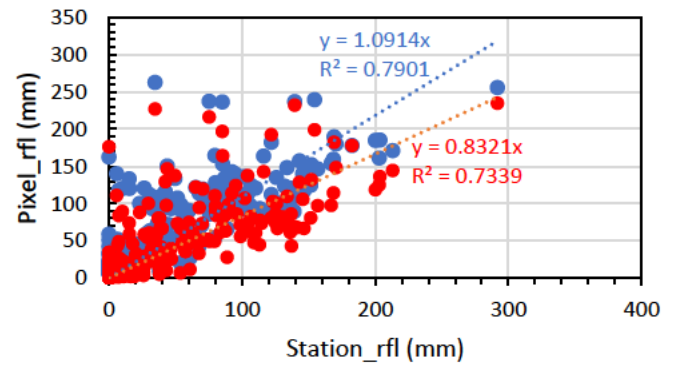
- Pixel\_rfl
- Corrected\_pixel\_rfl
- ..... Linear (Pixel\_rfl)
- ..... Linear (Corrected\_pixel\_rfl)

**Best Performing (0270086 A)**

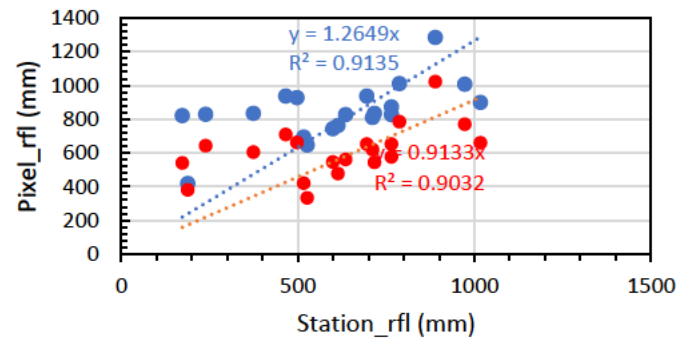
**Daily Scale**



**Monthly Scale**



**Annual Scale**



- Pixel\_rfl
- Corrected\_pixel\_rfl
- ..... Linear (Pixel\_rfl)
- ..... Linear (Corrected\_pixel\_rfl)

Figure 5.4: Assessment of performance of bias correction on a pixel-station basis for the best performing (0270086 A) and poorly performing (0269744 S) station

## 5.2 Catchment Rainfall Estimates

In this chapter, the catchment rainfall estimated using the areal weights of multiple stations (Weighted stations) was assessed against the catchment rainfall estimated using the other approaches.

### 5.2.1 Assessment on a daily scale

The catchment rainfalls were estimated and assessed using accumulated rainfall as presented in Figure 5.5 on a daily time scale. The catchment rainfall results from the two approaches show the potential of the Weighted pixel approach to accurately estimate catchment rainfall values. As seen in the Figure 5.5, the Driver pixel(pptcor) and Corrected GEE approach overestimate and underestimate catchment rainfalls, respectively. The Corrected GEE may be performing so poorly because of the poor distribution of rainfall stations across the catchments. The other approaches are not affected as such because the estimation of their RAW rainfall primarily depend on the location of the selected stations.

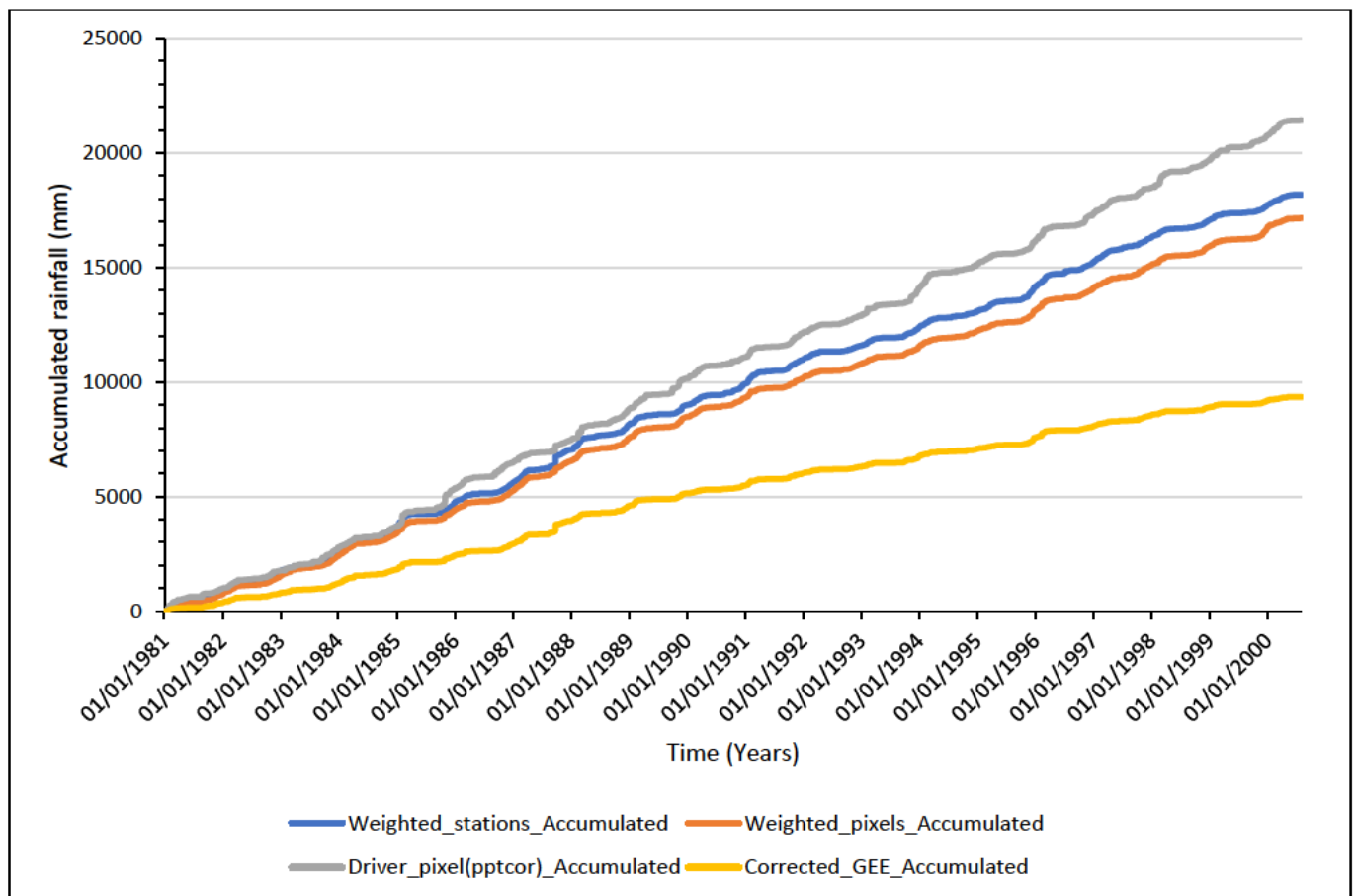


Figure 5.5: Accumulated daily catchment rainfalls for different approaches



Further assessment is presented in Figure 5.6 using the frequency distribution curve. As shown in Figure 5.6, the Weighted pixel approach has a distribution closer to the Weighted station approach except for the maximum value (100<sup>th</sup> percentile) which is much lower. This could have been due to values that were observed in Station 0270021W on 22/10/1996 and in Station 0269647W on 05/03/1995 which were higher compared to all the other stations on the same day and could be outliers. Generally, both Station 0270021W and Station 0269647W were occasionally estimating higher daily values compared to the other stations, and the values were not corresponding well with the estimated pixel values. This is supported by the MAE statistics in Table 5.2, where the Driver pixel(pptcor) has the highest value of MAE. The driver pixel selected was a pixel corresponding to Station 0270021W. Corrected GEE is poorly estimating the daily catchment values and has lower estimations of catchment rainfalls except in the 100<sup>th</sup> percentile. In higher non-exceedance percentiles, the driver pixel(pptcor) is overestimating catchment values. Overall, Weighted pixel approach showed the best performance with the MAE value of 2.86, followed by the Corrected GEE approach with the MAE value of 4.36.

Table 5.2: Daily catchment rainfalls MAE summary statistics for all approaches compared to the Weighted station approach

<b>Statistic</b>	<b>CR Corrected GEE</b>	<b>CR Weighted Pixel</b>	<b>CR Driver Pixel(pptcor)</b>
MAE	4.36	2.86	13.33

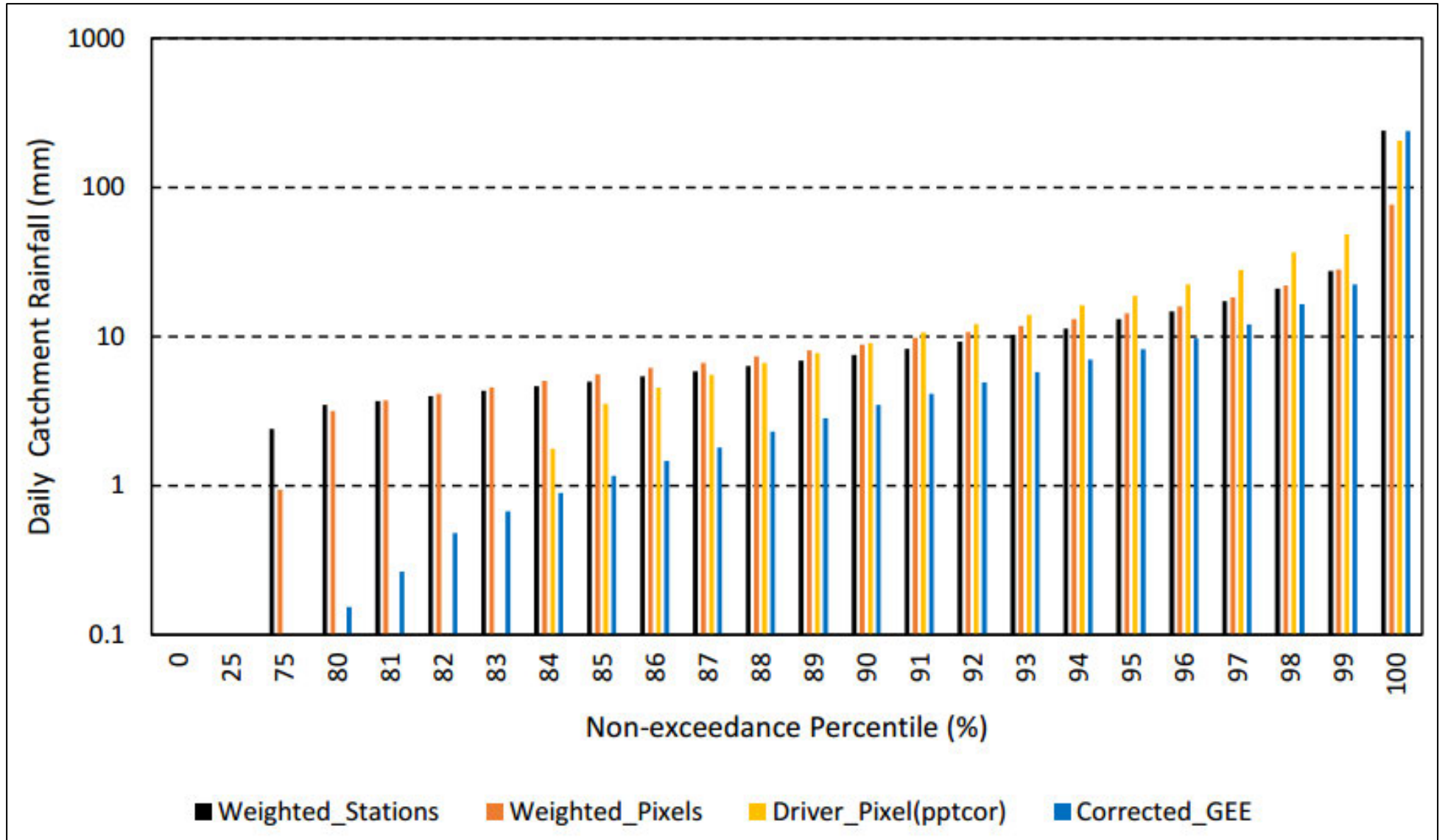


Figure 5.6: Frequency distribution for daily catchment rainfalls

### 5.2.2 Assessment on a monthly scale

The assessment on the monthly scale was done firstly using regression graphs presented in Figure 5.7. The graphs were analysed using the slope and the  $R^2$  values displayed on each chart. As seen in Figure 5.6, the comparison of catchment rainfall improved from the daily scale. This is evident in both the distribution of points and the regression statistics which shows good correlation for all approaches on a monthly scale. This could be due to time difference (08:00 – 08:00) relating to a day between observed and remotely sensed rainfalls which cannot be captured at monthly scale. The Weighted pixel approach has a good correlation of 0.9 and a slope of 1.1 while the Corrected GEE had the correlation of 0.9 but the slope was lower (0.6) compared to slope for other approaches. The Weighted pixels approach has the best catchment rainfall regression statistics.

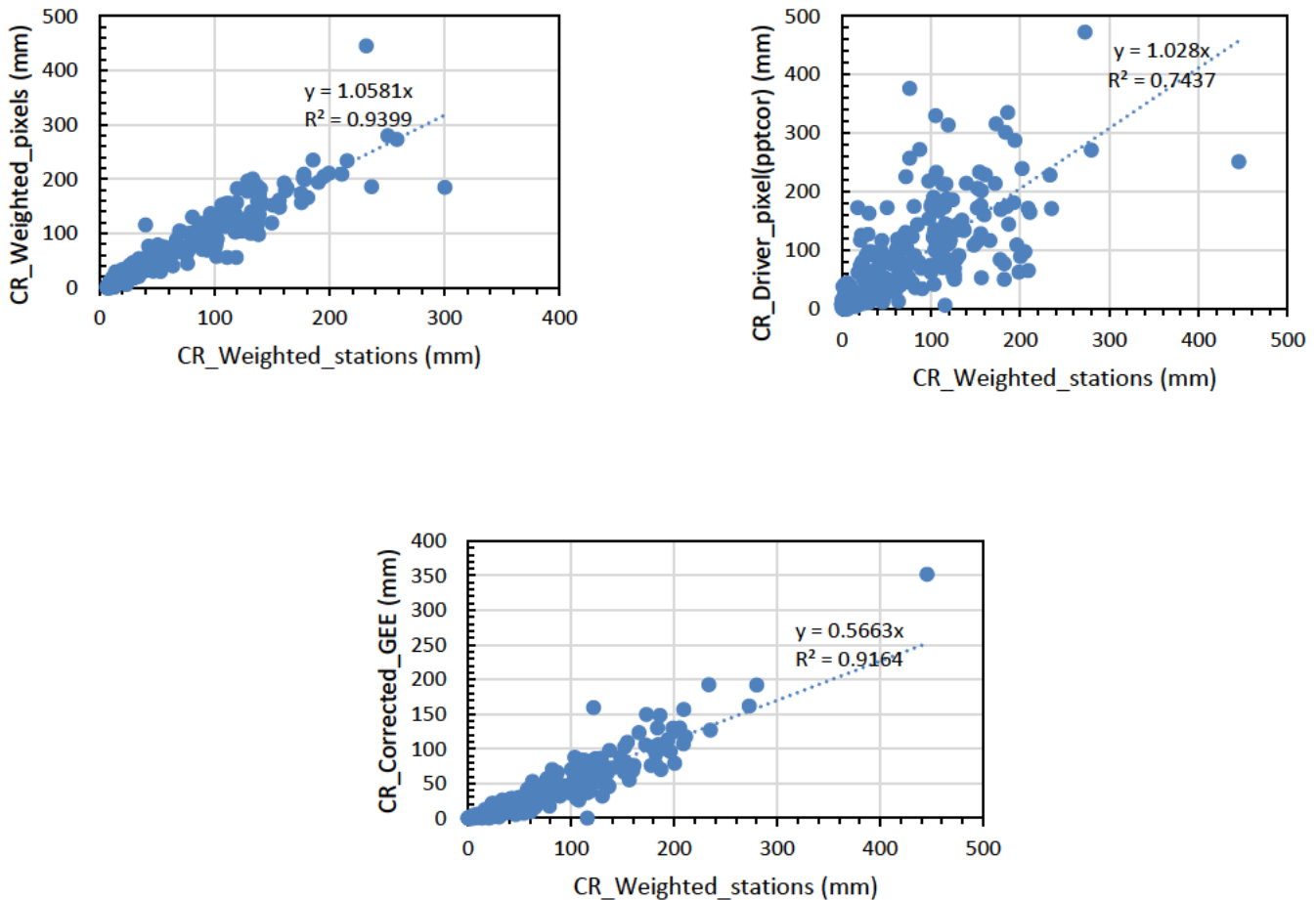


Figure 5.7: Catchment rainfalls comparison between different approaches

Based on results of regression statistics on monthly catchment rainfalls, both Weighted pixels and Corrected GEE were performing reasonably well. Therefore, further assessment was done using the frequency distribution. In Figure 5.8, the frequency distribution shows the non-exceedance percentile values for all the approaches. As per Figure 5.8, all the approaches follow a similar frequency distribution compared to the Weighted station approach. In this Catchment, the Driver pixel(pptcor) had a better performance compared to the Corrected GEE approach, unlike in Catchment S60A. This could be because the driver pixel used in this catchment had a higher contribution to the total estimated catchment rainfall. The Weighted pixel approach still has the best performance compared to all the other approaches followed by the Driver pixel(pptcor) approach. This is supported by the statistics in Table 5.3 which presents monthly catchment rainfalls MAE for all approaches against the Weighted station approach. The Weighted pixels approach has the lowest MAE value of 0.9 followed by the Driver pixel(pptcor) with a value of 2. Overall, the Weighted pixel approach is performing well while the Driver pixel(pptcor) and Corrected GEE is changing and inconclusive.

Table 5.3: Total monthly catchment rainfalls MAE statistics for all approaches compared to the weighted station approach

	<b>CR_Corrected GEE</b>	<b>CR Weighted Pixel(corrected)</b>	<b>CR Driver Pixel(pptcor)</b>
<b>MAE</b>	4.6	0.9	2.0

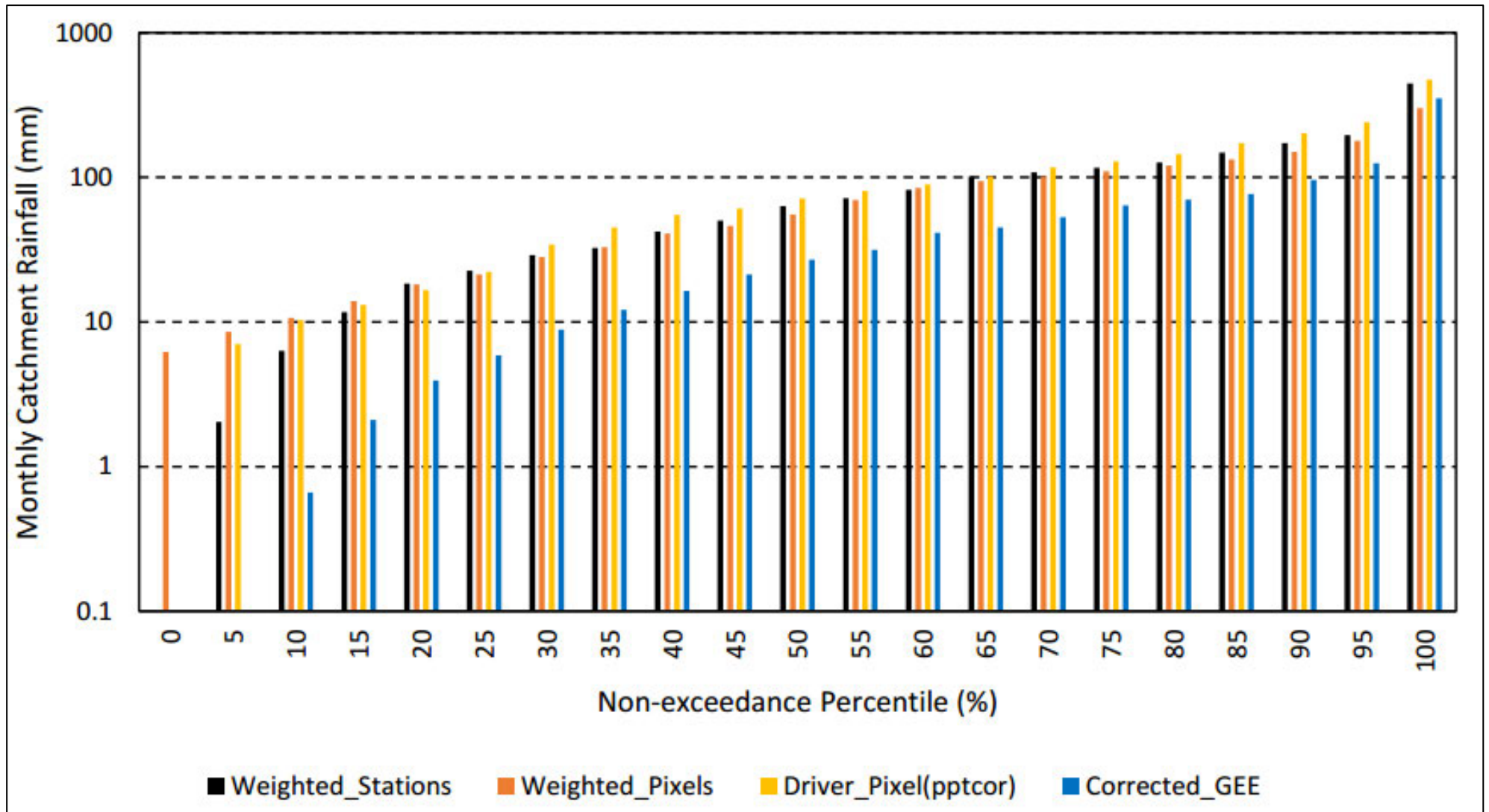


Figure 5.8: Frequency distribution curve for the monthly catchment values

### 5.2.3 Sensitivity to the spatial density and influence of Thiessen weights

This section assesses the sensitivity of estimation of catchment rainfall to the spatial density of raingauges. This assessment was done using Catchment U20F only because the stations in Catchment U20F were poorly distributed. The assessment was done to investigate how catchment rainfall estimation changes with different station spatial densities. Initially, catchment rainfall was estimated using the Weighted stations/pixels approach for all 10 stations, the second estimations were then done using 3 stations from the same catchment.

Figure 5.6 presents the distribution of the number of stations in Catchment U20F and the Thiessen polygons for 10 stations distribution and 3 stations distribution. The three stations were selected because they had extended record period lengths. However, for a fair comparison, the same record length was used for the assessment. For both the 10 and 3 station distribution scenarios, catchment rainfalls were estimated using areal averaged weights. In the 10 stations scenario, the weights that were estimated are presented in **Error! Reference source not found.** The Thiessen weights for the 3 stations scenario are 0.68, 0.17, and 0.15 for Stations 0270021 W, 0269712 W, and 0269647AW, respectively. The smaller Thiessen polygons were not included in the assessment because they had very small Thiessen weights ( $< 0,001$ ).

**10 stations distribution**

**3 stations distribution**

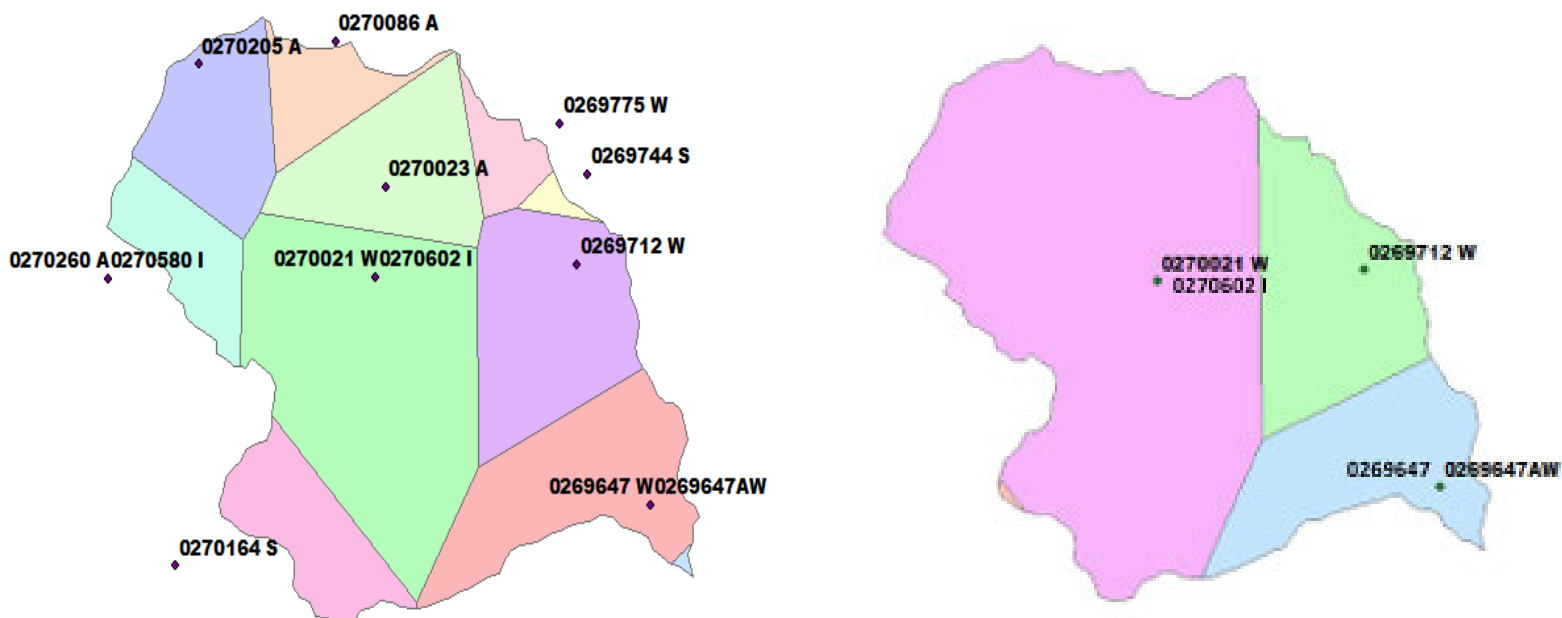


Figure 5.9: Catchment U20F showing the station's distribution and the Thiessen polygons.

### 5.2.3.1 Assessment using daily accumulation

According to the accumulated daily catchment rainfalls presented in Figure 5.10, there is evidence of a good correlation between the catchment rainfalls estimated using 10 stations/pixels and catchment rainfalls estimated using the 3 stations/pixels. In theory, the more the station is distributed in and around the catchment, the higher the accuracy of estimation. However, the results indicate that there is no significant difference between the accumulated daily catchment rainfalls estimated using 10 and 3 stations/pixels using the areal weighting of stations/pixels approach. With that fact, there should be a noticeable difference in the results of catchment rainfall estimation using 10 stations/pixels and using 3 stations/pixels with the weighted stations/pixels approach. It is the case in the presented estimations where the accumulated catchment rainfalls estimated using the 3 stations/pixels for both the weighted pixels and weighted stations approach is slightly overestimating catchment rainfall values. This observation is slightly increasing from the year 1984 and visibly increasing to the year 2000. Based on these results, there is no significant difference between the accumulated daily catchment rainfalls estimated using 10 and 3 stations/pixels by the areal weighting of stations/pixels approach.

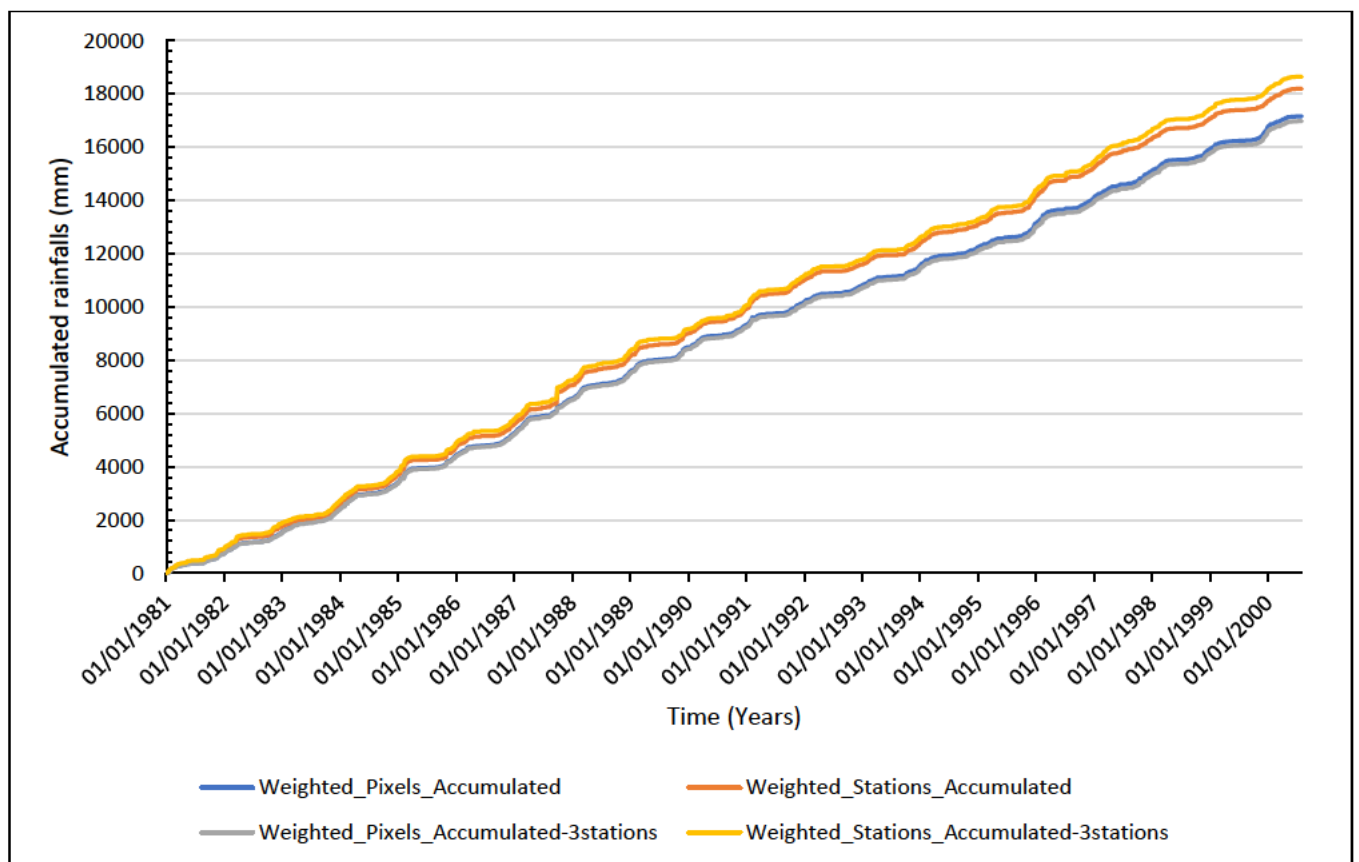


Figure 5.10: Accumulated daily catchment rainfalls estimated using weighted pixels

### **5.2.3.2 Assessment using regression statistics**

Further assessment of the impact of spatial density on estimation of catchment rainfall was done using the regression graphs presented in Figure 5.11. The graphs show results for the daily, monthly, and annual scales. As seen in the Figure 5.11, there is a good correlation between the catchment rainfalls estimated using 10 and 3 stations/pixels for all time scales. For the catchment rainfalls that were estimated using the weighted pixels approach, the correlation between the estimated values using 3 and 10 pixels is almost perfect with the values of  $R^2$  being 0.99 and the slope value of very close to 1 for all time scales. The catchment rainfall estimated using the weighted stations had a slightly lower value of  $R^2$  of 0.89 on a daily scale. This may be attributed to the extreme value of rainfall that was observed and seems to be an outlier. Overall, estimating catchment rainfall using 10 stations/pixels and using 3 stations/pixels showed no significant differences. This may be due to the 3 selected stations/pixels having high weight compared to the other 7 stations and therefore had more influence on the estimation of total catchment rainfall. In addition, the 10 stations that were initially used were not evenly distributed across the catchment and thus leaving some stations making a larger contribution to catchment rainfall compared to the others.



### Catchment rainfalls using Weighted stations

### Catchment rainfalls using Weighted pixels

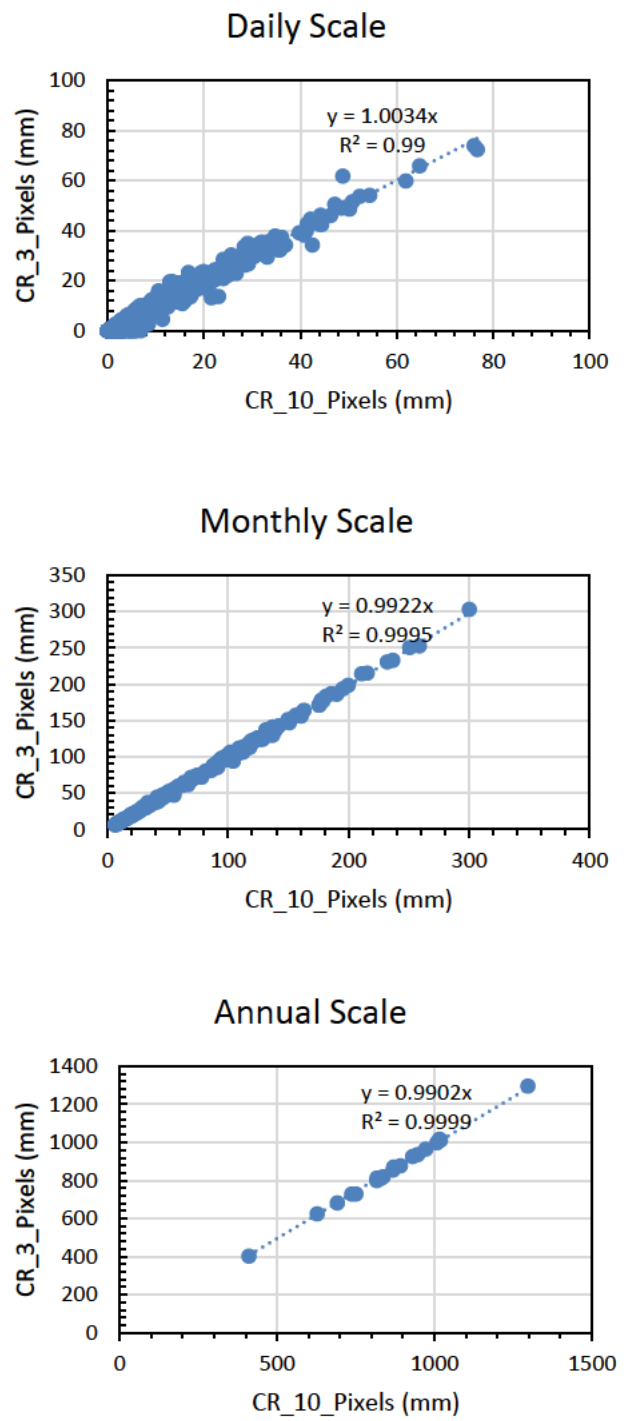
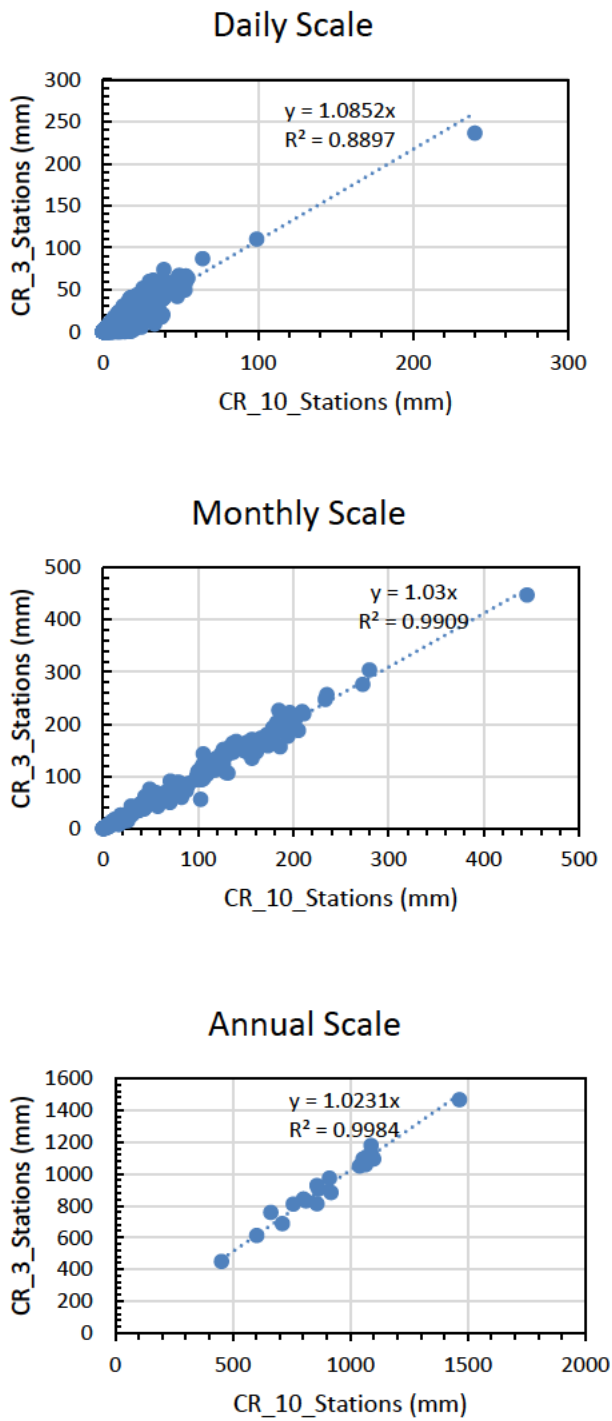


Figure 5.11: The estimation of catchment rainfalls using an areal weighting of stations/pixels for the 10 and 3 stations/pixels distribution

**5.3 Estimation of Catchment 1-Day Design Rainfall**

The catchment design rainfall results estimated for Catchment S60A suggested better performance to estimate catchment design rainfall through the Weighted pixel rainfall approach even though the other approaches (Driver pixel(pptcor) and Corrected GEE) still performed well, and the assumption was that the results will be the similar in Catchment U20F. Catchment S60A has 6 stations while Catchment U20F has 10 stations for catchment sizes of 328.34 km<sup>2</sup> and 458.99 km<sup>2</sup>, respectively. Thus, there the main differences in Catchments S60A and U20F are the different climatic regions and the distribution of stations across the catchment, which has an impact on Thiessen weights.

The results are presented in Figure 5.12 which shows the design values for each return period. Based on the graph, the approaches performed better compared to the Weighted stations approach from the Weighted pixels, Corrected GEE, Driver pixel(ARFs), and Driver pixel(pptcor) approach. The Driver pixel (pptcor) and the Driver pixel(ARFs) approaches overestimated the design values for most return periods while the Corrected GEE is slightly underestimating design values for all return periods except for the 10 year return period. The results show varied performance of all approaches against the Weighted station approach.

However, the MAE estimations in Table 5.4 show that Corrected GEE has the lowest estimated error followed by the Weighted pixel approach while the Driver pixel(pptcor) has the highest estimated error. Therefore, even though all approaches performed reasonably well, the Weighted pixel approach performed better. The switch between the Corrected GEE and the Weighted pixel approach in terms of which has the best estimate is influenced by the observation of an extreme observed design value of 240 mm at 20 year return period which resulted from an outlier that was observed in the observed rainfall dataset in March 2000. The MAE between Weighted stations and the Weighted pixel approach without the outlier value is 5.648. Therefore, without an outlier, the results prove that the Weighted pixel approach is the best estimate of catchment design rainfall.

Table 5.4: Catchment design rainfalls MAE statistics for all approaches compared to the weighted station approach

<b>Statistic</b>	<b>Corrected GEE</b>	<b>Weighted Pixel</b>	<b>Driver_Pixel (pptcor)</b>	<b>Driver pixel (ARF's)</b>
<b>MAE</b>	7.7	12.4	56.6	46.7

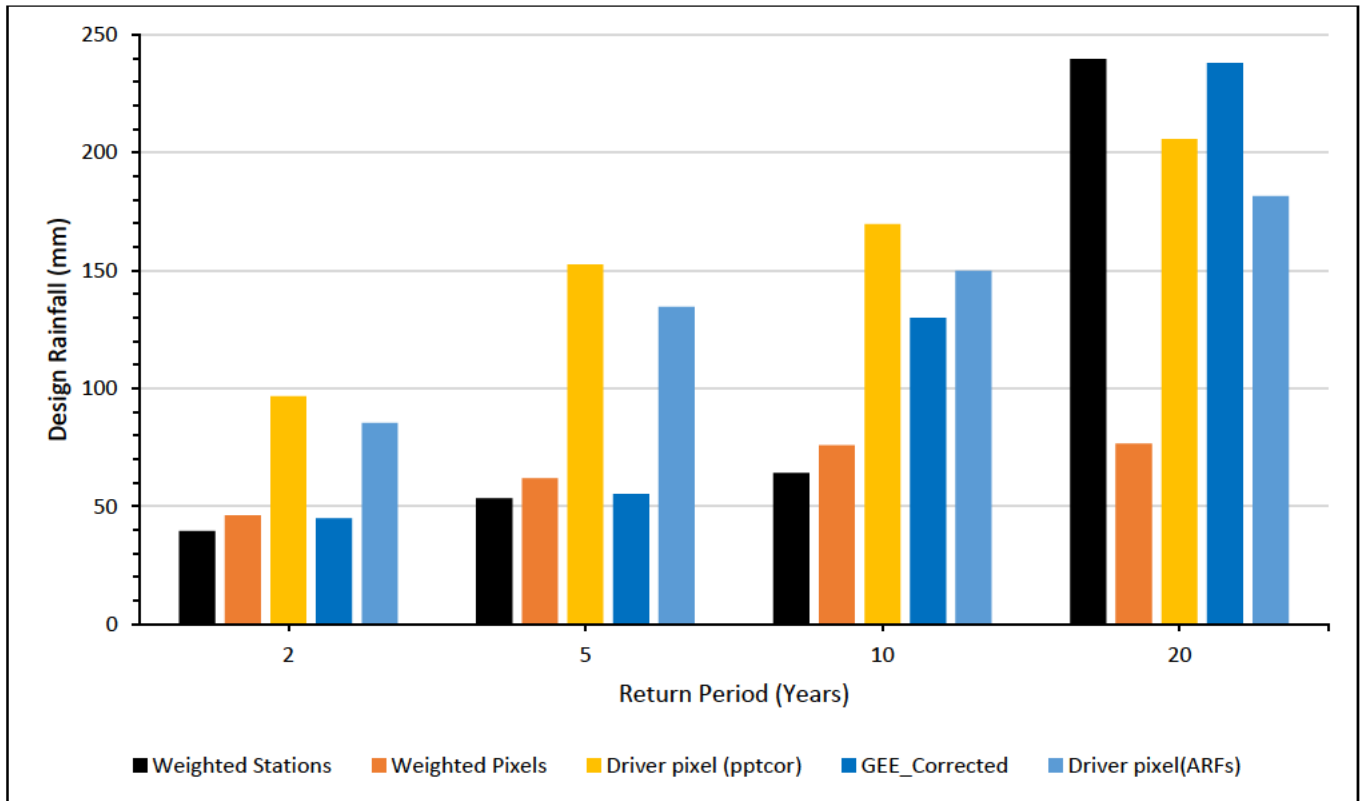


Figure 5.12: Estimation of 1-day catchment design rainfall values for different return periods

## 6. DISCUSSIONS, CONCLUSIONS, AND RECOMMENDATIONS

The main aims and objectives of this study were to use remotely sensed rainfall to improve the estimation of catchment rainfall for use in hydrological modelling and assess different methods of estimating both catchment rainfall and catchment design rainfall. This was done by using four different approaches based on the selected CHIRPS rainfall data and one approach based on the observed data. CHIRPS product was selected because it met the criteria that was set for this study. The four approaches were assessed against the observed rainfall data. This was done firstly using a pilot study in Catchment S60A and after, Catchment U20F was selected to verify the results that were obtained in the pilot study. The main results obtained in this project are bias correction, the estimation of catchment rainfalls, and the estimations of the catchment design rainfalls.

In the case of the bias correction results, the EQM approach was used in both catchments in this study. The results from both the catchments show a varied performance of bias correction. In terms of temporal scale, the performance of the bias correction method improved from daily scale to annual scale. The most improvement was observed in monthly scales where the statistics showed a large improvement compared to the daily scale statistics. In Catchment S60A, more than 50% of the selected pixels corresponding to stations had their monthly values highly reduced of bias. The results also showed a lack of improved bias in the RS values at two of the stations in Catchment U20F. However, good performance in terms of bias correction was obtained at two stations in Catchment U20F where the bias was reduced to zero.

Bias correction was assessed in terms of sensitivity of the period length selected. The results indicated that the performance of the bias correction using the EQM technique is not significantly affected by the change in period length. The use of areal weighted bias (based on the location of pixels) for the bias correction of catchment rainfall that was estimated using GEE showed good performance, however, the validation of the method was only done in Catchment S60A. Moreover, this method has not been used elsewhere and could be an area for future research. Generally, the results of bias correction resulted in improved performance in terms of reducing bias in the estimated RS pixel rainfall values. However, it is recommended that other methods of bias correction be investigated as bias correction performance depends on the accuracy and effectiveness of the method that was used to estimate raw RS data. Moreover, the CHIRPS RS product is an already bias corrected product and provides bias corrected raw data. However, the CHIRPS RS product bias correction was done on a large scale

and the results from this indicate that local bias correction is still necessary. Based on the results it is concerning that even after local bias correction was applied there was still some bias present in the data. Therefore, it is recommended that the method that is used in bias correcting the RAW CHIRPS data is re-evaluated and updated and that other methods may be used for local bias correction.

In this study, catchment rainfall was estimated using four approaches: Weighted stations, Weighted pixels, Driver pixel(pptcor), and the Corrected GEE approach. The assumption made was that the areal weighting of stations is the best estimate of actual catchment rainfall, and the performance of the other methods was compared against this approach. Based on the results obtained from Catchment S60A, further assessments were performed in Catchment U20F.

The performance of methods used to estimate catchment rainfalls were assessed for different time scales, using accumulated rainfalls, regression graphs, and frequency distributions. On a daily scale, the scatter plots were poor and unreadable owing to the poor phasing of observed and RS daily rainfall, and therefore assessments were done using accumulated daily rainfalls and frequency distribution. Based on the results, all approaches performed reasonably well against the Weighted station approach, However, Weighted pixels approach performed the best.

The results from the daily assessments were consistent with the monthly scale regression graphs and frequency distribution curves with the Weighted pixels having the best performance. This result is attributed to the method and weightings used in Weighted pixel approach being the same as for the Weighted station's approach, and the pixel values have been bias corrected against the station values. In addition, this could also mean that RS data was able to capture close values of point pixel rainfalls and that the bias correction method used was effective.

The results were the same for both catchments. The differences in Catchment S60A and Catchment U20F were the climatic regions, station density, and how the stations are distributed across the catchment which has an impact on the estimation of Thiessen weights.

A sensitivity analysis was done in Catchment U20F on the station's spatial density to estimate catchment rainfall using both Weighted stations and Weighted pixels approach. The estimations of catchment rainfall using three stations were compared with the estimation of catchment rainfall using the original selected stations (10). For this assessment, it was expected that there would be differences based on the assumption that more dense station distributions would estimate catchment rainfall more accurately. However, the results showed no considerable

differences between the catchment rainfalls that were estimated using three stations and 10 stations using the weighted stations and weighted pixels approaches. This could be because the 10 stations were not evenly distributed, and the 3 selected stations used had a higher weighted contributions to the total catchment rainfall when using the 10 stations. Overall, the results indicate the ability of local bias corrected RS CHIRPS data to provide accurate estimates of catchment rainfall because the results between catchment rainfall estimated using 3 and 10 stations by the weighted station's approach are similar to the results obtained using the weighted station's approach. In addition, RS is able to capture catchment rainfalls better at longer time scales.

The catchment 1-day design rainfalls were estimated up to a return period of 20 years. This was because of the limited record length used in the analysis due to the unavailability of quality rainfall beyond the year 2000. The estimated 1-day design catchment rainfall results were compared for the same approaches that were used to estimate catchment rainfalls for Catchment S60A and Catchment U20F, with the addition of the Driver pixel(ARFs).

In Catchment S60A, the Weighted pixels approach performed better than all other approaches and this was shown by the low value of MAE compared to the Weighted station's approach. In Catchment U20F, the Weighted pixel approach had the lowest MAE value. Corrected GEE approach also had a good performance with low value of MAE value compared to the Weighted station's approach. However, there was an unusually large value in the observed rainfall for Catchment U20F which was identified as an outlier and is believed to have influenced the smaller values of Weighted pixels approach and Corrected GEE approach because, with the removal of that observed value, the Weighted pixels approach was the best estimate of catchment 1-day design rainfall in Catchment U20F. While in practice the Corrected GEE will be more likely to be used to spatially estimate catchment rainfalls, it is important to acknowledge the traditional methods that make the use of RS point rainfalls to essentially estimate catchment rainfalls and catchment design rainfalls. Catchment rainfall from a single station by multiplied ARFs is commonly used in practice as the traditional method to estimate catchment design rainfall from a point, however, this approach (using point pixel value) only performed well in Catchment S60A compared to Catchment U20F.

Although the Weighted stations was assumed to be the best estimate of catchment rainfall in this study, there are limitations to this approach, and it will work best when there is a good spatial density of gauges.

This project aimed to use remotely sensed rainfall to improve the estimation of catchment rainfall for use in hydrological modelling and assess different methods of estimating both catchment rainfall and catchment design rainfall. This was undertaken to essentially address the challenge of a decreasing monitoring network with fewer stations with long records of rainfall data and the impacts of these when deriving catchment design rainfalls for flood studies in ungauged catchments. The bias corrected CHIRPS RS product was used to estimate remotely sensed catchment rainfall and, even though the performance of the RS products are location dependant, CHIRPS performed well for the selected study catchments. Approaches that use point observed rainfalls to estimate catchment rainfalls and catchment design rainfalls were successfully adjusted to use point pixel rainfalls and provided reasonable results. This study's aims and objectives have therefore been successfully met.

A limitation of this study was the record length available for the observed rainfall data at selected stations. This was due to the unavailability of rainfalls and the quality of observed rainfall data beyond the year 2000. Another limitation is the selection of catchments for use in the study which had an adequate number of stations with an even distribution of rainfall stations. These factors emphasize the need to use RS data in estimating rainfall. In addition, it was a challenge to obtain both RS and station data for the same daily time period (08:00 to 08:00 or 00:00 – 00:00) which could have had an impact on the results.

Overall, the results from using the bias corrected CHIRPS RS based data show good potential to estimate catchment rainfalls and 1-day catchment design rainfalls even though results from Catchment S60A and U20F varied. For example, accumulated plots and frequency distribution curves were good in Catchment S60A and poorer in Catchment U20F. This could be a result of the distribution of stations around the catchment. Both catchments had less dense stations, however, Catchment S60A had a good distribution of stations around the catchment. This had an impact on methods that involved the use of Thiessen weights as Thiessen weights are location dependant. To have more conclusive results on the daily catchment rainfalls comparison, it is recommended to assess the rain days in the observed and RS data and identify outliers. In Catchment U20F, sensitivity to spatial density and influence on Thiessen weights was done using 3 stations. For more conclusive results, it is recommended that future studies explore selection of different combination of stations to validate the results more and to analysis using the assigned bias correction rank values. It is of importance to note that the performance of the results presented are strictly for the catchments and stations selected for this project as

well as the methods selected to correct the bias. Therefore, it is recommended that a similar study is conducted in other regions where there is an even distribution of stations and a long record of quality observed rainfall (e.g. outside of South Africa) to increase the confidence in the estimation of design rainfalls.



## 7. REFERENCES

- Abtew, W, Obeysekera, J and Shih, GJ. 1995. Technical Notes: Spatial Variation of Daily Rainfall and Network Design. *American Society of Agricultural and Biological Engineers* 38 (3): 843-845.
- Adler, RF, Huffman, GJ, Chang, A, Ferraro, R, Xie, P-P, Janowiak, J, Rudolf, B, Schneider, U, Curtis, S and Bolvin, DJ. 2003. The version-2 global precipitation climatology project (GPCP) monthly precipitation analysis (1979–present). *Journal of Hydrometeorology* 4 (6): 1147-1167.
- Alexander, WJR. 1990. *Flood hydrology for southern Africa*. South African National Committee on Large Dams., Pretoria, South Africa.
- Allerup, P and Madsen, HJ. 1980. Accuracy of point precipitation measurements. *Hydrology Research* 11 (2): 57-70.
- Arnaud, P, Lavabre, J, Fouchier, C, Diss, S and Javelle, PJ. 2011. Sensitivity of hydrological models to uncertainty in rainfall input. *Hydrological Sciences Journal* 56 (3): 397-410.
- Artan, G, Gadain, H, Smith, JL, Asante, K, Bandaragoda, J, C and Verdin, JPJ. 2007. Adequacy of satellite derived rainfall data for stream flow modeling. *Natural Hazards* 43 (2): 167-185.
- Awange, J, Ferreira, V, Forootan, E, Andam-Akorful, S, Agutu, N and He, XJ. 2016. Uncertainties in remotely sensed precipitation data over Africa. *International Journal of Climatology: A Journal of the Royal Meteorological Society* 36 (1): 303-323.
- Ayugi, B, Tan, G, Ruoyun, N, Babaousmail, H, Ojara, M, Wido, H, Mumo, L, Ngoma, NH, Nooni, IK and Ongoma, VJW. 2020. Quantile mapping bias correction on rossby centre regional climate models for precipitation analysis over Kenya, East Africa. *Water* 12 (3): 801.
- Baboo, SS and Devi, MRJGJ. 2010. An analysis of different resampling methods in Coimbatore, District. *Global Journal of Computer Science and Technology* 75 (09): 4172.
- Bhatti, HA, Rientjes, T, Haile, AT, Habib, E and Verhoef, WJS. 2016. Evaluation of bias correction method for satellite-based rainfall data. *Sensors* 16 (6): 884.
- Blumenfeld, J. 2015. From TRMM to GPM: The Evolution of NASA Precipitation Data. [Internet]. NASA. Available from: <https://earthdata.nasa.gov/learn/articles/tools-and-technology-articles/trmm-to-gpm>. [Accessed: 15 March 2020].

- Chen, J, Brissette, FP, Chaumont, D and Braun, MJWRR. 2013. Finding appropriate bias correction methods in downscaling precipitation for hydrologic impact studies over North America. *Water Resources Research* 49 (7): 4187-4205.
- Chen, J, Wang, Z, Wu, X, Chen, X, Lai, C, Zeng, Z and Li, JJ. 2019. Accuracy evaluation of GPM multi-satellite precipitation products in the hydrological application over alpine and gorge regions with sparse rain gauge network. *Hydrology Research* 50 (6): 1710-1729.
- Ciach, GJJ. 2003. Local random errors in tipping-bucket rain gauge measurements. *Journal of Atmospheric Oceanic Technology* 20 (5): 752-759.
- Clark, D. 2019. *Development and assessment of an intergrated water resources accounting methodology for South Africa :Phase 2*. WRC Project K5/2512. Water Research Commission, Pretoria, South Africa.
- Darand, M and Zand, KS. 2016. Evaluation of the accuracy of the Global Precipitation Climatology Center (GPCC) data over Iran. *Iranian Journal of Geophysics* 10 (3): 95-113.
- Dee, DP, Uppala, SM, Simmons, A, Berrisford, P, Poli, P, Kobayashi, S, Andrae, U, Balmaseda, M, Balsamo, G and Bauer, DJ. 2011. The ERA-Interim reanalysis: Configuration and performance of the data assimilation system. *Quarterly Journal of the Royal Meteorological Society* 137 (656): 553-597.
- Dembélé, Moctar Zwart and %J, SJ. 2016. Evaluation and comparison of satellite-based rainfall products in Burkina Faso, West Africa. *International Journal of Remote Sensing* 37 (17): 3995-4014.
- Dent, M, Lynch, S and Schulze, R. 1989. *Mapping mean annual and other rainfall statistics in southern Africa*. Department of Agricultural Engineering. ACRU Report. University of Kwazulu-Natal, Durban, South Africa.
- Dinku, T, Funk, C, Peterson, P, Maidment, R, Tadesse, T, Gadain, H and Ceccato, PJ. 2018. Validation of the CHIRPS satellite rainfall estimates over eastern Africa. *Quarterly Journal of the Royal Meteorological Society* 144 (2): 292-312.
- Du Plessis, J and Kibii, JJJotSAIoCE. 2021. Applicability of CHIRPS-based satellite rainfall estimates for South Africa. *Journal of the South African Institution of Civil Engineering* 63 (3): 43-54.
- DWS. 2014. *Flood Frequency Estimation Methods*. Report No. 1060/1/03. Department of Water and Sanitation, Pretoria, South Africa.

- Enayati, M, Bozorg-Haddad, O, Bazrafshan, J, Hejabi, S and Chu, XJJoW. 2021. Bias correction capabilities of quantile mapping methods for rainfall and temperature variables. *Journal of Water and Climate Change* 12 (2): 401-419.
- Faisal, N and Gaffar, AJPJoM. 2012. Development of Pakistan's new area weighted rainfall using Thiessen polygon method. *Pakistan Journal of Meteorology* 9 (17): 1-10.
- Fang, G, Yang, J, Chen, Y and Zammit, C. 2014. Comparing bias correction methods in downscaling meteorological variables for hydrologic impact study in an arid area in China. *Hydrology and Earth System Sciences Discussions* 11 (11): 12659-12696.
- Frezghi, MS and Smithers, JJ. 2008. Merged rainfall fields for continuous simulation modelling (CSM). *Water SA* 34 (5): 523-528.
- Funk, C, Husak, G, Michaelsen, J, Love, T and Pedreros, D. 2007. Third generation rainfall climatologies: satellite rainfall and topography provide a basis for smart interpolation. *Proceedings of the JRC—FAO Workshop, Nairobi, Kenya*, 203.
- Funk, C, Michaelsen, J and Marshall, MT. 2017. Mapping Recent Decadal Climate Variations in Precipitation and Temperature across Eastern Africa. *United Nations Environment* 1097 (10): 354-578.
- Funk, C, Michaelsen, J and Marshall, MTJ. 2012. Mapping recent decadal climate variations in precipitation and temperature across eastern Africa. *Remote Sensing of Drought: Innovative Monitoring Approaches* 331 (7): 331-355.
- Funk, CC, Peterson, PJ, Landsfeld, MF, Pedreros, DH, Verdin, JP, Rowland, JD, Romero, BE, Husak, GJ, Michaelsen, JC and Verdin, APJ. 2014. A quasi-global precipitation time series for drought monitoring. *US Geological Survey data series* 832 (4): 1-12.
- Gericke, O and Du Plessis, JJWS. 2011. Evaluation of critical storm duration rainfall estimates used in flood hydrology in South Africa. *Water SA* 37 (4): 453-470.
- Gericke, OJ. 2018. Catchment response time and design rainfall: the key input parameters for design flood estimation in ungauged catchments. *Journal of the South African Institution of Civil Engineering* 60 (4): 51-67.
- Ghimire, U, Srinivasan, G and Agarwal, AJIJoC. 2019. Assessment of rainfall bias correction techniques for improved hydrological simulation. *International Journal of Climatology: A Journal of the Royal Meteorological Society* 39 (4): 2386-2399.
- Grimes, D, Pardo-Iguzquiza, E and Bonifacio, RJ. 1999. Optimal areal rainfall estimation using raingauges and satellite data. *Journal of Hydrology: Regional Studies* 222 (1-4): 93-108.

- Grody, NCJ. 1991. Classification of snow cover and precipitation using the Special Sensor Microwave Imager. *Journal of Geophysical Research: Atmospheres* 96 (D4): 7423-7435.
- Habib, E, Haile, AT, Sazib, N, Zhang, Y and Rientjes, TJ. 2014a. Effect of bias correction of satellite-rainfall estimates on runoff simulations at the source of the Upper Blue Nile. *Remote Sensing of Drought: Innovative Monitoring Approaches* 6 (7): 6688-6708.
- Habib, E, Haile, AT, Sazib, N, Zhang, Y and Rientjes, TJRS. 2014b. Effect of bias correction of satellite-rainfall estimates on runoff simulations at the source of the Upper Blue Nile. *Remote Sensing of Drought: Innovative Monitoring Approaches* 6 (7): 6688-6708.
- Haddad, K, Rahman, A and Green, J. 2011. Design rainfall estimation in Australia: a case study using L moments and generalized least squares regression. *Stochastic Environmental Research and Risk Assessment* 25 (6): 815-825.
- Harris, I, Jones, PD, Osborn, TJJ and %J, DH. 2014. Updated high-resolution grids of monthly climatic observations—the CRU TS3. 10 Dataset. *International Journal of Climatology: A Journal of the Royal Meteorological Society* 34 (3): 623-642.
- Haydon, S and Deletic, AJ. 2009. Model output uncertainty of a coupled pathogen indicator–hydrologic catchment model due to input data uncertainty. *Environmental Modelling Software* 24 (3): 322-328.
- Hersbach, H and Dee, DJ. 2016. ERA5 reanalysis is in production. *ECMWF Newsletter* 147 (7): 5-6.
- Hessels, TM. 2015. Comparison and validation of several open access remotely sensed rainfall products for the Nile Basin. Unpublished thesis, Department of Water Management, Delft University of Technology.
- Hoffmann, L, Günther, G, Li, D, Stein, O, Wu, X, Griessbach, S, Heng, Y, Konopka, P, Müller, R and Vogel, BJ. 2019. From ERA-Interim to ERA5: the considerable impact of ECMWF's next-generation reanalysis on Lagrangian transport simulations. *Atmospheric Chemistry Physics* 19 (5): 3097-3124.
- Hong, Y, Hsu, K-L, Sorooshian, S and Gao, XJ. 2004. Precipitation estimation from remotely sensed imagery using an artificial neural network cloud classification system. *Journal of Applied Meteorology* 43 (12): 1834-1853.
- Hosking, J, Wallis, JR and Wood, EFJHSJ. 1985. An appraisal of the regional flood frequency procedure in the UK Flood Studies Report. *Hydrological Sciences Journal* 30 (1): 85-109.

- Hu, Q, Li, Z, Wang, L, Huang, Y, Wang, Y and Li, LJW. 2019. Rainfall spatial estimations: A review from spatial interpolation to multi-source data merging. *Water* 11 (3): 579.
- Huffman, GJ, Adler, RF, Bolvin, DT and Nelkin, EJ. 2010. The TRMM multi-satellite precipitation analysis (TMPA). In: *Satellite rainfall applications for surface hydrology*. Springer.
- Hutchinson, PJ. 1974. Progress in the use of the method of optimum interpolation for the redesign of the Zambian raingauge network. *Geoforum* 5 (4): 49-62.
- Jinghao, ZCLLF, Yanli, HJMS and Technology. 2009. Development of Application Software on Agricultural Meteorology Database [J]. 3.
- Joyce, RJ, Janowiak, JE, Arkin, PA and Xie, PJ. 2004. CMORPH: A method that produces global precipitation estimates from passive microwave and infrared data at high spatial and temporal resolution. *Journal of hydrometeorology* 5 (3): 487-503.
- Joyce, RJ, Xie, P, Yarosh, Y, Janowiak, JE and Arkin, PA. 2010. CMORPH: A “morphing” approach for high resolution precipitation product generation. In: *Satellite rainfall applications for surface hydrology*. Springer.
- Katiraie-Boroujerdy, P-S, Rahnamay Naeini, M, Akbari Asanjan, A, Chavoshian, A, Hsu, K-I and Sorooshian, SJRS. 2020. Bias correction of satellite-based precipitation estimations using quantile mapping approach in different climate regions of Iran. *Remote Sensing of Drought: Innovative Monitoring Approaches* 12 (13): 2102.
- Kablouti, M, Ouerdachi, L and Boutaghane, HJ. 2012. Spatial interpolation of annual precipitation in Annaba-Algeria-comparison and evaluation of methods. *Energy Procedia* 18 468-475.
- Kruger, AC and Nxumalo, MJ. 2017. Historical rainfall trends in South Africa: 1921–2015. *Water SA* 43 (2): 285-297.
- Kummerow, C and Giglio, LJ. 1995. A method for combining passive microwave and infrared rainfall observations. *Journal of Atmospheric Oceanic Technology* 12 (1): 33-45.
- Kunz, RJ. 2004. Daily rainfall data extraction utility: User manual v 1.0. *Institute for Commercial Forestry Research, Pietermaritzburg, South Africa*.
- Lakew, HB, Moges, SA and Asfaw, DHJ. 2020. Hydrological performance evaluation of multiple satellite precipitation products in the upper Blue Nile basin, Ethiopia. *Journal of Hydrology: Regional Studies* 27 (4): 100-664.
- Liu, J, Duan, Z, Jiang, J and Zhu, AJ. 2015. Evaluation of three satellite precipitation products TRMM 3B42, CMORPH, and PERSIANN over a subtropical watershed in China. *Advances in Meteorology* 2015 (12): 151-239.

- Liu, Z, Ostrenga, D, Teng, W and Kempler, SJ. 2012. Tropical Rainfall Measuring Mission (TRMM) precipitation data and services for research and applications. *Bulletin of the American Meteorological Society* 93 (9): 1317-1325.
- Lynch, C, Hub, K, Atlas, MW, Water, S, Stuff, K, Guide, C, Water, F and Water, R. 2004. Development of a raster database of annual, monthly and daily rainfall for southern Africa. *Water SA*.
- Lynch, S. 2004. Development of a raster database of annual, monthly and daily rainfall for southern Africa. Report 1156/1/04. Water Research Commission, Pretoria, RSA.
- Maggioni, V, Meyers, PC and Robinson, MDJ. 2016. A review of merged high-resolution satellite precipitation product accuracy during the Tropical Rainfall Measuring Mission (TRMM) era. *Journal of Hydrometeorology* 17 (4): 1101-1117.
- Maidment, RI, Grimes, D, Allan, RP, Tarnavsky, E, Stringer, M, Hewison, T, Roebeling, R and Black, EJ. 2014. The 30 year TAMSAT African rainfall climatology and time series (TARCAT) data set. *Journal of Geophysical Research: Atmospheres* 119 (18): 10,619-10,644.
- Maidment, RI, Grimes, D, Black, E, Tarnavsky, E, Young, M, Greatrex, H, Allan, RP, Stein, T, Nkonde, E and Senkunda, SJ. 2017. A new, long-term daily satellite-based rainfall dataset for operational monitoring in Africa. *Scientific data* 4 170063.
- Makapela, L, Newby, T, Gibson, L, Majози, N, Mathieu, R, Ramoelo, A, Mengistu, M, Jewitt, G, Bulcock, H and Chetty, KJ. 2015. *Review of the use of Earth Observations Remote Sensing in Water Resource Management in South Africa*. Report No. KV329/15. Water Research Commission, Pretoria, South Africa.
- Maraun, DJJoC. 2013. Bias correction, quantile mapping, and downscaling: Revisiting the inflation issue. 26 (6): 2137-2143.
- Mashingia, F, Mtalo, F and Bruen, MJ. 2014. Validation of remotely sensed rainfall over major climatic regions in Northeast Tanzania. *Physics Chemistry of the Earth, Parts A/B/C* 67 (7): 55-63.
- Maswanganye, SE. 2018. A comparison of Remotely-Sensed Precipitation Estimates with observed data from rain Gauges in the Western Cape, South Africa. *Department of Earth Sciences, University of the Western Cape*
- Mei, Y, Nikolopoulos, EI, Anagnostou, EN, Zoccatelli, D and Borga, MJRS. 2016. Error analysis of satellite precipitation-driven modeling of flood events in complex alpine terrain. *Remote Sensing of Drought: Innovative Monitoring Approaches* 8 (4): 293.

- Mendez, M and Calvo-Valverde, LJPE. 2016. Assessing the performance of several rainfall interpolation methods as evaluated by a conceptual hydrological model. *Procedia Engineering* 154 (8): 1050-1057.
- Mishra, AKJ. 2013. Effect of rain gauge density over the accuracy of rainfall: a case study over Bangalore, India. *SpringerPlus* 2 (1): 311.
- Mitchell, TD and Jones, PDJ. 2005. An improved method of constructing a database of monthly climate observations and associated high-resolution grids. *International Journal of Climatology: A Journal of the Royal Meteorological Society* 25 (6): 693-712.
- Moulin, L, Gaume, E and Obled, CJH. 2009. Uncertainties on mean areal precipitation: assessment and impact on streamflow simulations. *Hydrology Earth System Sciences* 13 (2): 99-114.
- NCAR/UCAR. 2019. Climate Data Guide. [Internet]. NCAR. Available from: <https://climatedataguide.ucar.edu/climate-data>. [Accessed: 20 may 2020].
- Nomqophu, W. 2020. *Potential Remote Sensing technologies to enhance the monitoring and reporting of water flows*. WRC Report No. 486/1/95. Water Research Commission, Pretoria, South Africa.
- Novella, NS and Thiaw, WMJ. 2013. African rainfall climatology version 2 for famine early warning systems. *Journal of Applied meteorology Climatology* 52 (3): 588-606.
- Pegram, G, Scott, S, András, B, Plan, C, Hub, K, Atlas, MW, Water, S, Stuff, K, Guide, C, Water, F and Water, R. 2016. *New methods of infilling southern African raingauge records enhanced by annual, monthly and daily precipitation estimates tagged with uncertainty*. WRC Report No. 2241/1/15. Water SA, Pretoria, South Africa.
- Pietersen, J, Gericke, O, Smithers, J and Woyessa, YJJotSAIoCE. 2015. Review of current methods for estimating areal reduction factors applied to South African design point rainfall and preliminary identification of new methods. *Journal of the South African Institution of Civil Engineering* 57 (1): 16-30.
- Pike, A. 2004. *CalcPPTCor : A Utility to Assist in the Selection of Rainfall Stations and Adjustment of Rainfall Data*. In: Schulze, R.E. and Pike, A. (Eds). *Development and Evaluation of an Installed Hydrological Modelling System*. WRC Report, 1155/1/04. . Water Research Commission, Pretoria, South Africa.
- Pitman, WJWS. 2011. Overview of water resource assessment in South Africa: Current state and future challenges. 37 (5): 659-664.
- Pombo, S, de Oliveira, RP and Mendes, AJ. 2015. Validation of remote-sensing precipitation products for Angola. *Meteorological Applications* 22 (3): 395-409.

- Raybaut, PJAopo. 2009. Spyder-documentation.
- Rudolf, B and Schneider, U.2005. Calculation of gridded precipitation data for the global land-surface using in-situ gauge observations. *Proc. Second Workshop of the Int. Precipitation Working Group*, 231-247.
- SANRAL. 2013. *Drainage Manual (Sixth Edition)*. South African National Roads Agency Ltd, Pretoria, South Africa.
- Sawunyama, T and Hughes, DJ. 2008. Application of satellite-derived rainfall estimates to extend water resource simulation modelling in South Africa. *Water SA* 34 (1): 1-10.
- Schulze, R, Maharaj, M, Warburton, M, Gers, C, Horan, M, Kunz, R and Clark, DJ. 2007. *South African atlas of climatology and agrohydrology*. WRC Report 06/01/95. Water Research Commission, Pretoria, South Africa.
- Schulze, RE. 1995. *Hydrology and agrohydrology: A text to accompany the ACRU 3.00 agrohydrological modelling system*. WRC Report TT69/95. Water Research Commission, Pretoria, RSA.
- Shayeghi, A, Azizian, A and Brocca, LJ. 2020. Reliability of reanalysis and remotely sensed precipitation products for hydrological simulation over the Sefidrood River Basin, Iran. *Hydrological Sciences Journal* 65 (2): 296-310.
- Shepard, D.1968. A two-dimensional interpolation function for irregularly-spaced data. *Proceedings of the 1968 23rd ACM National Conference*, 517-524.
- Shrestha, M, Artan, G, Bajracharya, S, Gautam, D and Tokar, SJJofRM. 2011. Bias-adjusted satellite-based rainfall estimates for predicting floods: N arayani B asin. *Journal of Flood Risk Management* 4 (4): 360-373.
- Smithers, J, Pegram, G and Schulze, R. 2002. Design rainfall estimation in South Africa using Bartlett–Lewis rectangular pulse rainfall models. *Journal of Hydrology* 258 (1-4): 83-99.
- Smithers, J, Rowe, T, Horan, M and Schulze, RJ. 2018. Development and assessment of rules to parameterise the ACRU model for design flood estimation. *Water SA* 44 (1): 93-104.
- Smithers, J and Schulze, R. 2004b. The estimation of design rainfalls for South Africa using a regional scale invariant approach. *Water SA* 30 (4): 435-444.
- Smithers, JaS, RE. 1995. ACRU Agrohydrological modelling system: User Manual Version 3.00. Report TT 70/95. Water Research Commission, Pretoria, RSA.
- Smithers, JaS, RE. 2000. *Development and evaluation of techniques for estimating short duration design rainfall in South Africa*. WRC Report No. 681/1/00. , . Water Research Commission, Pretoria, South Africa.



- Smithers, JC and Schulze, R. 2003. *Design rainfall and flood estimation in South Africa*. Water Research Commission, Pretoria, South Africa.
- Smithers, JJ. 1996. Short-duration rainfall frequency model selection in Southern Africa. *Water SA* 22 (3): 211-217.
- Soriano, E, Mediero, L and Garijo, C.2018. Selection of bias correction methods to assess the impact of climate change on flood frequency curves. *Multidisciplinary Digital Publishing Institute Proceedings*, 14.
- Stellman, KM, Fuelberg, HE, Garza, R and Mullusky, MJW. 2001. An examination of radar and rain gauge-derived mean areal precipitation over Georgia watersheds. *Weather Forecasting* 16 (1): 133-144.
- Suleman, S. 2017. Assessment of satellite derived rainfall and its use in the ACRU hydrological model. Unpublished thesis.
- Suleman, S, Chetty, K, Clark, D and Kapangaziwiri, EJWS. 2020. Assessment of satellite-derived rainfall and its use in the ACRU agro-hydrological model. 46 (4): 547-557.
- Suleman, S, Chetty, KT, Clark, DJ and Kapangagaziwiri, E. 2020. Assessment of satellite-derived rainfall and its use in the ACRU agro-hydrological model. *Water SA* 46 (4): 547–557. .
- Taesombat, W and Sriwongsitanon, NJS. 2009. Areal rainfall estimation using spatial interpolation techniques. *Science Asia* 35 (3): 268-275.
- Thépaut, JN, Courtier, P, Belaud, G and Lemaître, GJ. 1996. Dynamical structure functions in a four-dimensional variational assimilation: A case study. *Quarterly Journal of the Royal Meteorological Society* 122 (530): 535-561.
- Thorne, V, Coakeley, P, Grimes, D and Dugdale, GJ. 2001. Comparison of TAMSAT and CPC rainfall estimates with raingauges, for southern Africa. *International Journal of Remote Sensing* 22 (10): 1951-1974.
- Tyson, PD, Preston-Whyte, R and Schulze, R. 1976. *The climate of the Drakensberg*. Town and Regional Planning Commission, Durban, South Africa.
- Van der Spuy, D and Rademeyer, PJDoW. 2016. Flood frequency estimation methods as applied in the Department of Water and Sanitation. *Department of Water Sanitation* 203 (3): 371.
- Wilheit, TT, Chang, AT and Chiu, LSJ. 1991. Retrieval of monthly rainfall indices from microwave radiometric measurements using probability distribution functions. *Journal of Atmospheric Oceanic Technology* 8 (1): 118-136.

- Wood, S, Jones, D and Moore, R. 2000. Accuracy of rainfall measurement for scales of hydrological interest. *Centre for Ecology and Hydrology* 4 (4): 531-543.
- Xie, P, Joyce, R, Wu, S, Yoo, S-H, Yarosh, Y, Sun, F and Lin, RJ. 2017. Reprocessed, bias-corrected CMORPH global high-resolution precipitation estimates from 1998. *Journal of Hydrometeorology* 18 (6): 1617-1641.
- Xu, H, Xu, C-Y, Chen, H, Zhang, Z and Li, LJ. 2013. Assessing the influence of rain gauge density and distribution on hydrological model performance in a humid region of China. *Journal of Hydrology: Regional Studies* 505 (4): 1-12.
- Xu, Y-P and Tung, Y-K. 2008. Constrained scaling approach for design rainfall estimation. *Stochastic Environmental Research and Risk Assessment* 23 (6): 697-705.
- Yang, T, Xu, C-Y, Shao, Q-X and Chen, X. 2010. Regional flood frequency and spatial patterns analysis in the Pearl River Delta region using L-moments approach. *Stochastic Environmental Research and Risk Assessment* 24 (2): 165-182.
- Yeh, N-C, Chuang, Y-C, Peng, H-S and Hsu, K-LJA-PJoAS. 2020. Bias Adjustment of Satellite Precipitation Estimation Using Ground-Based Observation: Mei-Yu Front Case Studies in Taiwan. *Asia-Pacific Journal of Atmospheric Sciences* 56 (3): 485-492.

## 8. APPENDIX A: PYTHON CODE TO EXTRACT CHIRPS RAINFALL DATA FROM MULTIPLE STATIONS

```
import geopandas as gpd
import os
import rasterio
import scipy.sparse as sparse
import pandas as pd
import numpy as np

# Create an empty pandas DataFrame called 'table'
table = pd.DataFrame(index = np.arange(0,1))

# Read the points shapefile using geopandas
stations = gpd.read_file('D:/CHIRPS RSDATA/CHIRPS
TS/Shapefiles/S81A_Stations.shp')
stations['Lon'] = stations['geometry'].x
stations['Lat'] = stations['geometry'].y

Matrix = pd.DataFrame()

# Iterate through the rasters and save the data as individual arrays to a
Matrix
for files in os.listdir(r'D:\CHIRPS RSDATA\CHIRPS TS'):
    print(files)
    if files[-4:] == '.tif':
        dataset = rasterio.open(r'D:\CHIRPS RSDATA\CHIRPS TS'+'\'+files)
        data_array = dataset.read(1)
        data_array_sparse = sparse.coo_matrix(data_array, shape =
(320,300))
        data = files[ :-4]
        Matrix[data] = data_array_sparse.toarray().tolist()
        print('processing is done for the raster: '+ files[ :-4])

# Iterate through the stations and get the corresponding row and column for
the related x,y coordinates
for index, row in stations.iterrows():
    station_name = str(row['ClimNo'])
    Lon = float(row['Lon'])
    Lat = float(row['Lat'])
    x,y = (Lon, Lat)
    row, col = dataset.index(x,y)
    print('processing:'+ station_name)

    # pick the rainfall value from each stored raster array and record it
into the previously created 'table'
    for records_date in Matrix.columns.tolist():
        a = Matrix[records_date]
        rf_value = a.loc[int(row)][int(col)]
        table[records_date] = rf_value
        transpose_mat = table.T
        transpose_mat.rename(columns = {0: 'Rainfall(mm)'}Ghimire et al.,
2019Maraun (2013), inplace = True)

transpose_mat.to_csv(r'D:\CHIRPS RSDATA\CHIRPS
TS\Rainfalls'+'\'+station_name+'.csv')
```

## 9. APPENDIX B: PYTHON SCRIPT TO EXTRACT CHIRPS RAINFALL DATA FROM A SINGLE STATION

```
import rasterio
import numpy as np
import os
import pandas as pd

table = pd.DataFrame(0, index = np.arange(1,14611), columns = ['Date',
'Rainfall(mm)'])
i = 0

for files in os.listdir(r'D:\CHIRPS RSDATA\CHIRPS(2006-2010)'):
    if files [-4:] == '.tif':
        i = i + 1
        dataset = rasterio.open(r'D:\CHIRPS RSDATA\CHIRPS(2006-
2010)+'\\'+files)
        x,y = (30.5297 , -29.3519)
        row, col = dataset.index(x,y)
        data_array = dataset.read(1)

        # copy the date to the 'Date' column in table during each
iteration
        table['Date'].loc[i] = files[:-4]

        #Fill in the rainfall value
        table['Rainfall(mm)'].loc[i] = data_array[int(row), int(col)]

        #Export the table file into a .csv
        table.to_csv(r'D:\CHIRPS RSDATA\CHIRPS(2006-2010)\Time
Series\Rainfall.csv')
```

## 10. APPENDIX C: CODE TO EXTRACT RESAMPLED CHIRPS DAILY RAINFALL IN GOOGLE EARTH ENGINE

```
Var chirps: ImageCollection "CHIRPS Daily...
  type: ImageCollection
  id: UCSB-CHG/CHIRPS/DAILY
  version: 1637190448908736
  bands: []
  properties: Object (25 properties)
    date_range: [347155200000,1632960000000]
    description: <p>Climate Hazards Group InfraRed Precipitation with
    Station data (CHIRPS)
    is a 30+ year quasi-global rainfall dataset. CHIRPS incorporates
    0.05° resolution satellite imagery with in-situ station data
    to create gridded rainfall time series for trend analysis and
    seasonal
    drought monitoring.</p><p><b>Resolution</b><br>5566 meters
    </p><p><b>Cadence</b><br>
    1 day
    </p><p><b>Bands</b><table class="eecat"><tr><th
    scope="col">Name</th><th
    scope="col">Description</th></tr><tr><td>precipitation</td><td><p>
    Precipitation</p></td></tr></table><p><b>Terms of
    Use</b><br><p>This datasets are in the public domain. To the
    extent possible under law,
    <a href="https://chc.ucsb.edu/people/pete-peterson">Pete
    Peterson</a>
    has waived all copyright and related or neighboring rights to
    Climate Hazards Group Infrared Precipitation with Stations
    (CHIRPS).</p><p><b>Suggested citation(s)</b><ul><li><p>Funk,
    Chris, Pete Peterson, Martin Landsfeld, Diego Pedreros, James
    Verdin, Shraddhanand Shukla, Gregory Husak, James Rowland, Laura
    Harrison, Andrew Hoell & Joel Michaelson. &quot;The climate
    hazards infrared precipitation with stations—a new environmental
    record for monitoring extremes&quot;. Scientific Data 2, 150066.
    <a
    href="https://doi.org/10.1038/sdata.2015.66">doi:10.1038/sdata.201
    5.66</a> 2015.</p></li></ul><style>
    table.eecat {
    border: 1px solid black;
    border-collapse: collapse;
    font-size: 13px;
    }
    table.eecat td, tr, th {
    text-align: left; vertical-align: top;
    border: 1px solid gray; padding: 3px;
    }
    td.nobreak { white-space: nowrap; }
    </style>
    keywords: List (6 elements)
    period: 1
    period_mapping: [347155200000,1632960000000]
    product_tags: List (4 elements)
    provider: UCSB/CHG
    provider_url: https://chc.ucsb.edu/data/chirps
```

```

sample: https://mw1.google.com/ges/dd/images/CHIRPS_sample.png
source_tags: ["ucsb","chg"]
system:is_global: 1
system:visualization_0_bands: precipitation
system:visualization_0_max: 17.0
system:visualization_0_min: 1.0
system:visualization_0_name: Precipitation
system:visualization_0_palette: 001137,0aab1e,e7eb05,ff4a2d,e90000
tags: List (6 elements)
thumb: https://mw1.google.com/ges/dd/images/CHIRPS_thumb.png
title: CHIRPS Daily: Climate Hazards Group InfraRed Precipitation
With Station Data (Version 2.0 Final)
type_name: ImageCollection
visualization_0_bands: precipitation
visualization_0_max: 17.0
visualization_0_min: 1.0
visualization_0_name: Precipitation
visualization_0_palette: 001137,0aab1e,e7eb05,ff4a2d,e90000

```

```

Var table : Table users/RS_DATA/S60A_Stations

```

```

  type: FeatureCollection
  id: users/RS_DATA/S60A_Stations
  version: 1636107686776604
  columns: Object (10 properties)
    ClimNo: String
    Concat: String
    Current_Or: String
    Lat: Float
    Lon: Float
    Province: String
    Record_Cou: Float
    StasName: String
    Year: Float
    system:index: String
  properties: Object (1 property)
    system:asset_size: 12359

```

```

Map.centerObject(station, 4)

```

```

var dontsa = station.filter(ee.Filter.eq('StasName', 'DONTSA PLANTATION'))

```

```

print(station)
var CHIRPS= chirps;
//The CHIRPS data is from 1981-01-01 to 2016-02-27
var precipAllYear = CHIRPS.filterDate('1981-01-01', '1981-03-31'); //change
the date here

```

```

var TS5 = ui.Chart.image.series(precipAllYear, dontsa, ee.Reducer.mean(),500,
'system:time_start').setOptions({
  title: 'Precipitation Full Time Series',
  vAxis: {title: 'mm/pentad'},
});

```

```

print(TS5);//

```

```

var chart = ui.Chart.image.series(
  precipAllYear.select(['precipitation']), station, ee.Reducer.mean(), 500)

```

```
.setSeriesNames(['daily-Prec'])  
.setOptions({  
  title: 'daily-Prec',  
  lineWidth: 1,  
  pointSize: 3,  
});
```

```
Map.addLayer(station);
```

```
Map.centerObject(station, 4)
```

## 11. APPENDIX D: A CODE TO ETRACT CHIRPS CATCHMENT RAINFALL FROM THE GOOGLE EARTH ENGINE

```
///1. Add region of interest
var ROI = S81A
Map.addLayer(ROI, {}, 'ROI')
Map.centerObject(ROI, 10)

///2. Define time of interest
// Ensure that the first image that is collected possesses data to
calculate NDVI otherwise the script will not work as required
var startdate = '2000-01-01'
var enddate = '2021-01-01'

var years = ee.List.sequence(ee.Date(startdate).get('year'),
ee.Date(enddate).get('year'));

// -----
// CHIRPS Daily Rainfall Data
// -----

/// Import image collections, filter by date and ROI, apply cloud mask
and clip to ROI

/// ERA5 Daily aggregates - Latest climate reanalysis produced by ECMWF
/ Copernicus Climate Change Service
var Rainfall = ee.ImageCollection('CHIRPS/DAILY')
  .filterBounds(ROI)
  .filterDate(startdate, enddate)
  .map(function(image){return image.clip(ROI)})
  .select("total_precipitation")

///Create a function to assign a time for every feature
var pointsmean = function(image) {
  var means = image.reduceRegions({
    collection: ROI, // used to be ROI.select(['Id'])
    reducer: ee.Reducer.mean(),
  })
}

/// assign time for every feature
means = means.map(function(f) { return f.set({date:
image.date().format("YYYY-MM-dd")}) })

  return means.copyProperties(image)
};

// Sort data in chronological order and select the date and mean
variables
var finalRainfall = Rainfall.map(pointsmean).flatten()
  .sort('date', true)
  .select(['date', 'mean'])
print(finalRainfall.limit(100), 'Rainfall')

// Export the mean rainfall for each polygon as a .csv file
Export.table.toDrive({
```



```
collection: finalRainfall,  
  description: 'CHIRPS_Rainfall'+startdate+'TO'+enddate,  
  folder: 'Genus_Exchange_GEE_Data',  
  fileFormat: 'CSV'  
});
```

## 12. APPENDIX E: EXAMPLES OF EXCEL SPREADSHEETS

Table E.1: An example spreadsheet of calculation of bias correction factors.

Day(Obs)	Observed rainfall	Day (Sim)	RS rainfall	Rank	Percentile	Correction Factors	Day (Sim)	Corrected RS rainfall	Day (Sim) sorted	Corrected RS rainfall sorted
01/01/1981	0	01/01/1981	0	1	0.0136874	0	01/01/1981	0	01/01/1981	0
03/01/1981	0	02/01/1981	0	2	0.0273748	0	02/01/1981	0	02/01/1981	0
04/01/1981	0	03/01/1981	0	3	0.0410621	0	03/01/1981	0	03/01/1981	0
07/01/1981	0	04/01/1981	0	4	0.0547495	0	04/01/1981	0	04/01/1981	0
08/01/1981	0	05/01/1981	0	5	0.0684369	0	05/01/1981	0	05/01/1981	0
10/01/1981	0	06/01/1981	0	6	0.0821243	0	06/01/1981	0	06/01/1981	0
11/01/1981	0	07/01/1981	0	7	0.0958117	0	07/01/1981	0	07/01/1981	0
12/01/1981	0	08/01/1981	0	8	0.109499	0	08/01/1981	0	08/01/1981	0
13/01/1981	0	10/01/1981	0	9	0.1231864	0	10/01/1981	0	09/01/1981	11.9
14/01/1981	0	11/01/1981	0	10	0.1368738	0	11/01/1981	0	10/01/1981	0
15/01/1981	0	12/01/1981	0	11	0.1505612	0	12/01/1981	0	11/01/1981	0
16/01/1981	0	13/01/1981	0	12	0.1642486	0	13/01/1981	0	12/01/1981	0
17/01/1981	0	15/01/1981	0	13	0.1779359	0	15/01/1981	0	13/01/1981	0
20/01/1981	0	16/01/1981	0	14	0.1916233	0	16/01/1981	0	14/01/1981	8.6
23/01/1981	0	19/01/1981	0	15	0.2053107	0	19/01/1981	0	15/01/1981	0
27/01/1981	0	20/01/1981	0	16	0.2189981	0	20/01/1981	0	16/01/1981	0
28/01/1981	0	22/01/1981	0	17	0.2326855	0	22/01/1981	0	17/01/1981	12.5
30/01/1981	0	23/01/1981	0	18	0.2463728	0	23/01/1981	0	18/01/1981	13.1
02/02/1981	0	27/01/1981	0	19	0.2600602	0	27/01/1981	0	19/01/1981	0
03/02/1981	0	28/01/1981	0	20	0.2737476	0	28/01/1981	0	20/01/1981	0
05/02/1981	0	29/01/1981	0	21	0.287435	0	29/01/1981	0	21/01/1981	4.7
09/02/1981	0	01/02/1981	0	22	0.3011224	0	01/02/1981	0	22/01/1981	0
10/02/1981	0	02/02/1981	0	23	0.3148097	0	02/02/1981	0	23/01/1981	0
11/02/1981	0	03/02/1981	0	24	0.3284971	0	03/02/1981	0	24/01/1981	6.5
12/02/1981	0	04/02/1981	0	25	0.3421845	0	04/02/1981	0	25/01/1981	19.4
13/02/1981	0	08/02/1981	0	26	0.3558719	0	08/02/1981	0	26/01/1981	3.6
14/02/1981	0	09/02/1981	0	27	0.3695593	0	09/02/1981	0	27/01/1981	0
15/02/1981	0	10/02/1981	0	28	0.3832466	0	10/02/1981	0	28/01/1981	0

Table E.2: An example of the calculation of catchment rainfall using areal weights

Hydr_Years	0270260A		0270205A		0270086A		0270023A		0270021W		02701645S		0269647W		0269712W		0269744S		0269775S		CR
Sta_Weights	0.06		0.09		0.05		0.11		0.29		0.08		0.14		0.14		0.01		0.03		1
01/01/1981	0	0	3.5	0.315	1.9	0.095	1	0.11	4.5	1.305	7	0.56	0	0	0	0	3.6	0.036	0	0	2.421
02/01/1981	10.1	0.61	1.6	0.144	0	0	0.9	0.099	0	0	1	0.08	9.5	1.33	0	0	6.4	0.064	0	0	2.323
03/01/1981	0	0	0	0	3.5	0.175	2.2	0.242	0	0	0	0	0	0	0	0	0	0	2	0.06	0.477
04/01/1981	0	0	4.4	0.396	0.1	0.005	0.1	0.011	6.5	1.885	3	0.24	0	0	0	0	0	0	0	0	2.537
05/01/1981	4	0.24	0	0	0	0	4.4	0.484	1	0.29	1.5	0.12	0	0	23	3.22	9	0.09	0	0	4.444
06/01/1981	2.5	0.15	0	0	0	0	0.6	0.066	0	0	0.7	0.056	8	1.12	2	0.28	4.4	0.044	0	0	1.716
07/01/1981	0	0	0	0	6.4	0.32	7.3	0.803	0	0	0	0	0	0	0	0	0	0	18	0.54	1.663
08/01/1981	0	0	5.8	0.522	0	0	3.5	0.385	24	6.96	9.5	0.76	41.5	5.81	19.5	2.73	18.4	0.184	0	0	17.351
09/01/1981	6.2	0.37	0	0	0	0	0.6	0.066	0	0	0	0	0	0	0	0	4.6	0.046	0	0	0.484
10/01/1981	0	0	0	0	2.1	0.105	1.7	0.187	0	0	0	0	0	0	0	0	0	0	3	0.09	0.382
11/01/1981	0	0	0.6	0.054	0	0	1.4	0.154	2.4	0.696	0	0	0	0	3	0.42	2.6	0.026	4	0.12	1.47
12/01/1981	0	0	0	0	0	0	0.1	0.011	0	0	0	0	0	0	0.5	0.07	1	0.01	0	0	0.091
13/01/1981	0	0	0	0	1.5	0.075	1.7	0.187	0	0	0	0	0	0	0	0	0	0	4	0.12	0.382
14/01/1981	0	0	1.2	0.108	0	0	1.2	0.132	0	0	1.6	0.128	7	0.98	6.5	0.91	8.6	0.086	0	0	2.344
15/01/1981	0	0	0	0	0	0	0.2	0.022	0	0	0.5	0.04	4	0.56	1	0.14	2.4	0.024	0	0	0.786
16/01/1981	0	0	0	0	3.1	0.155	5.2	0.572	0	0	0	0	0	0	16.7	2.338	0	0	3	0.09	3.155
17/01/1981	0	0	3	0.27	17.5	0.875	16.4	1.804	0	0	3.5	0.28	6	0.84	16.8	2.352	12.6	0.126	20	0.6	7.147
18/01/1981	5	0.3	14	1.26	0	0	0.9	0.099	84	24.36	24.5	1.96	30	4.2	0	0	28	0.28	2	0.06	32.519
19/01/1981	16	0.96	0	0	0.7	0.035	2.5	0.275	0	0	0	0	0	0	0	0	0	0	3	0.09	1.36
20/01/1981	0	0	0	0	2.7	0.135	1.4	0.154	0	0	7	0.56	8	1.12	0	0	0.2	0.002	0	0	1.971
21/01/1981	18.5	1.11	2.2	0.198	1.9	0.095	4.6	0.506	4.5	1.305	7.5	0.6	0	0	7	0.98	13.6	0.136	3	0.09	5.02
22/01/1981	4	0.24	0.5	0.045	11.8	0.59	6.4	0.704	0	0	0.3	0.024	0	0	0.5	0.07	0	0	0	0	1.673
23/01/1981	0	0	12	1.08	10.5	0.525	8.2	0.902	0	0	10.5	0.84	0	0	7.5	1.05	7.6	0.076	7	0.21	4.683
24/01/1981	11	0.66	8.3	0.747	3.5	0.175	2.8	0.308	0	0	7.5	0.6	21	2.94	0	0	6.8	0.068	0	0	5.498
25/01/1981	6.2	0.37	6.2	0.558	0	0	5.4	0.594	27	7.83	4	0.32	6.5	0.91	27	3.78	3.4	0.034	0	0	14.398
26/01/1981	4	0.24	0	0	0	0	0.4	0.044	0	0	0	0	0	0	0	0	0	0	0	0	0.284

Table E.3: Results of the catchment median rainfalls, station median rainfalls, and the adjustment factors for the selected driver station in Catchment S60A.

Month	Station Median	Catchment Median	Catchment/station
Jan	123	89.46087	0.727324146
Feb	108	97.626087	0.90394525
Mar	106	97.652174	0.921246925
Apr	55	47.313043	0.860237145
May	9	24.008696	2.667632889
Jun	15	13.252174	0.883478267
Jul	8	10.504348	1.3130435
Aug	18	19.2	1.066666667
Sep	50	36.547826	0.73095652
Oct	88	70.052174	0.796047432
Nov	122	79.582609	0.652316467
Dec	93	80.982609	0.870780742

Table E.4: Results of the catchment median rainfalls, station median rainfalls, and the adjustment factors for the selected driver pixel in catchment U20F.

Month	Station Median	Catchment Median	Catchment/station
Jan	122.011	145.876712	1.195602954
Feb	90.6065	140.19863	1.547335235
Mar	100.5435	114.239726	1.136221894
Apr	38.919	53.486301	1.374297926
May	15.76	17.458904	1.107798477
Jun	12.115	6.308219	0.520694924
Jul	9.6515	8.486301	0.879272756
Aug	20.705	20.910959	1.009947307
Sep	29.476	44.760274	1.51853284
Oct	88.486	89.541096	1.011923875
Nov	112.163	118.993151	1.060894867
Dec	126.882	140.19863	1.10495287

### 13. APPENDIX F: CODE TO ESTIMATE CATCHMENT DESIGN RAINFALLS IN THE R-STUDIO

```
## load catchment data ##

data <- read.table("Daily_Peaks.csv", header=T, sep = ",", col.names = c("Date",
"Obs_Qpeak"), as.is = TRUE)

## Data in date format ##

data$Date <- as.POSIXct(data$Date, "%Y/%m/%d", tz = "UTC")

## Data in date time format ##

#data$Date <- as.POSIXct(data$Date, "%Y/%m/%d %H:%M", tz = "UTC")

### AMS Extraction Per Hydro Year and GEV Fitting ####

Start <- min(data$Date)

End <- max(data$Date)

Start.year <- format(Start,"%Y")

Start.year <- as.numeric(Start.year)+1

End.year <- format(End,"%Y")

End.year <- as.numeric(End.year)

Length <- (End.year-Start.year)+2

require(lubridate)

## DATA MUST START IN JANUARY - OTHERWISE CHANGE THIS TO MAKE THE START MONTH
OCTOBER

month(Start) <- month(Start) + 9

## Use vector of November 1st dates to cut data into hydro-years
```

```

breaks <- seq(as.POSIXct(Start, tz = "UTC"), length=Length, by="year")

data$hydroYear <- cut(data$Date, breaks, labels=Start.year:End.year)

require(data.table)

Data <- as.data.table(data)

AMS <- Data[Data[, .I[Obs_Qpeak == max(Obs_Qpeak)], by=hydroYear]$V1]

## Certain AMS values can be removed if desired to match other record lengths
##

AMS <- AMS[!duplicated(AMS$hydroYear), ]

AMS <- AMS[-c(1),]

AMS <- AMS[order(Obs_Qpeak, decreasing = T)]

L2 <- (length(AMS$hydroYear))

AMS <- cbind(AMS, "Rank" = c(1:L2))

AMS <- cbind(AMS, "RP" = (L2+1)/(AMS$Rank))

library(extRemes)

# Fit GEV Dist to AMS #

fit_AMS <- fevd(AMS$Obs_Qpeak, AMS, method = "Lmoments", units="mm")

GEV_out_and_ciAMS <- (ci(fit_AMS, return.period=c(2,5,10,20, 50, 100,200)))

GEV_out_and_ci_AMS <- as.data.frame(GEV_out_and_ciAMS[1:7,1:3])

GEV_out_and_ci_AMS <- cbind(GEV_out_and_ci_AMS, "RP" = c(2,5,10,20, 50, 100,
200))

library(ggplot2)

ggplot() +

```

```

geom_line(data = GEV_out_and_ci_AMS, aes(x = GEV_out_and_ci_AMS$RP, y =
GEV_out_and_ci_AMS$Estimate, colour = "GEV Obs")) +

#geom_line(data = GEV_out_and_ci_AMS, aes(x = GEV_out_and_ci_AMS$RP, y =
GEV_out_and_ci_AMS$`2.5%`), linetype = "dashed", color = "red") +

#geom_line(data = GEV_out_and_ci_AMS, aes(x = GEV_out_and_ci_AMS$RP, y =
GEV_out_and_ci_AMS$`97.5%`), linetype = "dashed", color = "red") +

geom_point(data = AMS, aes(x = RP, y = AMS$Obs_Qpeak, colour = "GEV Obs"),
size = 1) +

scale_colour_manual("",
                    breaks = c("GEV Obs"),
                    values = c("red")) +

ylab("Rainfall (mm)") +

xlab("Return Period (Years)") +

scale_x_log10(expand = c(0, 0), breaks = c(2,5,10,20,50,100,200), limits =
c(1,200))+

#coord_cartesian(ylim=c(0,40)) - use to avoid warnings if limiting y-axis
range

#scale_y_continuous(limits = c(0,15)) +

theme_bw() +

theme(axis.text = element_text(size=12), axis.title = element_text(size = 12,
face = "bold"))+

theme(legend.position = "bottom")

```

## 14. APPENDIX G: RESULTS OF BIAS CORRECTION STATISTICS IN CATCHMENT S60A

Table G.1: Bias correction statistics at a daily scale

Station	Rainfall	MBE	RMSE	MAE	D	% BIAS
0079396 2	RAW	0.31	8.15	3.17	0.37	31
	CORRECTED	-0.06	7.57	2.85	0.42	-6
0079485 1	RAW	-0.26	10.21	3.1	0.3	-26
	CORRECTED	-0.072	11.041	4.12	0.32	-7.2
0079490 X	RAW	-0.49	9.05	3.78	0.33	-49
	CORRECTED	-0.34	9.29	3.89	0.35	-34
0079632 6	RAW	-0.5	10	3.94	0.34	-50
	CORRECTED	-0.19	10.84	4.19	0.34	-19
0079730 0	RAW	-0.4	8.41	3.56	0.41	-40
	CORRECTED	-0.36	8.21	3.56	0.43	-36
0079754 2	RAW	0.146	9.92	3.67	0.28	14.6
	CORRECTED	-0.017	10.11	3.57	0.311	-1.7
0101719A8	RAW	0.34	7.89	3.25	0.35	34
	CORRECTED	-0.2	6.87	2.8	0.36	-20

Table G.2: Bias correction statistics at a monthly scale

Station	Rainfall	MBE	RMSE	MAE	D	% BIAS
0079396 2	RAW	9.459	28.506	20.96	0.92	945.9
	CORRECTED	-1.78	26.23	18.41	0.923	-178
0079485 1	RAW	-7.885	36.348	24.365	0.915	-788.5
	CORRECTED	-2.197	33.483	22.987	0.937	-219.7
0079490 X	RAW	-15.044	40.414	26.758	0.892	-1504.4
	CORRECTED	-10.304	38.97	25.976	0.902	-1030.4
0079632 6	RAW	-15.213	42.614	28.561	0.9	-1521.3
	CORRECTED	-5.655	38.83	26.559	0.926	-565.5
0079730 0	RAW	-12.085	31.248	21.425	0.928	-1208.5
	CORRECTED	-10.979	32.504	22.273	0.919	-1097.9
0079754 2	RAW	4.442	44.176	26.759	0.87	444.2
	CORRECTED	-0.503	43.892	25.977	0.873	-50.3
0101719A8	RAW	10.19	32.438	21.913	0.907	1019
	CORRECTED	-6.081	27.229	18.73	0.913	-608.1



Table G 3: Bias correction statistics at an annual scale

Station	Rainfall	MBE	RMSE	MAE	D	% BIAS
0079396 2	RAW	113.513	144.154	122.726	0.744	11351.3
	CORRECTED	-21.35	88.699	73.51	0.886	-2135
0079485 1	RAW	-94.617	140.194	111.701	0.8	-9461.7
	CORRECTED	-26.365	103.307	80.975	0.902	-2636.5
0079490 X	RAW	-180.532	224.263	180.532	0.605	-18053.2
	CORRECTED	-123.645	186.056	132.125	0.699	-12364.5
0079632 6	RAW	-182.551	238.13	206.117	0.679	-18255.1
	CORRECTED	-67.86	154.827	126.01	0.863	-6786
0079730 0	RAW	-145.019	174.849	152.708	0.74	-14501.9
	CORRECTED	-131.75	166.338	142.18	0.763	-13175
0079754 2	RAW	59.336	66.297	63.962	0.962	5933.6
	CORRECTED	6.035	159.49	107.975	0.789	603.5
0101719A8	RAW	122.275	161.472	137.733	0.697	12227.5
	CORRECTED	-72.97	116.728	91.18	0.784	-7297

## 15. APPENDIX H: RESULTS OF BIAS CORRECTION STATISTICS IN CATCHMENT U20F

Table H.1: Bias correction statistics at a daily scale

Stations	Rainfall	MBE	RMSE	MAE	D	% BIAS
0270260A	RAW	0.197	7.486	3.042	0.531	19.7
	CORRECTED	-0.116	7.846	2.864	0.502	-11.6
0270205A	RAW	0.205	7.033	2.678	0.62	20.5
	CORRECTED	0.088	7.494	2.514	0.614	8.8
0270086A	RAW	-0.097	6.888	2.768	0.613	-9.7
	CORRECTED	-0.136	6.69	2.714	0.717	-13.6
0270023A	RAW	-0.04	7.109	2.767	0.618	-4
	CORRECTED	-0.064	7.523	2.752	0.657	-6.4
0270021W	RAW	-0.087	8.774	3.309	0.466	-8.7
	CORRECTED	0	9.84	3.386	0.518	0
02701645S	RAW	0.121	7.678	2.96	0.62	12.1
	CORRECTED	-0.067	8.361	2.91	0.607	-6.7
0269647W	RAW	-0.715	9.514	3.996	0.444	-71.5
	CORRECTED	-0.19	10.858	4.387	0.447	-19
0269712W	RAW	-0.419	8.425	3.283	0.538	-41.9
	CORRECTED	-0.058	8.958	3.489	0.631	-5.8
0269744S	RAW	-1.076	8.32	3.423	0.591	-107.6
	CORRECTED	-0.207	9.133	3.858	0.652	-20.7
0269775S	RAW	0.666	7.467	3.015	0.384	66.6
	CORRECTED	0	7.452	2.579	0.371	0

Table H.2: Bias correction statistics for the monthly scale

Stations	Rainfall	MBE	RMSE	MAE	D	% BIAS
0270260A	RAW	5.991	29.043	18.619	0.938	599.1
	CORRECTED	-3.538	27.788	17.044	0.941	-353.8
0270205A	RAW	6.243	30.988	19.894	0.929	624.3
	CORRECTED	-2.68	30.006	17.554	0.934	-268
0270086A	RAW	-2.939	31.073	17.774	0.931	-293.9
	CORRECTED	-4.151	23.681	15.472	0.96	-415.1
0270023A	RAW	-1.205	32.233	20.497	0.928	-120.5
	CORRECTED	-1.954	32.21	19.973	0.936	-195.4
0270021W	RAW	-2.643	34.18	23.119	0.921	-264.3
	CORRECTED	0	38.122	25.467	0.924	0
02701645S	RAW	3.685	34.009	20.147	0.93	368.5
	CORRECTED	-2.034	38.993	22.76	0.912	-203.4
0269647W	RAW	-21.757	62.776	38.797	0.829	-2175.7
	CORRECTED	-5.769	60.44	37.764	0.867	-576.9

0269712W	RAW	-12.746	44.848	25.607	0.89	-1274.6
	CORRECTED	-1.758	38.708	22.73	0.935	-175.8
0269744S	RAW	-32.742	51.911	35.209	0.873	-3274.2
	CORRECTED	-6.315	32.654	22.028	0.961	-631.5
0269775S	RAW	20.278	42.435	28.453	0.838	2027.8
	CORRECTED	0	39.341	25.761	0.834	0

Table H 3: Bias correction statistics for the annual scale

Stations	Rainfall	MBE	RMSE	MAE	D	% BIAS
0270260A	RAW	70.389	107.945	92.665	0.911	7038.9
	CORRECTED	-41.57	86.39	66.93	0.939	-4157
0270205A	RAW	73.351	101.753	80.957	0.913	7335.1
	CORRECTED	-31.485	78.819	65.325	0.947	-3148.5
0270086A	RAW	-34.536	130.561	110.241	0.888	-3453.6
	CORRECTED	-48.77	125.874	96.71	0.913	-4877
0270023A	RAW	-14.16	132.06	102.156	0.878	-1416
	CORRECTED	22.96	124.549	94.57	0.909	-2296
0270021W	RAW	-31.06	113.942	99.11	0.904	-3106
	CORRECTED	0	127.025	105.86	0.911	0
02701645S	RAW	43.299	143.96	110.218	0.886	4329.9
	CORRECTED	-23.905	132.505	89.345	0.91	-2390.5
0269647W	RAW	-255.649	399.331	301.432	0.525	-25564.9
	CORRECTED	-67.79	322.066	251.32	0.676	-6779
0269712W	RAW	-149.769	247.819	208.951	0.74	-14976.9
	CORRECTED	-20.66	194.477	122.31	0.862	-2066
0269744S	RAW	-384.719	405.671	384.719	0.465	-38471.9
	CORRECTED	-74.2	144.664	128.29	0.913	-7420
0269775S	RAW	238.267	306.489	250.111	0.487	23826.7
	CORRECTED	0	202.636	172.97	0.637	0